

Supercooled dynamics of glass-forming liquids and polymers under hydrostatic pressure

C M Roland¹, S Hensel-Bielowka², M Paluch² and R Casalini^{1,3}

¹ Naval Research Laboratory, Chemistry Division, Code 6120, Washington, DC 20375-5342, USA

² Institute of Physics, Silesian University, ul. Uniwersytecka 4, 40-007 Katowice, Poland

³ Chemistry Department, George Mason University, Fairfax, VA 22030, USA

Received 11 March 2005

Published 19 May 2005

Online at stacks.iop.org/RoPP/68/1405

Abstract

An intriguing problem in condensed matter physics is understanding the glass transition, in particular the dynamics in the equilibrium liquid close to vitrification. Recent advances have been made by using hydrostatic pressure as an experimental variable. These results are reviewed, with an emphasis in the insight provided into the mechanisms underlying the relaxation properties of glass-forming liquids and polymers.

(Some figures in this article are in colour only in the electronic version)

Contents

	Page
1. Introduction	1407
2. Experimental techniques	1408
2.1. Viscosity measurements	1408
2.2. Dielectric spectroscopy	1410
2.3. Light scattering measurements	1411
2.4. Neutron scattering	1412
2.5. Nuclear magnetic resonance	1414
2.6. Thermal analysis	1414
3. Pressure coefficient of the glass transition temperature	1416
4. Models for the effect of pressure and temperature on the relaxation time and viscosity	1419
4.1. Phenomenological equations	1419
4.2. Free volume models	1421
4.2.1. Cohen and Turnbull	1421
4.2.2. Hole model of Simha–Somcynsky	1423
4.2.3. Dynamic lattice liquid model	1423
4.2.4. Cohen and Grest	1424
4.2.5. Defect diffusion model	1425
4.3. Entropy models	1425
4.3.1. Avramov	1425
4.3.2. Adam and Gibbs	1426
5. Pressure dependence of the structure factor	1428
6. Quantifying the volume and temperature dependences	1431
7. Dynamic crossover	1443
8. Secondary relaxations	1444
8.1. Johari–Goldstein secondary relaxation	1446
8.2. The excess wing	1450
8.3. Temperature dependence of τ_{JG} near T_g	1452
8.4. Properties of secondary relaxations below T_g	1458
9. Decoupling phenomena	1458
10. Dielectric normal mode	1463
11. Blends	1466
12. Summary	1470
Acknowledgments	1470
References	1470

1. Introduction

Glass-formation on earth may be as old as the planet itself. Natural silica glasses include tektite, formed from the heat and pressure of meteor impacts; fulgurites, created when lightning causes melting and fusion of sand; and diatomaceous earth, the fossilized skeletons of microscopic sea animals. Some amber, formed by polymerization and vitrification of tree resin, is more than 300 million years old. Utilization of naturally-occurring glasses dates to the beginning of recorded history. For example, around 75 000 BC, tools were made from obsidian, a silica glass formed from quenched volcanic lava. The first synthetic glasses, silicate artifacts, appeared in Mesopotamia and Egypt, about 3500 years ago. However, glazed (vitreous) surfaces were produced as early as the 5th millennium BC. A verse in one of the oldest books of the bible (about 2000 BC) indicates the great value of vitreous material in antiquity: ‘*Gold and glass cannot equal [wisdom]*’ (Job 28:17, ASV). Modern glass-making is a highly developed technology, used to produce not only inorganic glasses but also metallic glasses and many plastics. It is a testament to the complexity of the process that despite such a long history, the factors governing vitrification are still vigorously investigated. Near the glass transition, viscosities become so large that the material behaves as a solid, yet retains the microscopic disorder of the liquid state. Small changes in thermodynamic conditions can alter the time scale for molecular motions from nanoseconds to a duration exceeding the human lifespan. Because of the complexity of the supercooled dynamics, theoretical efforts remain at the model-building stage and a quantitatively accurate theory of real materials is lacking.

There are many routes to the glassy state: (i) thermal quenching at a rate sufficient to avoid crystallization; (ii) application of hydrostatic pressure; (iii) condensation of gas at low temperature (e.g. include the water in comets and the Mt Palomar mirror); (iv) solvent evaporation or sublimation; (v) irradiation of crystalline materials to disrupt the unit cell; (vi) using chemical methods, such as polymerization, hydrolysis of organosilicon compounds, or condensation of chemically reacted vapours (e.g. to produce fibre optics). Although theorists often ascribe vitrification to an underlying thermodynamic transition, from an experimental viewpoint the glass transition is a kinetic process, associated with departure from the equilibrium liquid structure, as the experimental time-scale becomes shorter than the characteristic time for the relevant molecular motions. Although this transition is accompanied by spectacular changes in physical properties (above T_g the material assumes the shape of its container, while the glass can serve as the container), there are no changes in the molecular configuration. Both the liquid and glassy states lack long-range order (no translational symmetry) and are distinguished by their dynamic, rather than static, properties.

Historically, studies of the dynamics of molecules approaching the glassy state are focused on the effect of temperature, owing in part to experimental convenience. Isobaric measurements of relaxation times and viscosities are carried out as a function of temperature. (Previous studies relied on the less useful method of scanning temperature and measuring the response to a fixed-frequency perturbation.) While much has been learned from these studies, more groups have begun to exploit pressure as an experimental variable. This has led to important insights into glass formation in liquids and polymers. The earliest use of pressure to study the dynamics was probably the dielectric measurements of Gilchrist *et al* (1957) on propanol and glycerol at pressures as high as 100 MPa. Bridgman (1964) carried out very early viscosity measurements at elevated pressure. The most influential work involved dielectric spectroscopy measurements on polymers by Williams (Williams 1964a, 1964b, 1965, 1966a, 1966b, 1979, Williams and Edwards 1966, Williams and Watts 1971a, McCrum *et al* 1991) and by Sasabe and co-workers (Sasabe and Saito 1968, Saito *et al* 1968, Sasabe *et al* 1969).

Skorodumov and Godovskii (1993) reviewed the effect of pressure on the glass transition temperature of polymers. More recently, Floudas (2003) reviewed the use of pressure in dielectric relaxation measurements on polymers, covering selected works on the glass transition. Floudas (2004) has also reviewed the dynamics of liquid crystalline and other ordered polymers under pressure. The focus herein is the supercooled dynamics, by which we mean the relaxation and transport properties of the equilibrium liquid or polymer in the vicinity of its glass transition. Strictly speaking, 'supercooled' refers to a sufficiently fast temperature reduction, such that crystal nuclei do not form and the liquid remains in an amorphous state. For many polymers such quenching is unnecessary, since their rate of crystallization is inherently slow (*cis*-1,4-polyisoprene, polyethylene terephthalate, polyether ether ketone, polyphenylene sulfide, etc) or they lack sufficient steric regularity of their chain backbone to crystallize (e.g. copolymers and atactic homopolymers). Rapidly bringing a material to conditions at which vitrification is imminent and the dynamics markedly slowed can also be accomplished by hydrostatic pressure. In fact, pressure quenching can be much more effective than cooling, since stresses equilibrate within the material faster (at approximately the speed of sound) than thermal equilibration. This is especially true for polymers, which have low thermal diffusivities (although pressure enhances the rate of crystallization (Thiessen and Kirsch 1938, Floudas *et al* 2003)). For convenience, herein we retain the term 'supercooling' for both temperature and pressure quenching.

Although the focus is on the dynamics associated with the glass transition (the dielectric α -process, which for polymers is also referred to as local segmental relaxation), high-pressure studies of other relaxation processes in glass-forming materials, including secondary relaxations at higher frequencies and the slower normal mode (involving polymeric chain modes), are also discussed within the context of their relationship to the glass transition.

Although work to date has been limited to elevated pressure, in principle negative pressure (triaxial tension) can also be used to alter the dynamics. Interestingly, models for the dynamics of liquids (see section 4) make different predictions for the effect of negative pressure. However, existing negative pressure experiments have addressed primarily the effect on the phase boundaries of mixtures (Imre *et al* 2002).

2. Experimental techniques

2.1. Viscosity measurements

Viscosity, η , is a measure of the resistance to flow, and as the temperature of a normal liquid is lowered toward the glass transition temperature, η increases over an extremely broad range. Simple liquids at normal temperatures (well above T_g) have viscosities near 0.1 Pa s, values of the order of 10^{12} Pa s are achieved near T_g . This same effect can be induced by increasing the pressure. However, it is an experimental challenge to measure the viscosity over several decades under elevated pressure, and thus different measurement techniques are used. Figure 1 illustrates most of the techniques for high-pressure viscosity measurements; all have some limitations with respect to both pressure and viscosity range.

Using a falling body viscometer, Bridgman (1926) was the first to measure precise viscosities at pressures of up to 1.2 GPa. In this type of viscometer, the liquid and a cylindrical weight are enclosed in a cylinder, with an attached bellows to transmit the pressure. The entire apparatus is mounted inside a high-pressure chamber, with pressure generated by a hydraulic press. The viscosity is determined from the descent under gravity of the weight in the liquid, with the range of measurable η only about three decades. To extend this range, Bridgman (1964) utilized a swinging vane apparatus which provided viscosities of up to about 10^5 Pa s at pressures of as high as 3 GPa.

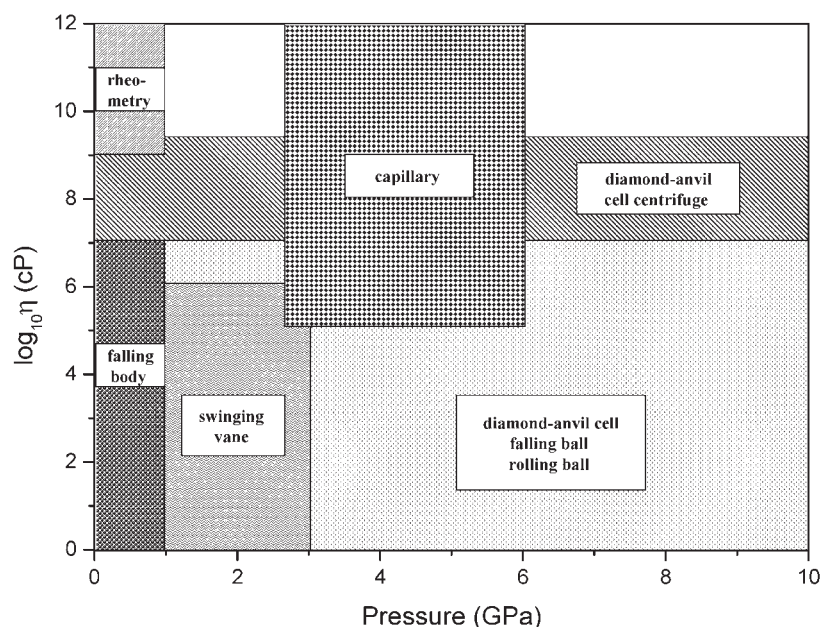


Figure 1. The viscosity and pressure range of various viscometers (reprinted with permission from Cook *et al* (1993), copyright American Chemical Society).

Capillary-type viscometers (Barnett and Bosco 1969) can measure viscosities of as high as 10^{11} Pa s at pressures of up to 6 GPa. In this method, the flow time of the test liquid is measured for two parts of a viscometer that are under slightly different pressures. However the precision of the data is low, with uncertainties in η of about 60%.

An advancement in viscosity measurements under high pressures is the use of a diamond pressure cell (Jayaraman 1983). In the pioneering work by Piermarini *et al* (1978), a diamond anvil cell was used to pressurize a falling-sphere viscometer; pressures of the order of 10 GPa could be achieved. In this type of viscometer, the proximity of the falling sphere to the wall results in large drag forces, which introduces significant uncertainty into the determination of η . With careful corrections for the wall effect, absolute viscosities with a 10% uncertainty can be obtained (Munro *et al* 1978). Higher precision data were obtained by King *et al* (1992) by using a rolling ball, rather than the falling ball technique. The ball is constrained to roll along one of the diamond anvils by tilting the cell. A high-pressure diamond anvil cell viscometer is depicted in figure 2. Pressure can be generated by the use of a mechanical clamp (Jayaraman 1983), with a small piece of ruby used as manometer (Barnet *et al* 1973, King and Prewitt 1980).

An advantageous feature of falling or rolling ball viscometers is that the sample is visible throughout the experiment. Simple rolling-ball diamond anvil cell viscometers yield η in the range of 10^{-2} – 10^6 Pa s. To measure higher viscosities, a method was developed by Cook and co-workers, who used centrifugal force, rather than gravity, to move the ball in the diamond anvil cell viscometer (Cook *et al* 1993). This extended the range of η to 10^4 – 10^8 Pa s, with a precision of 8%.

Koran and Dealy (1999) have developed a rheometer capable of measuring the shear-rate dependent viscosity of polymers under shear flow to pressures of up to 70 MPa. The dynamic viscosity (no flow) under pressure can be measured using a quartz-resonator (Theobald *et al* 1994, 2001); there is no control of the strain amplitude. Commercial rheometers are available which impose moderate pressures (<20 MPa) pneumatically. However, the geometry is usually

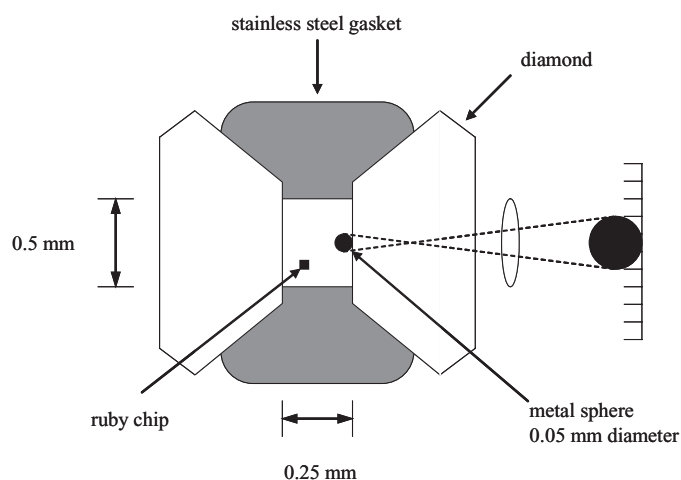


Figure 2. The diamond-anvil pressure cell utilizing a rolling-sphere viscometer. The tilt necessary to obtain a rolling sphere trajectory is not shown (reprinted with permission from King *et al* (1992), copyright American Institute of Physics).

limited to Couette flow, and since gas is used as the pressurizing medium, the potential exists for plasticization of the sample.

2.2. Dielectric spectroscopy

Dielectric spectroscopy allows observation of both the movement of ionic species, that is, migration of charged carriers in the presence of an electrical field, and the reorientational motions of dipolar molecules. The time scales of the dc-conductivity and the various relaxation modes, and their change with thermodynamic conditions (e.g. T and P), span an enormously wide range. This makes dielectric spectroscopy especially useful, because it enables the different processes to be monitored in a single experiment. At ambient pressure dielectric spectra can be obtained over 16 decades of frequency ($10^{-4} < \nu$ (Hz) $< 10^{12}$), although at high pressures the highest accessible frequency is about 10^7 Hz.

For a typical dielectric experiment, the sample is placed in a capacitor connected to the appropriate analyser (impedance or time domain analyser), which measures capacitance (C) and resistance (R) from which the real and imaginary parts of dielectric permittivity (or the dielectric modulus) are determined. To control both temperature and pressure during the measurements, the capacitor is installed in a special high-pressure cell. The capacitor uses wires in insulated sleeves leading out of the cell. Many high-pressure set-ups are non-commercial and differ among laboratories. Common features are described below. A description of a commercial high-pressure dielectric instrument was given by Reisinger *et al* (1997).

To exert pressure on the sample within the pressure chamber, two methods are in use. Pressurization can be by means of a hydraulic pump using a non-polar liquid (Urbanowicz *et al* 1995, Theobald *et al* 2001, Reiser *et al* 2004); the general scheme is shown in figure 3. To increase the pressure on the side of the sample, the pump can be used in conjunction with a pressure intensifier, which are commercially available. Since the capacitor is embedded in the pressure-transmitting liquid, it is usually physically separated by a flexible membrane (typically thin Teflon film). A disadvantage is that during the course of an experiment, with continual changes of temperature and pressure (the latter sometimes very

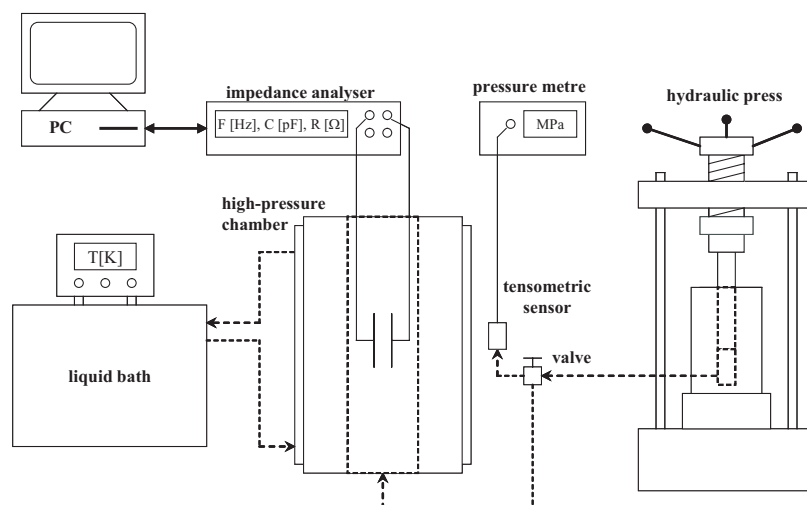


Figure 3. High-pressure dielectric cell using a pressure-transmitting liquid. Hydraulic connections are denoted by dashed lines and electrical connections by solid lines.

abrupt), the sample may be contaminated by the pressure-transmitting liquid. The transmitting liquid must be nonpolar, noncorrosive to electrical connections and maintain a low viscosity at low temperatures and high pressures. Silicon oils are a popular choice as are perfluorinated alkanes (e.g. Fluorinert from 3M Co.). These can be mixed with alkanes such as heptane to allow measurements at lower temperatures. Hydraulic pumps using pressurizing fluids allow pressures of above 1 GPa (Casalini and Roland 2004a). To obtain higher pressures, a different construction of the dielectric cell is used.

In the second type (figure 4), the cylindrical pressurizing cell is filled with the sample, which is squeezed by pistons in conjunction with a hydraulic press (Gilchrist *et al* 1957, Johari and Whalley 1972, Forsman *et al* 1986). Thus, in this method the sample serves as its own pressure-transmitting fluid, and pressures of as high as 2.5 GPa can be achieved. A limitation of the approach is that for experiments below T_g , the sample solidifies and can no longer exert hydrostatic stress. Another potential problem is friction between the cylinder and pistons.

The capacitor plates used during the high-pressure dielectric measurements are usually flat and parallel, although cylindrical plates are also employed (Johari and Whalley 1972, Forsman *et al* 1986, Koplinger *et al* 2000). Teflon or quartz spacers are used to maintain a fixed distance between the plates. The former introduces a small uncertainty into the absolute value of the capacitance, since the capacitance of Teflon changes with pressure. A representative illustration is shown in figure 5.

The usual ways to measure the pressure are calibrated bourdon gauges and tensometric manometers. For temperature control, the high-pressure cell is immersed in either a thermostatic bath or other environmental chamber.

2.3. Light scattering measurements

Another experimental technique for the study of the molecular motions under high pressure is dynamic light scattering (figure 6). A typical set-up includes a laser, a high-pressure light scattering cell, a diode detector and a digital correlator. The sample chamber is made of hardened steel equipped with optical windows. Both the polarized and depolarized scattered light can be measured, although the depolarized component is used to study molecular

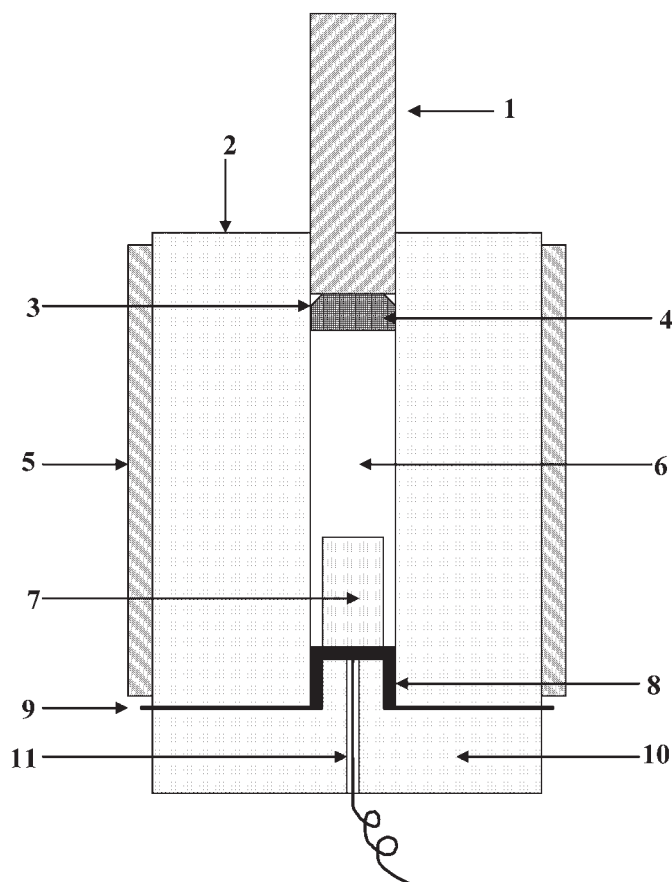


Figure 4. High-pressure dielectric cell for pressures up to 2.5 GPa: 1—piston, 2—cylinder, which is both the high electrode and a vessel for the sample, 3—anti-extrusion ring, 4—seal, 5—safety ring, 6—sample, 7—solid cylinder, which serves as the low electrode, 8—mica sheet insulating parts 2 from 9, 9—support which serves as ground electrode and 10—electrical contact to part 7, 11—the ceramic-insulated stainless-steel-sheathed wire (figure from Johari and Whalley (1972)).

reorientations. Typical experiments are limited to moderate pressures, of up to about 200 MPa, with pressure applied via a gas and membrane compressor (Fytas *et al* 1982a, 1982b, 1982c, 1983, 1984, Paluch *et al* 2000a, 2001a, 2003, Patkowski *et al* 2002, Gapinski *et al* 2002, Comez *et al* 2002, 2004). To extend light scattering measurements to the gigapascal range, a diamond anvil cell can be used. Relaxation times in the gigahertz regime at 12 GPa have been reported (Oliver *et al* 1991).

2.4. Neutron scattering

There are several methods which probe dynamical processes in the GHz–THz regime. Among these techniques, quasielastic neutron scattering (QENS) is the most versatile. No special features of the sample (e.g. dipole moment or optical transparency) are required, allowing QENS to be applied to virtually any materials. Inelastic coherent and incoherent scattering are proportional to the space and time Fourier transforms of the pair-correlation and the self-correlation functions, respectively, and are used to probe the dynamics (see section 5).

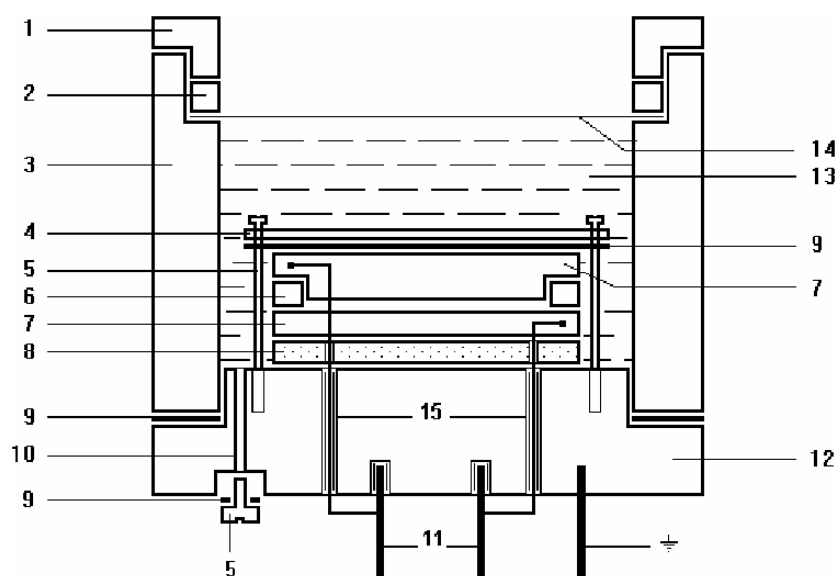


Figure 5. Capacitor for pressure experiments: 1—clamp nut, 2—pressure ring, 3—cylindrical encapsulation of capacitor, 4—clamp cover plate, 5—screws, 6—quartz spacer, 7—plates, 8—Teflon insulator, 9—Teflon washer, 10—filler hole, 11—connection wires, 12—capacitor base, 13—sample, 14—Teflon membrane for transmission of pressure, 15—bushing (Urbanowicz *et al* 1995).

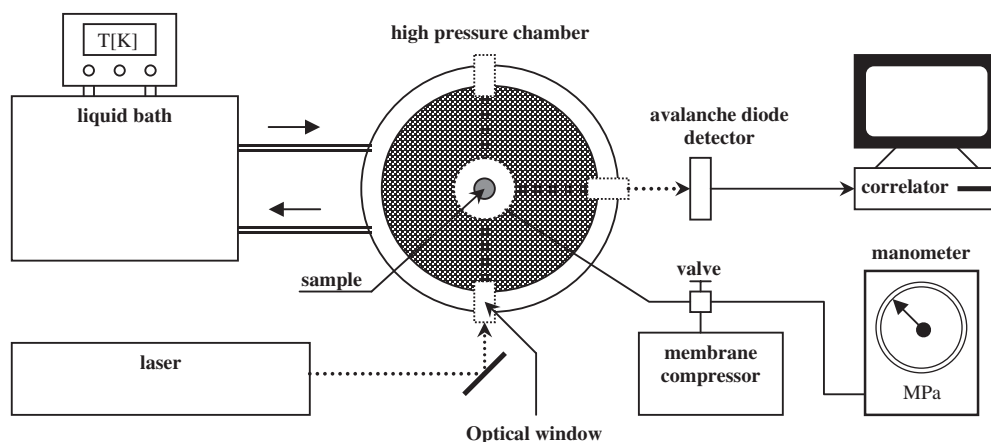


Figure 6. Schematic illustration of the light scattering technique used for high pressure measurements.

The two sources of neutrons are nuclear reactors and particle accelerators (spallation sources). The neutrons are moderated to obtain energies comparable to that associated with thermal motion of molecules in condensed phase; this corresponds to a wavelength close to 1 \AA (Lovesey 1984). The quantity measured in neutron scattering experiments is the dynamic structure factor $S(Q, \omega)$, which is a function of both the wave-vector Q (momentum transfer) and the energy $\omega (= 2\pi\nu)$ (see section 5). Neutron scattering is the only method that provides both types of information. At constant ω one obtains the static structure factor $S(Q)$, while measurements at fixed Q are used to investigate molecular motions.

Neutron scattering experiments can be carried out as a function of both temperature and pressure. However, investigations at high pressure are rare (Frick and Alba-Simionesco 1999, Tölle 2001, Calliaux *et al* 2003, Frick *et al* 2003). A problem is to select a high-pressure vessel with the appropriate strength, size and wall thickness, while minimizing background scattering and absorption by the cell walls (Tölle 2001). The frequency range of neutron spectrometers is relatively narrow. Time domain instruments provide the largest, just over three decades of frequency. Thus, data from different spectrometers is often combined, or master curves are constructed.

2.5. Nuclear magnetic resonance

Nuclear magnetic resonance (NMR) is a well-known and oft-exploited technique to study the relaxation dynamics of liquids and polymers. The molecular site specificity arising from the chemical shift and from isotopic labelling offers advantages over other spectral methods. Slow chain motions in polymers, reflecting their local segmental dynamics, can be detected from the NMR relaxation times T_1 and T_2 (Zeeman and quadrupolar). NMR lineshapes that are dominated by chemical shift anisotropy or the quadrupole interaction are also sensitive to slow local segmental dynamics. In this regard, deuterium NMR is often used because the quadrupole lineshape is very sensitive to small-angle reorientations.

Such measurements can be carried out at elevated pressures, using either a pressurizing liquid or gas (Rössler *et al* 1985, Kulik and Prins 1993, Hollander and Prins 2001). The latter avoids problems with contamination of the spectra; however, plasticization of the sample by the gas is hard to avoid. Helium is commonly used, since it has a relatively small (but not insignificant) solubility in most materials. Xenon is an interesting pressurizing gas, since the NMR spectrum of ^{129}Xe is very sensitive to environment (Miller *et al* 1993, Miller and Roland 1995). This means the pressurizing gas can be used to probe the dynamics. A few NMR studies using xenon at elevated pressure have been published recently (Miyoshi *et al* 2002, Omi *et al* 2004). Different probe designs for high-pressure NMR experiments have been described in the literature (Shimokawa and Yamada 1983, Huber *et al* 1984, Delangen and Prins 1995, Ballard *et al* 1998, Castro and Delsuc 1998, Zahl *et al* 2004).

2.6. Thermal analysis

To delineate the respective contributions of density and thermal energy to the dynamics, it is essential to know the volume and its change with temperature and pressure. *PVT* measurements also directly yield the glass transition temperature (from the discontinuity in the thermal expansion) and its pressure dependence. Properties such as the thermal expansivity and compressibility are also central to thermodynamic interpretations of the glass transition.

There are two basic techniques for obtaining *PVT* data (Zoller 1986). In the first, a rigid cylinder is filled with the sample, then closed with a piston. The volume of the sample is calculated from the displacement of the piston, induced by changes in pressure and temperature. There are serious disadvantages to this method. The sample must remain a liquid; when it solidifies, the state of hydrostatic compression is lost. Seals are required to minimize leakage of low-viscosity samples around the piston; however, this introduces friction and uncertainty regarding the applied pressure. The piston/cylinder technique is not widely used, primarily because of these problems.

A more popular method is to use a confining fluid (Tribone *et al* 1989, Zoller and Walsh 1995, Takahara *et al* 1998). The sample, either liquid or solid, is immersed in a fluid inside a cell capped by a flexible bellows. External pressure is applied, causing a change in

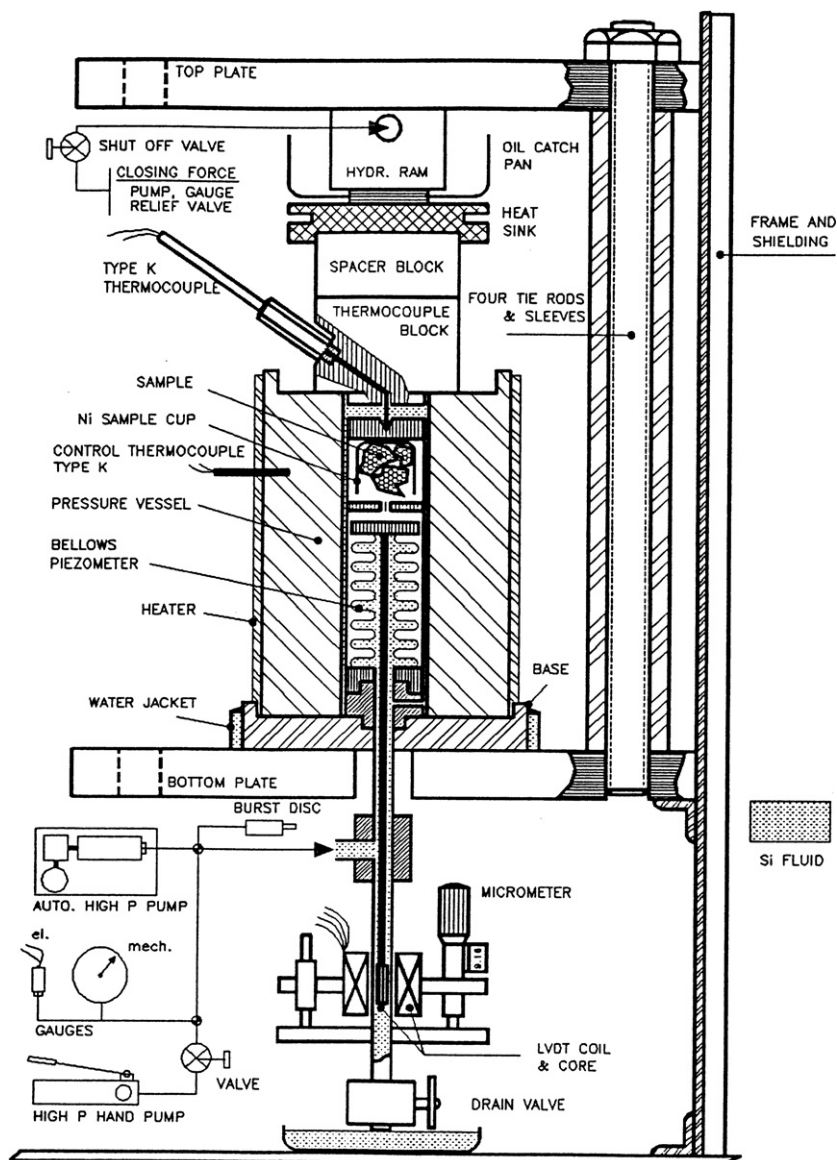


Figure 7. GNOMIX apparatus for PVT measurements (from Zoller and Walsh (1995), with permission).

bellows dimensions in relation to changes in the sample/fluid volume. The change in length of the bellow is monitored magnetically. The volume of the sample is determined by subtracting the volume of the confining fluid. The latter is usually silicone oil or mercury, although other liquids have also been used (Takahara *et al* 1998). Drawbacks to the technique include possible interaction between the sample and the confining liquid, and the need to maintain the latter in a fluid state. A schematic of the commercial GNOMIX apparatus is shown in figure 7.

The measurement of the heat capacity at atmospheric pressure is a very common method for the characterization of liquid and glasses owing to the commercial availability of good quality instruments and the relative simplicity of the measurements. For measurements under high

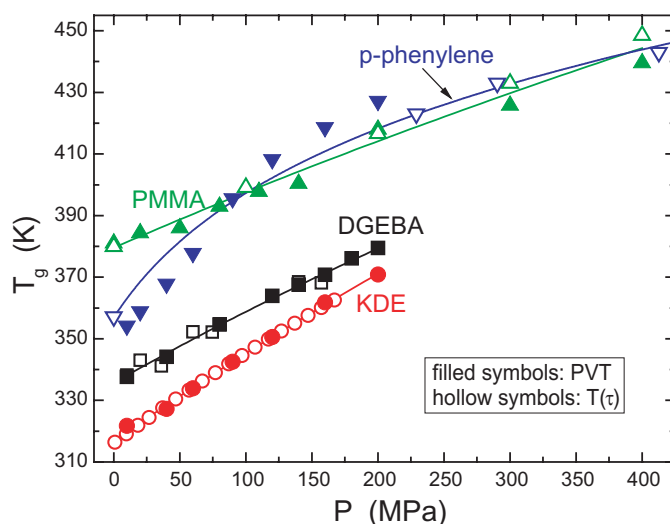


Figure 8. Comparison of the glass transition temperature determined from the change in the volume expansivity (●, ■, ▲, ▼) to the temperature at which: (○) the dielectric relaxation time equals 10 s for cresolphthalein-dimethylether (Paluch *et al* 2002e); (□) the relaxation time measured by dynamic light scattering equals 40 s for diglycidylether of bisphenol A (Paluch *et al* 2003); (△) the dielectric relaxation time equals 100 s for poly(methylmethacrylate) (extrapolated from the data of Theobald *et al* (2001)); (▽) the dielectric relaxation time equals 100 s for *p*-phenylene (Gitsas *et al* 2004). The solid lines represent fits to equation (1).

pressure, the pressuring medium is generally a gas, which can readily dissolve in the material if not isolated, although liquids can also be used (Williams and Angell 1977). Commercial scanning calorimeters are restricted to relatively low pressures ($P < 20$ MPa). Specially developed instruments can achieve pressures as high as 400 MPa (Williams and Angell 1977, Atake and Angell 1979, Takahara *et al* 1994, 1999a, Alba-Simionesco 1994, Leyser *et al* 1995, Yamamuro *et al* 1995).

3. Pressure coefficient of the glass transition temperature

The effect that pressure has on the dynamics varies widely among liquids and polymers. A convenient measure of pressure sensitivity is the change of the glass transition temperature with pressure. Dynamic measurements usually yield the pressure coefficient of some characteristic temperature, corresponding to a constant value of the principal reorientational relaxation time; i.e. $\tau_\alpha(T_g) = \text{constant}$. In figure 8 are shown data for four glass-formers, in which the glass transition temperature obtained from *PVT* data (as the change in slope of the volume versus temperature curve) is compared with the temperature associated with a fixed value of the relaxation time. The correspondence between the two measurements of T_g is maintained at all pressures (Skorodumov and Godovskii 1993, Hollander and Prins 2001). Of course, the particular value of $\tau_\alpha(T_g)$ varies with the material, at least in part owing to differences in the rates at which *PVT* measurements are carried out. In terms of the dynamics, the glass transition is viewed as a kinetic phenomenon, so that the value of τ_α used to define T_g is arbitrary.

For a wide range of molecular and polymeric glass-formers, values of dT_g/dP , taken in the limit of low pressure, are collected in table 1. Although so coarse a metric has limited

Table 1. Pressure coefficient of T_g in the limit of low pressure.

Material	T_g (K)	dT_g/dP (K GPa ⁻¹)	Method	Reference
Polystyrene	373	360	PVT	Roland and Casalini 2003b
	373	303	DTA	Rehage and Oels 1977 <i>High Temp.—High Press.</i> 9 545
Polymethyltolylsiloxane	261	340	Dielectric	Paluch <i>et al</i> 2002b
	250	380	Dielectric	Mpoukouvalas and Floudas 2003
Poly(2-vinylpyridine)	337	340	Dielectric	Papadopoulos <i>et al</i> 2004
Bisphenol-A polycarbonate	413	320	DTA	Colucci <i>et al</i> 1997
Cresolphthalein-dimethylether (KDE)	313	307	Dielectric	Casalini <i>et al</i> 2003b
64% chlorinated biphenyl (PCB64)	278	310	Dielectric	Roland and Casalini 2005
52% chlorinated biphenyl (PCB52)	251	300	Dielectric	Roland and Casalini 2005
1,1'-di(4-methoxy-5-methylphenyl) -cyclohexane (BMMPC)	261	270	Dielectric	Casalini <i>et al</i> 2003c
	263	227	Light scattering	Patkowski <i>et al</i> 2004
<i>o</i> -terphenyl (OTP)	246	260	DTA	Atake and Angell 1979
<i>m</i> -terphenyl/OTP (1/4)	247	260	DTA	Atake and Angell 1979
Triphenylchloromethane/OTP (1/3)	243	260	PVT	Naoki <i>et al</i> 1986
42% chlorinated biphenyl (PCB42)	225	240	Dielectric	Roland and Casalini 2005
Polyvinylacetate	302	250	Dielectric	Roland and Casalini 2003a
	298	220	PVT	O'Reilly 1962
1,2-polybutadiene	253	240	Dielectric	Roland <i>et al</i> 2003a
1,1'-bis(<i>p</i> -methoxyphenyl) cyclohexane (BMPC)	241	240	Dielectric	Casalini <i>et al</i> 2003c
	247	182	Light scattering	Patkowski <i>et al</i> 2004
Polymethylmethacrylate	378	240	PVT	Olabisi and Simha 1975
Poly(4-vinylphenol)	473	222	PVT	Zhang <i>et al</i> 2003
Polymethylmethacrylate	380	145	PVT	Theobald <i>et al</i> 2001
	390	170	Dielectric	Theobald <i>et al</i> 2001
Polyisobutene	198	240	PVT	O'Reilly 1962
Polycyclohexylmethacrylate	380	224	PVT	Olabisi and Simha 1975
<i>o</i> -phenylphenol/OTP (1/2)	233	206	Diel	Roland <i>et al</i> 2004a
Poly(<i>n</i> -butyl methacrylate)	293	204	PVT	Olabisi and Simha 1975
Salol	221	204	Dielectric	Casalini <i>et al</i> 2003a
B ₂ O ₃	520	200	PVT	O'Reilly 1962
Polypropyleneglycol	210	192	Dielectric	Casalini and Roland 2003c
Polyvinylchloride	352	189	PVT, dielectric	Naoki and Owada 1984
Oligomeric epoxy (4,4'-methylene- bis(N,N-diglycidylaniline))	257	180	Dielectric	Casalini <i>et al</i> 2004
1,4-polyisoprene	201	178	Diel	Dalal and Phillips 1983
Polyvinylmethylether	247	177	Dielectric	Casalini and Roland 2003a
Polyvinylethylether	241	215	Dielectric	Mpoukouvalas <i>et al</i> 2005
Triphenylomethane triglycidyl ether	281	167	Dielectric	Paluch 2001
Atatic polypropylene	252	158	2H NMR	Hollander and Prins 2001
Polyethylvinylacetate	258	158	Dielectric	Zhang <i>et al</i> 2003
Polybisphenol A-co-epichlorohydrin, glycidyl endcapped (PBGD)	258	156	Dielectric	Paluch <i>et al</i> 1999
Polyoxybutylene	199	155	Dielectric	Casalini and Roland 2005b
Poly(phenyl glycidyl ether)-co- formaldehyde	258	154	Dielectric	Paluch <i>et al</i> 2000c
Polydimethylsiloxane	148	143	QENS	Roots <i>et al</i> 1999
17% chlorobenzene/decalin	130	120	Diel	Koplinger <i>et al</i> 2000
Ethylammonium/ α -picolinium chlorides	218	110	DTA	Williams and Angell 1977

Table 1. (Continued.)

Material	T_g (K)	dT_g/dP (K GPa ⁻¹)	Method	Reference
Propylene glycol trimer	206	109	Dielectric	Casalini and Roland 2003c
Nylons	337–341	100–160	Mechanical	Parry and Tabor 1973
Polychlorotrifluoroethylene	368	100	Mechanical	Parry and Tabor 1973
Ethanolaminium/ α -picolinium chlorides	215	82	DTA	Williams and Angell 1977
<i>m</i> -fluoroaniline	171	81	Dielectric	Reiser <i>et al</i> 2004
Propylene glycol dimer	210	80	Dielectric	Casalini and Roland 2003c
1-propanol	95	70	PVT	O'Reilly 1962
Ca/KNO ₃ mixtures	350–333	57–64	DTA	Williams and Angell 1977
<i>m</i> -toluidine	182	45	PVT	Alba-Simionescu <i>et al</i> 1997
<i>d</i> -sorbitol	267	43	DTA	Atake and Angell 1979
Cyclohexanol	150	40	DTA	Atake and Angell 1979
Glycerol	183	40	PVT	O'Reilly 1962
	188	27	Dielectric	Johari and Whalley 1972
Propylene glycol	185	37	Dielectric	Casalini and Roland 2003c
Selenium		37	MD simulation	Caprion and Schober 2002
	303	130	PVT	O'Reilly 1962

utility, as noted by Atake and Angell (1979) some time ago, the pressure coefficient of T_g distinguishes associated liquids from van der Waals materials, the latter having significantly larger values. While this observation is clearly borne out by the data in table 1, no other trends are so marked. With many exceptions, polymers as a class tend to have somewhat larger values than molecular glass-formers.

For all glass-formers, the change in T_g with pressure is linear at low pressures, but dT_g/dP decreases with increasing pressure. A second-order polynomial can be fitted to experimental data (Hollander and Prins 2001), although often the empirical relation proposed by Andersson and Andersson (1998)

$$T_g = k_1 \left(1 + \frac{k_2}{k_3} P \right)^{1/k_2} \quad (1)$$

is used, with k_1 , k_2 and k_3 material constants. An equation having the identical form is used to describe the melting point of simple crystals (Babb 1963, March and Tosi 2003). Equation (1) for the pressure coefficient at ambient pressure, $\lim_{P \rightarrow 0}(dT_g/dP)$, is equal to the ratio of k_1/k_3 . Equation (1) can also be used to describe the Vogel temperature, $T_0(P)$ (see, equation (2)) and pressure $P_0(T)$ (equation (5)). These parameters are obtained by fitting relaxation times measured for isobaric and isothermal conditions, respectively (section 4). Although the pressure dependences *per se* of T_g and the Vogel temperature may be the same in the low-pressure limit, they usually exhibit different pressure dependences (Hensel-Bielowka *et al* 2002a, Paluch *et al* 2002a, 2002b, Papadopoulos *et al* 2004). This behaviour is illustrated in figure 9 for a siloxane polymer. A specific relationship can be derived between the glass transition and Vogel temperatures (Patkowski *et al* 2003).

Metallic glasses, formed by the quenching of metallic alloys, have the disordered, amorphous structure of organic and inorganic glasses. Although changes with pressure in the T_g of metallic glasses are reported in the literature, these invariably refer to the pressure applied during glass formation. Using conventional calorimetric methods, the glass transition

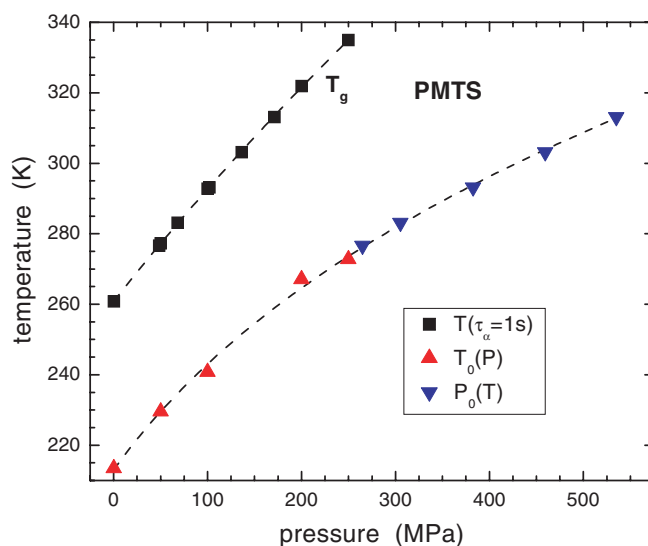


Figure 9. The pressure dependence of T_g (■), the Vogel temperature (▲, equation (2)) and the corresponding pressure parameter (▼, equation (5)) for polymethyltolylsiloxane. The curves through the data are respective fits to equation (1), with $k_1 = 261$, $k_2 = 1.9$ and $k_3 = 776$ for T_g and $k_1 = 213$, $k_2 = 4.1$ and $k_3 = 571$ for $T_0(P)$ and $P_0(T)$ (Paluch *et al* 2002b).

temperature is subsequently measured at ambient pressure. For this reason, the dT_g/dP are quite low: 3–6 K GPa⁻¹ (Kamwer *et al* 1999, Jin *et al* 2003a, 2003b, Pan *et al* 2004, Wen *et al* 2004) and cannot be compared with the pressure coefficients in table 1.

4. Models for the effect of pressure and temperature on the relaxation time and viscosity

The number of models for the glass transition seems to be inversely proportional to the degree to which any one can adequately describe the myriad properties. While the fundamental mechanisms underlying the glass transition continue to be vigorously debated, even parameterization of experimental data can be useful. Measurements over a large interval of temperature and pressure (figure 10) provide a stern test of any model of the supercooled dynamics. A liquid in a given ‘dynamic state’ can be investigated at various pressures and temperatures, that is, different thermodynamic conditions, corresponding to different material densities and glass transitions temperatures, can be associated with a fixed value of the relaxation time. In the following section we briefly review models of the dynamics that offer predictions, or at least expressions, for the temperature and pressure dependence of the primary α -relaxation time, τ_α . Jäckle (1986) authored a more comprehensive review of older models.

4.1. Phenomenological equations

In the vicinity of the glass transition, below the temperature of the dynamic crossover (see section 7), the structural relaxation time of liquids and polymers is often described using the divergent Vogel–Fulcher–Tammann–Hesse (VFTH) equation (Vogel 1921, Fulcher 1923, Tammann and Hesse 1926).

$$\tau_\alpha(T) = \tau_0 \exp\left[\frac{B}{T - T_0}\right], \quad (2)$$

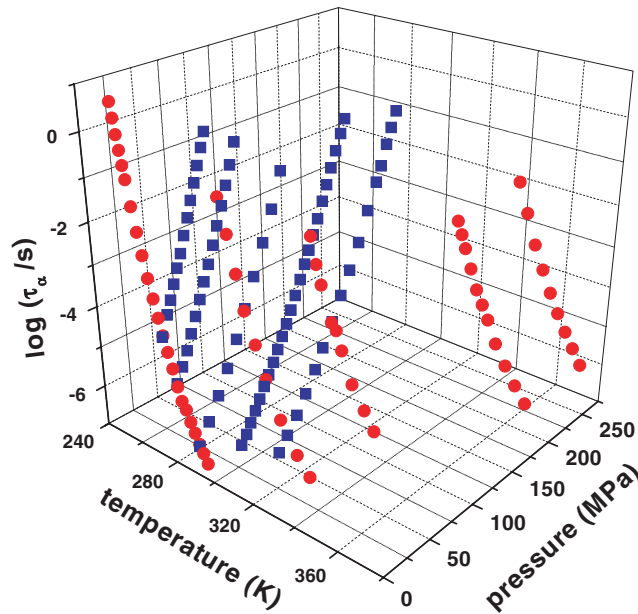


Figure 10. Dielectric relaxation times for poly(methyltolylsiloxane); circles were measured as a function of temperature at $P = 0.1, 50, 100, 200$ and 250 MPa, and squares are data obtained versus pressure at $T = 277, 283, 293, 303$ and 313 K (Paluch *et al* 2002b).

where B , τ_0 and $T_0 (< T_g)$ are constants. Equation (2) is equivalent to the Williams–Landel–Ferry (WLF) (Ferry 1980). Both the VFTH and the WLF equations have some theoretical underpinning, e.g. the Adam and Gibb (AG) entropy model (Adam and Gibbs 1965) and the free volume model (Ferry 1980) are both discussed. Using equation (2) as a starting point, several empirical equations to describe the pressure dependence of τ_α have been derived.

One obvious approach is to consider the α -relaxation a volume-activated process, with an activation volume ΔV^\ddagger ,

$$\tau_\alpha(T, P) = \tau_\alpha(T, 0) \exp\left[\frac{P\Delta V^\ddagger}{RT}\right], \quad (3)$$

where R is the gas constant and $\tau_\alpha(T, 0)$ is the value of τ_α at atmospheric pressure. ΔV^\ddagger is ostensibly a measure of the empty volume necessary for local motion (equivalently defined as the difference between the volumes of activated and non-activated species). A linear dependence on pressure of $\log(\tau_\alpha)$ in isothermal measurements is, however, almost never observed in supercooled liquids. Since ΔV^\ddagger invariably varies both with P and (inversely) with T (O'Reilly 1962, Williams 1964b, Naoki and Matsushita 1983, Forsman *et al* 1986, Floudas *et al* 1999a, Casalini *et al* 2003a, Paluch *et al* 2003, 2003b), the applicability of equation (3) is limited. Nevertheless, the value of ΔV^\ddagger in the limit of low pressure is a common metric for the pressure sensitivity of τ_α . Its magnitude is of the same order of the molecular (or repeat unit) size.

Fytas *et al* (1983) introduced a modification of equation (2)

$$\tau_\alpha(T, P) = \tau_0 \exp\left[\frac{B + b_F P}{T - (T_0 + a_F P)}\right], \quad (4)$$

where a_F and b_F are additional constants. This function can describe experimental data only over limited ranges of pressure, and for materials for which the activation volume is a weak

function of pressure. Since this equation predicts a linear dependence of the Vogel temperature T_0 with pressure, a sixth parameter is required, if T_0 varies superlinearly with pressure (Corezzi *et al* 1999a, Paluch *et al* 2001a).

A different empirical modification of the VFTH was introduced by Johari and Whalley (1972) to describe high P data

$$\tau_\alpha(T, P) = \tau_\alpha(T, 0) \exp\left(\frac{D_P P}{P_0 - P}\right), \quad (5)$$

where D_P and P_0 are functions of T only. In particular, P_0 is the pressure for which τ_α would diverge. This equation is capable of describing pressure dependences for data wherein there is a variation of the activation volume with pressure, and in which T_0 varies nonlinearly with P (Paluch 2001, Paluch *et al* 1998, 2001, 2002a, 2002b, Roland *et al* 2003a, Suzuki *et al* 2002, Floudas *et al* 2003). The usefulness of equation (5) comes from the fact that the parameter D_P is constant over a wide range of P and T (Paluch *et al* 1998, 2001, 2002a, 2002b, 2002c, Roland *et al* 2003a). For the case in which D_P is a constant and considering a quadratic dependence of P_0 in T this equation requires four additional parameters to the VFTH.

4.2. Free volume models

Free volume models rest on a simple concept of the dynamics of liquids. The assumption is that the vacant space available to each molecule governs its local motion, with the latter transpiring in a background potential owing to interactions among neighbouring molecules. Impetus to a free volume approach comes from studies using positron annihilation lifetime spectroscopy (PALS) (Dlubek *et al* 2004a, Cangialosi *et al* 2004, Faupel *et al* 2004). In organic glasses, *o*-positronium (the bound state of a positron) accumulates in regions of low electron density. Regarding such regions as the unoccupied volume, the lifetime of the *o*-positronium can be used to deduce information about the size of the free volume cavities, while its intensity relates to the concentration of vacancies. These characteristics of the free volume are then related to the local dynamics (Malhotra and Pethrick 1983, Vass *et al* 1999, Bartos and Kristiak 2000, Bartos *et al* 2000, Ngai *et al* 2001).

4.2.1. Cohen and Turnbull. The earliest free volume model is due to Cohen and Turnbull (1959), who defined free volume V_f as the difference between the specific volume V and an occupied volume V_∞ . The approach of Cohen and Turnbull formalized the empirical equation of Doolittle for the temperature dependence of the viscosity (Doolittle and Doolittle 1957),

$$\eta = a_D \exp\left(b_D \frac{V_\infty}{V_f}\right), \quad (6)$$

where a_D and b_D are constants, the latter approximately unity.

A recent analysis of dielectric data on polyvinylacetate (PVAc) concluded that the α -relaxation times decrease faster than can be accounted for by the free volume shrinkage as deduced from the Cohen–Turnbull model (Dlubek *et al* 2005a). From relaxation times and viscosities, measured as a function of temperature and pressure but plotted versus specific volume (figure 11), it is clear that V is not the dominant control variable. Therefore, for equation (6) to be valid, the temperature and pressure dependences of V_f have to differ from those of the specific volume. Fits of equation (6) to experimental data, with V_∞ taken to be constant or at least pressure independent at fixed T , show deviations beyond any experimental error (Schug *et al* 1998, Corezzi *et al* 1999a, Paluch 2001). Improved fitting is achieved by allowing b_D to vary with temperature, becoming much larger than unity (Cook *et al* 1994).

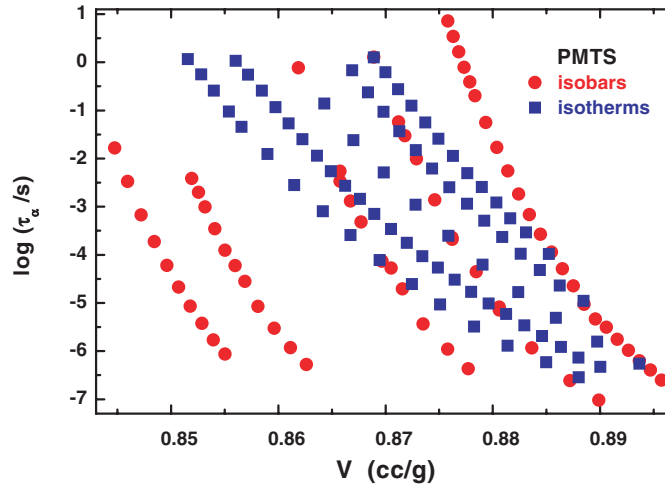


Figure 11. Dielectric relaxation times from figure 10 replotted versus specific volume.

Alternatively, the fractional free volume, defined as the ratio of the free and occupied volumes, $f = V_f/V_\infty$, is assumed to depend on temperature and pressure according to (Ferry 1980)

$$f(T, P) = f(T_{\text{ref}}, P_{\text{ref}}) + \alpha_f(T - T_{\text{ref}}) - \beta_f(P - P_{\text{ref}}), \quad (7)$$

where T_{ref} and P_{ref} are a reference temperature and pressure, $f(T_{\text{ref}}, P_{\text{ref}})$ is the fractional free volume calculated at these reference conditions and $\alpha_f (= (1/V_f)(\partial V_f/\partial T)_P)$ and $\beta_f (= -1/V_f(V_f/\partial P)_T)$ are, respectively, the free volume expansion coefficient and compressibility. Equation (7) implies that f changes roughly linearly with T and P . For simplicity taking $P_{\text{ref}} = 0$, substitution of equation (7) into equation (6) yields

$$\tau_\alpha(T, P) = a_D \exp\left(\frac{b_D}{\alpha_f(T - T_\infty)}\right) \exp\left(\frac{b_D}{\beta_f(P_\infty - P)}\right), \quad (8)$$

where $T_\infty = T_{\text{ref}} - f_{\text{ref}}/\alpha_f$ and $P_\infty = f_{\text{ref}}/\beta_f$. For $P = 0$ (atmospheric pressure) this equation is equivalent to the VFTH expression (equation (2)); that is, this equation is formally equivalent to the empirical equation (5) with the constant $D_P = b_D/(f_{\text{ref}})$. If b_D is set equal to unity, equation (8) allows determination of β_f and α_f from experimental data (Ferry 1980). These free volume quantities can then be compared with the compressibility and expansion coefficient for the total volume. The results are $\alpha_f \sim \alpha$ and $\beta_f \sim 0.5\beta$, suggesting that most of the volume change at atmospheric pressure is due to changes in free volume, while during an isothermal pressure change, only half of the volume change can be attributed to a change in free volume (Ferry 1980).

Large differences between β and β_f are evident in many materials, for example, from weaker volume sensitivities for isothermal conditions compared with isobaric conditions. This is quantified more directly from the relative magnitudes of the activation enthalpies at constant volume and constant pressure (see section 6). As discussed later, given the strong contribution from thermal energy, especially for polymers and more so for hydrogen-bonded materials, interpretations of the glass transition based on free volume seem ill-fated.

4.2.2. Hole model of Simha–Somcynsky. The model of Simha and Somcynsky (SS) (1969) is based on the cell model for polymers originally proposed by Prigogine and Mathot (1952). The basic idea is that each monomer is trapped by its surroundings, with an activation barrier at the centre of the cell described by the Lennard–Jones (LJ) 6–12 potential. In the SS model, holes (defects) are necessary to permit motion. The SS equation of state (EOS) provides for a direct estimate of the free volume

$$\frac{\tilde{P}}{\tilde{T}} = \frac{(y\tilde{V})^{1/3}}{\tilde{V}[(y\tilde{V})^{1/3} - 2^{-1/6}y]} - \frac{2y}{\tilde{T}\tilde{V}} \left(\frac{1.2045}{(y\tilde{V})^2} - \frac{1.011}{(y\tilde{V})^4} \right), \quad (9)$$

where y is the fraction of lattice cells containing molecules, and thus $1 - y$ is the fractional free volume. The reduced variables in equation (9) are defined as ratios of the experimental quantities to constants characteristic of the particular fluid, $\tilde{V} \equiv V_m/V^*$, $\tilde{T} \equiv T/T^*$ and $\tilde{P} \equiv P/P^*$ where V_m is the molar volume and T^* and P^* are material constants. The quantity y must satisfy the condition

$$\left(\frac{s}{3c} \right) \left[1 + \frac{\ln(1-y)}{y} \right] = - \frac{[(y\tilde{V})^{1/3}/3 - 2^{-1/6}y]}{[(y\tilde{V})^{1/3} - 2^{-1/6}y]} - \frac{y}{6\tilde{T}} \left(\frac{2.409}{(y\tilde{V})^2} - \frac{3.033}{(y\tilde{V})^4} \right), \quad (10)$$

where $s/3c$ is the ‘flexibility ratio’, usually set equal to unity. Although the SS EOS can describe experimental $V(T, P)$ results, this requires the simultaneous solution of equations (9) and (10). To avoid this, an approximate version of the EOS can be used

$$\tilde{V} = 0.9018 \exp(23.835\tilde{T}^{3/2}) \{1 - 0.089 \ln[1 + 1.0472\tilde{P} \exp(49.22\tilde{T})]\}. \quad (11)$$

The use of the SS model to determine the free volume from $V(T, P)$ measurements leads to the counter-intuitive result that the compressibility of the occupied volume is almost as large as the free volume compressibility (Dlubek *et al* 2004b, 2005b). Using the SS model to calculate the free volume, and substituting directly into the Cohen–Turnbull equation (equation (6)) yields different curves for different experimental isobars, demonstrating limits of this free volume approach (Dlubek *et al* 2004b).

4.2.3. Dynamic lattice liquid model. The dynamic lattice liquid (DLL) model (Pakula and Teicmann 1997, Pakula 2000) is a model wherein molecules are assigned to lattice sites. This determines the presence of nearest neighbours, but not the distance between them. According to the DLL model the rates of rearrangement are thermally activated, with the activation energy barriers dependent on local density. The nature of this density dependence is assumed.

The local volume v assigned to each molecule fluctuates, but cannot be less than v_0 . With the excess volume $(v - v_0)$ distributed exponentially, the probability of local rearrangement is given by

$$p(v, T) = \exp\left(-\frac{E(v)}{kT}\right), \quad (12)$$

where k is Boltzmann’s constant. Four simple cases can be considered for $E(v)$ (Pakula 2000):

- (i) $E(v)$ is a constant, obtained from an observed Arrhenius dependence of τ_α .
- (ii) $E(v)$ changes discontinuously from infinity below a volume v_c to $E(v) = 0$ above v_c .

The relaxation time is then given as

$$\tau_\alpha = \tau_{\text{DLL}} \exp\left(\frac{v_c - v_0}{\bar{v} - v_0}\right), \quad (13)$$

where \bar{v} is the average molecular volume, analogous to the free volume (equation (6)).

- (iii) Case (ii) but E is finite below v_c and nonzero: $E = E_2$ for $v > v_c$, $E = E_1$ for $v_0 < v < v_c$. This gives

$$\tau_\alpha = \tau_{\text{DLL}} \left\{ \exp\left(\frac{-E_1}{kT}\right) \left[1 - \exp\left(\frac{v_0 - v_c}{\bar{v} - v_0}\right) \right] + \exp\left(\frac{-E_2}{kT}\right) \exp\left(\frac{v_0 - v_c}{\bar{v} - v_0}\right) \right\}, \quad (14)$$

which for $E_1 \rightarrow \infty$ becomes equivalent to the formula of Macedo and Litovitz (1965).

- (iv) E decreases linearly from E_1 to E_2 in the range v_0 to $v'_c (> v_c)$, with the relaxation time given by

$$\tau_\alpha = \tau_{\text{DLL}} \left\{ \frac{1}{1 + ((E_1 - E_2)(\bar{v} - v_0)/kT(v_0 - v'_c))} \left[\exp\left(\frac{-E_1}{kT}\right) - \exp\left(\frac{-E_2}{kT}\right) \exp\left(\frac{v_0 - v'_c}{\bar{v} - v_0}\right) + \exp\left(\frac{-E_2}{kT}\right) \exp\left(\frac{v_0 - v'_c}{v' - v_0}\right) \right] \right\}^{-1}. \quad (15)$$

The predictions of the first two cases are at odds with most experimental data. A test of the two predictions (equations (14) and (15)) was carried out by Pasterny *et al* (2004), who obtained $\tau_{\text{DLL}} \sim 10^{-49}$ s (a physically unreasonable value), and only rough agreement with experimental data.

4.2.4. Cohen and Grest. The Cohen and Grest (CG) model (Cohen and Grest 1979, 1984, Grest and Cohen 1980, 1981) considers diffusion to be dominated by the free volume. The system is considered to be dynamically heterogeneous, with solid-like and liquid-like cells coexisting. Only the latter have free volume, with molecular motion requiring some continuity of the liquid-like cells. The temperature dependence of the relaxation time is given by

$$\log(\tau_\alpha(T)) = A_{\text{CG}} + \frac{B_{\text{CG}}}{T - T_{\text{CG}} + [(T - T_{\text{CG}})^2 + C_{\text{CG}}T]^{1/2}}, \quad (16)$$

where A_{CG} , B_{CG} , C_{CG} and T_{CG} are material constants, the latter identified as the temperature at which continuity of the liquid-like cells is attained. This percolation threshold requires each liquid-like cell to be in contact with at least two other liquid-like cells. Equation (16) has four free parameters, one more than the VFTH equation (equation (2)). However, the CG equation can describe $\tau_\alpha(T)$ over a wider range of temperature, encompassing the crossover at temperatures above T_g . Two different VFTH equations are required for fitting over this range (Cohen and Grest 1979, Grest and Cohen 1981, Cummins 1996, Cummins *et al* 1997, Schneider *et al* 1999a, Paluch *et al* 2003c). In fact, the crossover temperature T_B has been shown to equal T_{CG} (Paluch *et al* 2003c).

Cohen and Grest incorporated the effect of pressure by introducing an additional term, proportional to pressure, into their expression for the local free energy (Cohen and Grest 1979, Grest and Cohen 1981). The resulting temperature and pressure dependences of the relaxation time are given by

$$\log(\tau_\alpha(T, P)) = A_{\text{CG}} + \frac{B_{\text{CG}}(1 + P/\xi_0)}{T - T_{\text{CG}}^* + [(T - T_{\text{CG}}^*)^2 + C_{\text{CG}}(1 + P/\xi_0)T]^{1/2}}, \quad (17)$$

where $T_{\text{CG}}^* = T_{\text{CG}} + (C_{\text{AG}}/4\xi_0)P$ and ξ_0 is a constant with the dimension of pressure. It has been shown that this expression fares poorly in describing experimental high-pressure data (Corezzi *et al* 2000, Paluch *et al* 2003c, Comez *et al* 2004).

4.2.5. Defect diffusion model. The defect diffusion (DD) model was developed originally by Bendler and Schlesinger (1987, 1988) to interpret ionic conduction in polymer electrolytes, and it was recently extended to include the effect of pressure (Bendler *et al* 2001a). In this model for polymer electrolytes, an ion moves when it encounters a single ‘defect’. Since the defects can be identified as regions of local free volume, the DD model is a dynamical free volume model. As temperature decreases or pressure increases, these defects cluster, reducing their number density. This accounts for decreased conductivity. The glass transition occurs when the clusters percolate; i.e. form continuous geometric pathways. For zero pressure, the defect clustering gives rise to equation (2). The model leads to Arrhenius behaviour if the defects repel each other, so that there is no clustering (Bendler *et al* 2003a).

The DD equation for the temperature and pressure dependences is (Bendler *et al* 2001a, 2003b)

$$\tau_{\alpha}(T, P) = \frac{A_{\text{DD}}}{T(1 - \delta_{\text{DD}}(T, P))^{1/\beta}} \exp \left[- \frac{B_{\text{DD}} T_{\text{DD}}}{(T - T_{\text{DD}})^{3/2} (1 - \delta_{\text{DD}}(T, P))} \right], \quad (18)$$

where A_{DD} and B_{DD} are constants, and δ_{DD} is a measure of the specific volume defined as $1 - \delta_{\text{DD}}(T, P) = V(T, P)/V(T, 0)$. Note that the critical temperature, T_{DD} , is the temperature at which single clusters cease to exist, and this always occurs below the glass transition temperature. T_{DD} is assumed to have a pressure dependence given by equation (1), or alternatively by a second-order polynomial (Bendler *et al* 2001a). In this respect, the DD model differs from the other free volume models and the theoretical approaches discussed later, which attempt to derive a theoretical justification for the pressure dependence.

The DD equation for $\tau_{\alpha}(T, P)$ has five adjustable parameters and yields good fits to conductivity, dielectric relaxation and viscosity data for materials in the vicinity of their glass transition but below the dynamic crossover (Bendler *et al* 2001a, 2001a, 2003a, 2003b, 2004).

One feature of the DD model is that it offers an interpretation of the correlation (Böhmer *et al* 1993) between the isobaric fragility, $m_P \equiv d \log(\tau)/d(T_g/T)|_{T=T_g}$, and the breadth of the dielectric relaxation function (the latter quantified by the stretch exponent, β_{KWW} , of the Kohlraush–William–Watts (KWW) relaxation function (Williams and Watts 1970). The DD prediction is $m_P = D_{\text{DD}}/\beta_{\text{KWW}}$, with D_{DD} a constant, experimentally found to equal ~ 42 (Bendler *et al* 2003a). Of course, such a strict correlation between m_P and β_{KWW} is violated by several materials (Böhmer *et al* 1993, Roland *et al* 2003b). Moreover, at high pressure, the usual situation is for the fragility to decrease without a concomitant change in the Kohlraush exponent (Paluch *et al* 2000b, 2002a, 2003, Paluch and Roland 2003, Casalini and Roland 2005a).

4.3. Entropy models

4.3.1. Avramov. Avramov (2000) introduced a model to interpret the temperature and pressure dependences of the viscosity. The starting hypothesis is that the cooperative motions underlying the glass transition are thermally activated. By calculating the average jump frequency for an assumed Poisson distribution of local energy barriers, the following relationship is obtained between η and the entropy of the system

$$\eta = \eta_{\infty} \exp \left\{ \frac{E_{\text{max}}}{\sigma_{\text{Av}}} \exp \left[- \frac{2(S - S_r)}{ZR} \right] \right\}, \quad (19)$$

where η_{∞} is the limiting viscosity at high temperature and atmospheric pressure, E_{max} is the maximum value of the activation energy and σ_{Av} the dispersion of the reference state having entropy S_r . Z , the degeneracy of the system, reflects the number of available pathways for local relaxation of a polymer segment, which depends on the short range order. So similarly to

the AG model (Adam and Gibbs 1965) discussed later, the dynamics slows down (increasing viscosity) because of a decrease of entropy. However, the Avramov model is concerned with the total entropy, whereas the relevant quantity in the AG model is the configurational entropy.

From the thermodynamic considerations, the following equation for the temperature and pressure dependences of the viscosity follows from equation (19)

$$\eta(T, P) = \eta_{\infty} \exp \left[30 \left(\frac{T_r}{T} \right)^{a_{AV}} \left(1 + \frac{P}{\Pi} \right)^{b_{AV}} \right] \quad (20)$$

with $a_{AV} = 2C_P/ZR$ and $b_{AV} = (2\alpha V_m/ZR)\Pi$. T_r is a reference temperature at which the entropy equals S_r , $\alpha_P (= V^{-1}(dV/dT)|_P)$ the isobaric thermal expansion coefficient, C_P the heat capacity at atmospheric pressure and Π a constant having the dimensions of pressure.

By defining T_g as the temperature at which $\tau_{\alpha} = 10^2$ s, from equation (20) it follows that the pressure dependence of T_g is (Paluch *et al* 2000b)

$$T_g(P) = T_r \left[\frac{30 \log(e)}{2 - \log(\tau_0)} \right]^{1/a_{AV}} \left(1 + \frac{P}{\Pi} \right)^{b_{AV}/a_{AV}}. \quad (21)$$

This expression has the same form as equation (1), the empirical relation of Andersson and Andersson (1998).

Equation (20) describes well the respective temperature and pressure dependences of the viscosity (Avramov 2000), the dielectric relaxation data (Roland and Casalini 2003a, Paluch 2001, Paluch *et al* 2000b, 2001b, 2002a, 2002d, 2002e, 2003) and light scattering data (Paluch *et al* 2003a, Patkowski *et al* 2004) below the dynamic crossover, at least for low pressures for materials in which the fragility depends at most only weakly on P . In fact, the Avramov model (equation (20)) predicts the fragility m_P to be (Paluch *et al* 2000b)

$$m_P = a_{AV}[2 - \log(e)] \quad (22)$$

and thus independent of pressure. This is contrary to many results (Paluch *et al* 2002a, 2003, Paluch and Roland 2003, Casalini and Roland 2005a), leading to a modification of the model with the introduction of an extra parameter (Paluch and Roland 2003).

Apart from the utility of the Avramov model to describe simultaneously temperature and pressure dependences, the parameters in equation (20) are related to measurable thermodynamics properties. However, at least for PVAc, the Avramov parameters obtained from fitting relaxation data differed significantly from values deduced from other properties, raising questions about the validity of the model (Roland and Casalini 2003a).

4.3.2. Adam and Gibbs. The AG model (Adam and Gibbs 1965) is probably the most widely used to interpret experimental data on the glass transition dynamics (the original paper has been cited over 2400 times till date). The model is based on the idea of cooperatively rearranging regions (CRR), which represent the minimum volume of the liquid able to relax independently of its environment (no interactions among CRR). The slowing down of the relaxation as temperature is reduced is due to an increasing size of the CRR. In turn, the size of the CRR depends on the configurational entropy S_c (i.e. to the number of available configurations). The resulting expression for the relaxation times is

$$\tau_{\alpha} = \tau_{AG} \exp \left(\frac{C_{AG} \Delta\mu}{T S_c} \right), \quad (23)$$

where C_{AG} is a constant, $\Delta\mu$ is the free energy barrier (per molecule) to rearrangement. S_c is defined as the entropy of the liquid minus the vibrational contribution, $S_c = S_{liq} - S_{vib}$. However, since S_{vib} cannot be measured experimentally, it is commonly assumed to be equal

to the entropy of the crystal, $S_{\text{vib}} \sim S_{\text{cryst}}$ (Adam and Gibbs 1965, Richert and Angell 1998), so that $S_{\text{c}} \sim S_{\text{exc}}$ with S_{exc} the excess entropy. At atmospheric pressure, the temperature dependence of τ_{α} is obtained by calculating the configurational entropy using

$$S_{\text{c}}(T) = \int_{T_{\text{K}}}^T \frac{\Delta C_P}{T'} dT'. \quad (24)$$

T_{K} is the temperature at which S_{c} is zero at atmospheric pressure and ΔC_P is the excess heat capacity of the melt with respect to the crystal. The integral in equation (24) can be approximated by $(S_{\infty} - a_{\text{AG}}/T)$, where S_{∞} is the configurational entropy in the limit of high temperature and a_{AG} is a constant. Thus, calculating $S_{\text{c}}(T)$ from equation (24), equation (23) at atmospheric pressure yields the empirical VFTH equation (identifying with $T_{\text{K}} = T_0$), for temperatures up to the crossover temperature T_{B} (Richert and Angell 1998). A better assumption than $S_{\text{c}} \sim S_{\text{exc}}$ is $S_{\text{c}} \sim 0.7S_{\text{exc}}$, as shown by measurements and simulations for atmospheric pressure (Scala *et al* 2000, Sastry 2001, Angell and Borick 2002, Martinez and Angell 2002).

An increase of pressure, similarly to a decrease of temperature, reduces the configurational entropy and, according to equation (23), slows down the α -relaxation. An extension of the AG model for elevated P assumes $S_{\text{c}} = S_{\text{exc}}$, and calculates $S_{\text{c}}(T, P)$ using the Maxwell relation $\partial S/\partial P = -\partial V/\partial T$ (Casalini *et al* 2001a)

$$S_{\text{c}}(T, P) = \int_{T_{\text{K}}}^T \frac{\Delta C_P}{T'} dT' - \int_{P_{\text{atm}}}^P \Delta \left(\frac{\partial V}{\partial T} \right)_{P'} dP', \quad (25)$$

where $\Delta(\partial V/\partial T)_P$ is the excess expansivity of the melt with respect to the crystal. The predicted pressure behaviour is in reasonable agreement with experimental results for both polymers (Casalini *et al* 2001b, 2002a) and molecular glass formers (Casalini *et al* 2002b Paluch *et al* 2002f). However, a strict test of equation (25) is limited by the availability of values of C_P and the thermal expansivity for both the crystal and the melt. One approach is to determine the integral (equation (24)) from a VFTH fit to atmospheric pressure data, and estimate the a_{AG} from the excess heat capacity of the melt over that of the glass (Casalini *et al* 2002a, 2002b). Interestingly, similar to results for atmospheric pressure (Richert and Angell 1998), the AG model extended to high pressure does not describe the data for relaxation times shorter than the crossover relaxation time observed at atmospheric pressure at T_{B} (Casalini *et al* 2002a, 2003b).

Alternatively, the proportionality between S_{c} and S_{exc} can be taken to differ for isobaric versus isothermal conditions, which yields for the configurational entropy (Prevosto *et al* 2003, Comez *et al* 2004)

$$S_{\text{c}}(T, P) = g_T(P_{\text{atm}}) \int_{T_{\text{K}}}^T \frac{\Delta C_P}{T'} dT' - f_P(T) \int_{P_{\text{atm}}}^P \Delta \left(\frac{\partial V}{\partial T} \right)_{P'} dP', \quad (26)$$

where $g_T(P)$ and $f_P(T)$ are respective functions of P and T . For molecular glass formers, the available data suggest that $g_T(P_{\text{atm}})/f_P(T) \sim 0.7$ (Prevosto *et al* 2003, Comez *et al* 2004, Roland *et al* 2004a). Substituting equation (26) into equation (23) gives

$$\tau_{\alpha}(T, P) = \tau_{\text{AG}} \exp \left(\frac{D_{\text{AG}} T_{\text{K}}^*(T, P)}{T - T_{\text{K}}^*(T, P)} \right). \quad (27)$$

In this equation, the characteristic temperature, T_{K}^* , is defined as

$$T_{\text{K}}^*(T, P) = \frac{T_{\text{K}}}{1 - (f_P(T)/g_T(P_{\text{atm}})S_{\infty}) \int_0^P \Delta(\partial V/\partial T)_{P'} dP'}, \quad (28)$$

where $D_{AG} = C_{AG} \Delta\mu / [g_T(P_{atm})a]$ and T_K is the diverging temperature at atmospheric pressure (equation (20)). Simulations indicate a negligible variation of C_{AG} with pressure for density changes of up to 20% (Scala *et al* 2000, Sastry 2001); in typical experiments the density varies by less than 10%. In calculating the integral in equation (28), the pressure dependence of $(\partial V / \partial T)^{cryst}$ is negligible with respect to $(\partial V / \partial T)^{melt}$ for P as large as hundreds of megapascals (Naoki *et al* 1987, Van Krevelen 1997, Theobald *et al* 2001), so that it can be taken to be constant. The pressure dependence of the parameter D_{AG} is also usually taken as constant, which is satisfactory for small pressures.

In the limit of zero pressure equation (27) is reduced to the VFTH function (equation (2)). This VFTH behaviour for isobaric measurements will be maintained as long as the temperature dependence of T_K^* is negligible. Moreover, the isothermal behaviour of equation (27) for small pressures reduces to a VFTH-like equation for the pressure dependence of the α -relaxation (equation (5)), although it clearly deviates at high pressure.

Since the quantity $\Delta(\partial V / \partial T)_P$, can be measured independently, the only free parameter, beyond those necessary to describe the data at atmospheric pressure, is the function f_P . However, f_P is found to be unity, within the limits of the experimental error (Prevosto *et al* 2003, Comez *et al* 2004). If the temperature dependence of T_K^* is negligible over the range of interest, then defining the glass transition such as $\tau_\alpha(T = T_g, P) = 10^2$ s, it follows that the T_g is proportional to T_K^* ; therefore,

$$T_g(P) \simeq T_K^*(P) \left(\frac{D_{AG} \log(e) + 2 - \log(\tau_0)}{2 - \log(\tau_0)} \right), \quad (29)$$

which describes a nonlinear dependence on P .

In the limit of low pressure, the steepness index at the glass transition is given by

$$m_P = \log(e) \frac{D_{AG}(T_K^*(T, P)/T_g(P))}{(1 - (T_K^*(T, P)/T_g(P)))^2}, \quad (30)$$

which is independent of P only if the temperature dependence of T_K^* is negligible over the relevant range of T and P . This requires that the function f_P and the excess expansivity are both independent of temperature, which is not true for the latter at least.

Johari (2003) has criticized the extended AG model (equations (25)–(29)) for its neglect of any pressure dependences of $\Delta\mu$ and the crystal thermal expansivity. These effects are expected to be small and could, in principle, be accommodated through the introduction of additional parameters. The AG model also assumes exponential relaxation of identical CRRs, whereas stretched exponential behaviour is invariably observed (Angell *et al* 2000). Other aspects of the AG model have been debated (see, e.g. Ngai (1999a), Goldstein (2005) and Prevosto *et al* (2005)).

5. Pressure dependence of the structure factor

A useful measure of the short range order of a liquid is the pair distribution function $g(r)$, which for a monatomic species gives the probability of finding two atoms separated by a distance r . The quantity $4\pi r g(r) r^2 dr$ is thus the mean number of atoms inside a spherical shell, of radius r and thickness dr , around a given atom. The pair distribution is related to the liquid static structure factor $S(Q)$ by

$$S(Q) = 1 + \rho \int [g(r) - 1] e^{iQ \cdot r} dr. \quad (31)$$

For a completely disordered system, $S(Q) = 1$ (corresponding to $g(r) = 1$), which is the asymptotic value of $S(Q)$ for large Q , given the absence of long-range order in a liquid.

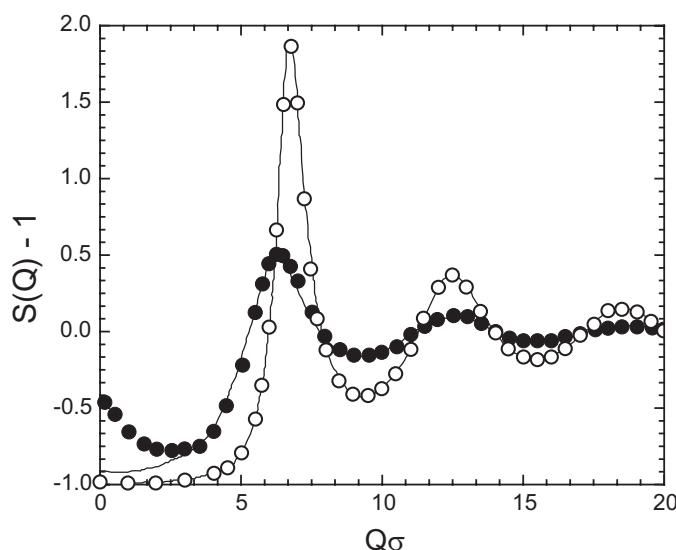


Figure 12. Static structure factor for a fluid having only the repulsive interactions of a LJ potential in an expanded state at high temperature (●) and as dense cold fluid (○), along with simulation data for the complete LJ potential including attractive interaction (—). Data from Chandler and Weeks (1970).

The structure factor is directly determined by neutron or x-ray scattering experiments, with $g(r)$ obtained by Fourier inversion of the equation (31). For systems more complex than monatomic, partial scattering functions have to be considered. The main feature of the structure factor for a monatomic liquid (figure 12) is a prominent peak, reflecting the range of first-neighbour distances. The short-range order (amorphous halo) may be enhanced by lower temperature, as reflected in a steeper and narrower peak $S(Q)$. The peak also shifts to larger Q (closer packing) with decreasing T or increasing pressure (Alba-Simionseco *et al* 1998).

The structure factor also depends on the interactions among atoms. For example, for a LJ liquid (figure 12), simulations reveal (Chandler and Weeks 1970) that the main features of $S(Q)$ depend on the repulsive part of the potential, but not on the attractive part (which in any case is neglected in many simulations (Bernu *et al* 1987, Roux *et al* 1989, Nauroth and Kob 1997)).

Experimental results for the $S(Q)$ of OTP under high pressure were reported by Tölle (2001). By comparing the static structure factor measured under isothermal, isobaric, isochoric and isochronic (constant τ) conditions (figure 13), Tölle observed that for constant T or P ' $S(Q)$ evolves continuously, it is nearly identical along an isochore and an isochron'. However, these results do not appear to be general, as shown by Frick and co-workers (Frick *et al* 2003, Calliaux *et al* 2003), who measured $S(Q)$ for 1,4-polybutadiene (PB) (figure 14). The interesting result is their finding that significant changes in $S(Q)$ being observed for isochronic conditions. These experiments extended to higher pressures (4 GPa) than the OTP measurements; however, even over an equivalent pressure range, the dynamic structure factor of PB appears to be more sensitive to pressure than is the case for OTP (see figure 2 in Calliaux *et al* (2003) and figure 31 in Tölle (2001)). At very high pressure, the first peak in $S(Q)$ for PB becomes much weaker, indicating a substantial decrease in the short-range order.

The pressure dependence of $S(Q)$ is particularly important for evaluating mode coupling theory (MCT). According to MCT, the structure factor governs the dynamics, implying that

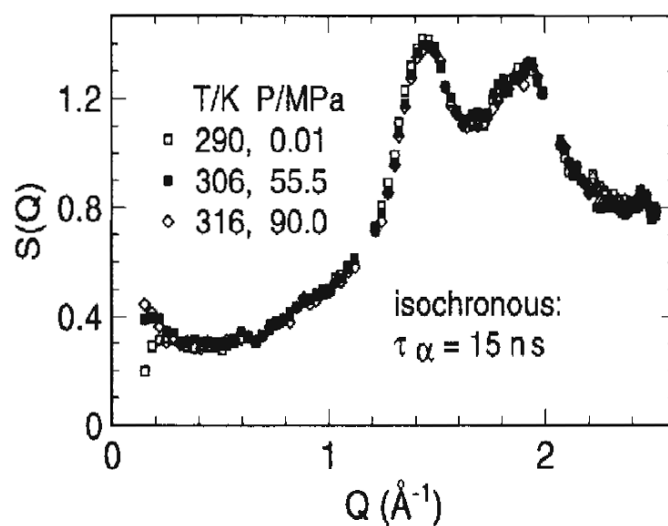


Figure 13. Static structure factor for *o*-terphenyl under isochronic conditions (reproduced from Tölle (2001)).

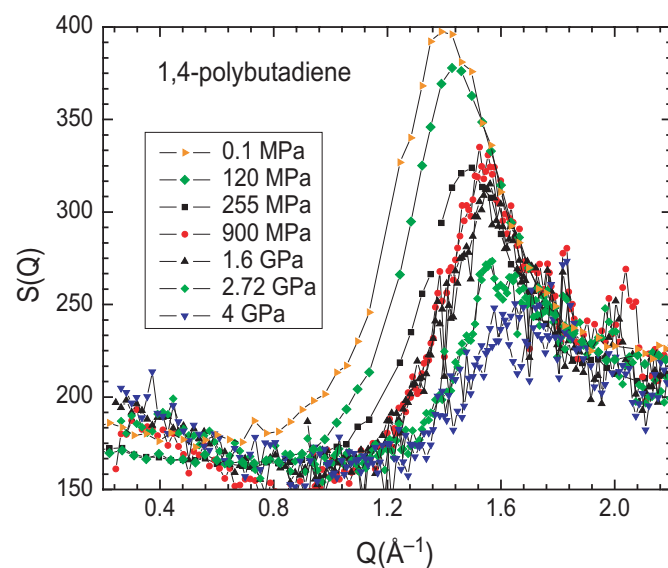


Figure 14. Static structure factor for 1,4-polybutadiene at 295 K and various pressures. Data from Calliaux *et al* (2003).

$S(Q)$ should be the same for conditions of constant τ_α . This prediction is verified for OTP but not for PB. However, there are significant differences in the character of the dynamics of these two materials. As discussed later (section 6), temperature tends to be the dominant variable controlling the relaxation behaviour of polymers, such as PB. On the other hand, for OTP, density exerts an influence as strong as that from thermal energy; the two effects are equally important in determining the variation of τ_α with T . This distinction between

polymers and small molecules arises from the insensitivity to pressure of the intramolecular bonds (which are profuse for polymers). Although the dynamics in PB is dominated primarily by temperature, $S(Q)$ is strongly affected by pressure, and therefore by volume changes alone. Again, this reflects the importance of intramolecular interactions, which are relatively unaffected by pressure.

6. Quantifying the volume and temperature dependences

The extreme complexity of condensed matter precludes analysis of relaxation data in terms of the mutual interactions of molecules, at least without simplifying assumptions. Computer simulations are carried out at fixed volume (constant ρ (see, e.g. Sastry *et al* (1998), Sastry (2001), Debenedetti and Stillinger (2001) and Middleton and Wales (2001)), with a few exceptions (Middleton and Wales 2002, Mukherjee *et al* 2002). Simulations of the glass transition usually employ the LJ potential (Grabow and Andersen 1986, Jonsson and Andersen 1988, Dasgupta *et al* 1991, Dasgupta and Ramaswamy 1992, Lewis and Wahnström 1994, Kob and Andersen 1995, Shumway *et al* 1995, Fujiwara and Yonezawa 1996, Nauroth and Kob 1997, Mueser *et al* 1998, Sastry *et al* 1998, Kob *et al* 2000, Li 2000, Sastry 2001, Vollmayr-Lee *et al* 2002, Sampoli *et al* 2003, Vollmayr-Lee 2004), which takes into account only two-body interactions. In generalized form, the LJ potential energy is

$$U(r) = 4\varepsilon \left[\left(\frac{\sigma}{r} \right)^{3\gamma} - \left(\frac{\sigma}{r} \right)^{3\gamma/2} \right], \quad (32)$$

where r is the molecular separation, and ε , a microscopic energy and σ , a molecular size, are constants. The parameter γ accounts for the ‘softness’ of the LJ interaction; commonly, $\gamma = 4$. The LJ potential describes strong, short-ranged repulsive forces and weaker, longer-ranged attractions. The force on any molecule is the vector sum of the contributions, $-dU(r)/dr$, from all other molecules. In condensed matter, each molecule (or polymer segment) has many neighbours, implying that the attractive forces tend to cancel locally (Widom 1999). This leads to the classic van der Waals model for liquids, in which the arrangement of molecules (liquid structure) is governed by steric effects and local packing, with the attractions manifested as a uniform background pressure (Widom 1967, Chandler *et al* 1983, Stillinger *et al* 2001). This idea is consistent with the static structure factor being sensitive only to the repulsive part of the potential (Weeks *et al* 1971, Hansen and McDonald 1986, Tölle *et al* 1998) (see section 5). Although the local structure is not substantially affected by the nature of the attractive potential, the attractions are important for thermodynamic properties, such as the EOS.

Emphasis on the role of the short-range repulsive interactions in governing the local structure in non-associated liquids leads to a generalized repulsive potential, the inverse power-law, $U(r) \propto r^{-3\gamma}$ (Hoover and Ross 1971, March and Tosi 2003).

$$U(r) = 4\varepsilon \left(\frac{\sigma}{r} \right)^{3\gamma}. \quad (33)$$

This purely repulsive potential (with a mean field attraction) has been utilized in recent simulation studies to investigate the local dynamics of the glass transition (Debenedetti *et al* 1999, Shell *et al* 2003, De Michele *et al* 2004). Whether the supercooled dynamics, with cooperative length scales extending a few nanometres (Rizos and Ngai 1999, Tracht *et al* 1999, Hempel *et al* 2000, Donth *et al* 2001, Reinsberg *et al* 2001, Schroeder and Roland 2002, Ellison *et al* 2005) can be regarded as local is an open question. The cohesive energy density, which is directly connected to the attractive potential, plays a role in the activated barrier hopping as described by energy landscape models.

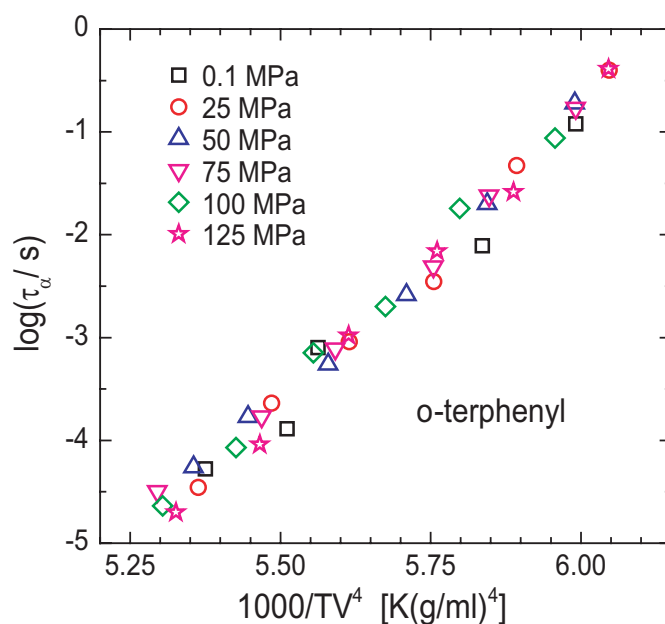


Figure 15. Relaxation times measured by dynamic light scattering for OTP plotted versus the inverse of the product of the temperature times the specific volume, with the latter raised to the 4th power. Data from Dreyfus *et al* (2004).

Nevertheless, for *o*-terphenyl, the dynamic structure factor (the transform of the van Hove correlation function (Lovesey 1984)) is invariant when measured over a series of temperatures and pressures, subject to the condition that the quantity TV^4 remains constant (Tölle *et al* 1998, Tölle 2001). Similarly, Dreyfus *et al* (2003, 2004) were able to superimpose dynamic light scattering relaxation times for OTP, measured at various T and P , by plotting as a function of ρ^4/T (figure 15). The same coefficient, $\gamma = 4$, has also been determined from superposition of viscosity data for OTP (Tarjus *et al* 2004a).

Such results are consistent with the accuracy of the LJ 6–12 potential for OTP (Lewis and Wahnström 1994, Roland *et al* 1995, Tölle *et al* 1998), notwithstanding the rather complex structure of the molecule. Expanding on the idea that for local properties the repulsive forces are paramount, this approach was generalized (Casalini and Roland 2004b, Roland *et al* 2004a). Treating the exponent γ in equation (33) as a material-specific constant, relaxation times for various molecular (figure 16) and polymeric (figure 17) glass-formers can be expressed as a unique function of ρ^γ/T . The data in these figures span a broad range of temperatures and pressures, yet a single material constant allows construction of master curves.

Similar superpositioning of relaxation times measured by light scattering on different materials was reported by Dreyfus (Dreyfus *et al* 2004). In table 2, we compare the results for a large number of glass-formers. The agreement between the different experiments is quite good, with the exponent varying in the range $0.1 < \gamma < 9$.

Note that the scaling method extends to non-spherical molecules, and even some hydrogen-bonded liquids (e.g. glycerol and sorbitol), for which a power-law repulsive potential is clearly inadequate. Nevertheless, the non-Arrhenius nature of relaxation times in the supercooled regime, along with the variation in τ_α with isothermal pressure changes, demonstrates unequivocally that there are two relevant control parameters governing the dynamics: temperature and density. An interpretation of the scaling in figures 15–17 is that local

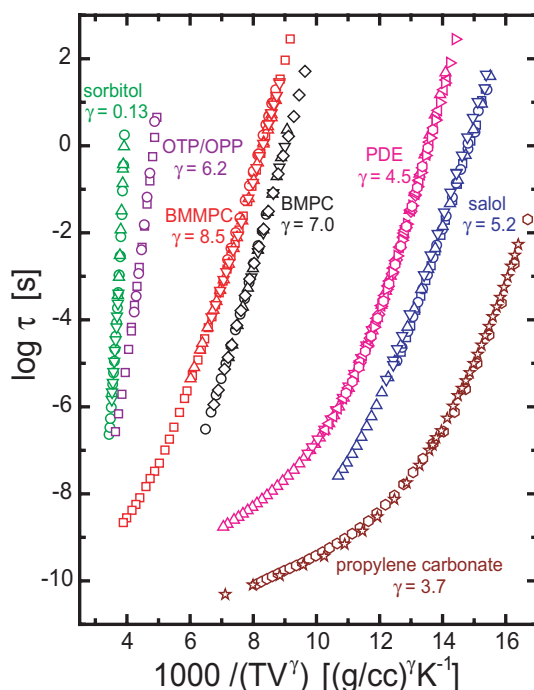


Figure 16. Dielectric α -relaxation times of molecular liquids as a function of the reciprocal of temperature times the specific volume, with the latter raised to the indicated power of γ (Roland and Casalini 2004, Casalini and Roland 2004b).

motion reflects activated transport over free energy barriers, whose height is density (pressure) dependent (Macedo and Litovitz 1965, Li and Keyes 1999, Pakula 2000, Alba-Simionesco *et al* 2002, Solunov 2002)

$$\tau = \tau_0 \exp \left[\frac{E_a(\rho)}{RT} \right]. \quad (34)$$

Explicit functional forms for τ_α , incorporating the empirical fact that $E_a(\rho) \propto \rho^\gamma$, have been proposed (Tölle 2001, Dreyfus *et al* 2004, Tarjus *et al* 2004a). Note that normalizing temperature by ρ^γ makes the behaviour in figures 15–17 almost Arrhenius over most of the range of the data. This suggests that the non-Arrhenius behaviour of isobaric data reflects the influence of density on the energy landscape.

Notwithstanding the success of the superpositioning, justification of the method based on a connection to the intermolecular potential is tenuous. For small values of $\gamma (<3)$, there is a breakdown of the underlying assumption that the repulsive interactions are sufficiently short-range in comparison with the attractions (so that the latter can be ignored for local processes). This scaling approach cannot necessarily be extended to other properties. Certainly the EOS, which always depends on the attractive part of the potential, requires inclusion of the attractive potential; thus, *PVT* data cannot be represented as a function of ρ^γ/T . Nevertheless, as a merely phenomenological means to superpose relaxation times, the method has substantial utility, as described later.

Alternative forms of the density dependence of the activation energy have been proposed (Alba-Simionesco *et al* 2002, Tarjus *et al* 2004a). For example, the scaling variable, $\rho - \rho^*$, where ρ^* is a material constant, has been shown to yield good superpositioning of Arrhenius

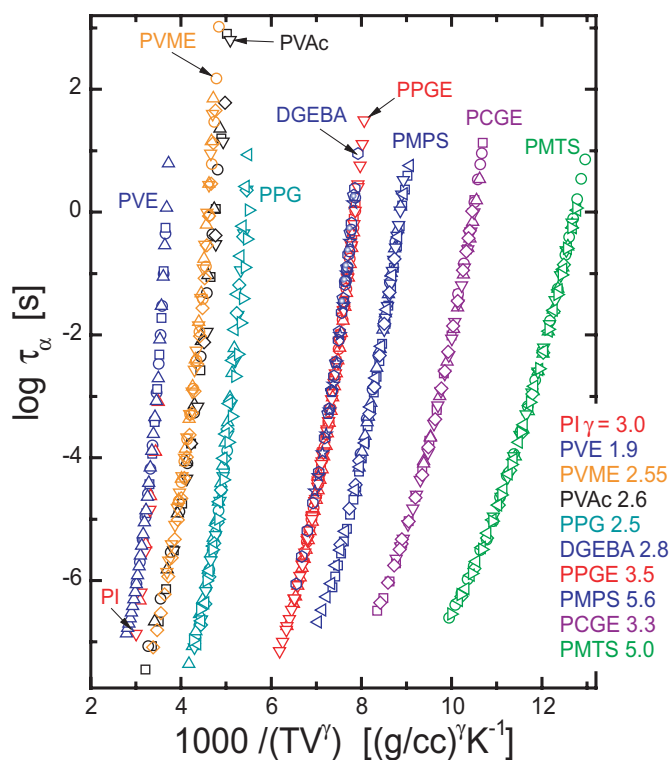


Figure 17. Dielectric α -relaxation times of polymers as a function of the reciprocal of temperature times the specific volume, with the latter raised to the indicated power of γ (Roland and Casalini 2004, Casalini and Roland 2004d).

plots of relaxation times and viscosities, over most of the range of published data (Alba-Simionseco *et al* 2004, Tarjus *et al* 2004b); this is illustrated in figures 18 and 19. However, over larger ranges of T and ρ , or for larger values of γ this linear approximation breaks down (figures 20 and 21).

Since the parameter γ captures the effect of density on $\tau(T, P)$, it must be related to other measures of how T and V govern the relaxation times. These relaxation times are a function of TV^γ , and taking the derivatives of this (unspecified) function, we can obtain an expression for the quantity E_V/E_P . E_V is the activation enthalpy at constant volume ($E_V(T, V) = R(\partial \ln \tau_\alpha / \partial T^{-1})|_V$) and E_P the activation enthalpy for constant pressure ($E_P(T, V) = R(\partial \ln \tau_\alpha / \partial T^{-1})|_P$). This ratio characterizes the relative effects of density and temperature on the variation of τ with temperature (Jobling and Lawrence 1951, Mac Kenzie 1958, Hoffman *et al* 1966, Williams 1997). The result is (Casalini and Roland 2004b)

$$\frac{E_V}{E_P} = \frac{1}{1 + \alpha_P T \gamma}. \quad (35)$$

In figure 22, data for E_V/E_P at $T \sim T_g$ are plotted versus γ for 20 glass-formers; the fit of equation (34) yields $\alpha_P T_g = 0.182 \pm 0.009$. The approximate constancy of this product for polymers is known as the empirical Boyer–Spencer rule, $\alpha_P T_g = 0.2$, or the Bondi rule, $\alpha_P T_g = 0.16$ (Boyer and Spencer 1944, Van Krevelen 1990). It should be emphasized that the derivation of equation (35) from the scaling of the relaxation times does not rely on or show that $\alpha_P T_g$ is roughly constant; this is only an empirical observation.

Table 2. Relaxation parameters (for $\tau = 1$ s).

Material	T_g (K)	E_V/E_P	γ	dm/dP (GPa $^{-1}$)	Reference
<i>o</i> -terphenyl	244	0.55			Naoki <i>et al</i> 1987
			4		Dreyfus <i>et al</i> 2003
			4		Tarjus <i>et al</i> 2004a
			4		Tölle 2001
Diglycidylether of bisphenol A	335	0.6	2.8	≈ 0	Paluch <i>et al</i> 2003c
			3.6		Dreyfus <i>et al</i> 2004
KDE	313	0.49			Paluch <i>et al</i> 2002b
			4.5	-17	Casalini and Roland 2005a
			4.8		Dreyfus <i>et al</i> 2004
Phenylphthalein-dimethylether (PDE)	249	0.53		≈ 0	Paluch <i>et al</i> 2002f
					Patkowski <i>et al</i> 2002
			4.5	-30	Casalini and Roland 2005a
			4.4		Dreyfus <i>et al</i> 2004
Propylene carbonate	159	0.64	3.7		Roland <i>et al</i> 2003b
				-18	Pawlus <i>et al</i> 2004
				-18	Casalini and Roland 2005a
Isopentylcyanobiphenyl	221			-17	Drozd-Rzoska <i>et al</i> 2005
PCB62	274	0.38	8.5	-45	Casalini and Roland 2005a
PCB54	252	0.50	6.7		Roland and Casalini 2005
PCB42	225	0.56	5.5		Roland and Casalini 2005
Salol	220	0.43	5.2		Casalini <i>et al</i> 2003a
				-11	Casalini and Roland 2005a
Glycerol	188	0.94			Ferrer <i>et al</i> 1998
			1.8		Dreyfus <i>et al</i> 2004
				+35	Paluch <i>et al</i> 2002c
				+40	O'Reilly 1962
Sorbitol	273	0.87			Hensel-Bielowka <i>et al</i> 2002
			0.13		Casalini and Roland 2004b
BMMPC	263	0.41			Paluch <i>et al</i> 2003b
			8.5	-23	Casalini and Roland 2005a
			7.5		Dreyfus <i>et al</i> 2004
BMPC	243	0.39			Paluch <i>et al</i> 2003b
			7		Casalini and Roland 2004b
			6.4		Dreyfus <i>et al</i> 2004
				-25	Gapinski <i>et al</i> 2002
Polystyrene	373	0.64			Roland and Casalini 2003b
				-160	Huang <i>et al</i> 2002
Polyvinylacetate	311	0.6	2.6	≈ 0	Roland and Casalini 2003a
			1.4		Alba-Simionescu <i>et al</i> 2004
				0	Huang <i>et al</i> 2002
Poly(2-vinylpyridine)	337	0.72			Papadopoulos <i>et al</i> 2004
Polymethyltolylsiloxane	261	0.55	5.0	-27	Paluch <i>et al</i> 2002b
	250	0.59			Mpoukouvalas and Floudas 2003
Poly(phenol glycidyl ether) -co-formaldehyde	258	0.63		≈ 0	Paluch <i>et al</i> 2000b
			3.5		Casalini and Roland 2004d

Table 2. (Continued.)

Material	T_g (K)	E_V/E_P	γ	dm/dP (GPa ⁻¹)	Reference
1,2-polybutadiene	253	0.70			Roland <i>et al</i> 2003a
			1.9	-35	Casalini and Roland 2005a
Polybutadiene (55% 1,2-45% 1,4-copolymer)				0	Huang <i>et al</i> 2002
1,4-polybutadiene			1.8		Alba-Simionseco <i>et al</i> 2004
Polyvinylmethylether	251	0.69	2.5	-4	Casalini and Roland 2003a
			2.7		Alba-Simionseco <i>et al</i> 2004
Polyvinylethylether	241	0.81			Mpoukouvalas <i>et al</i> 2005
Polymethylphenylsiloxane	246	0.52	5.6	≈ 0	Paluch <i>et al</i> 2002a
Polypropylene oxide	198	0.55*			Williams 1965
Polyepichlorhydrin			2.7		Alba-Simionseco <i>et al</i> 2004
Polypropylene glycol	202			>0	Andersson and Andersson 1998
		0.67	2.5		Roland <i>et al</i> 2004d
Polymethylacrylate	276	0.78*		-180	Williams 1964b
					Huang <i>et al</i> 2002
Polymethylmethacrylate			1.25		Alba-Simionseco <i>et al</i> 2004
1,4-polyisoprene	250	0.76	3.0		Roland <i>et al</i> 2004d
		0.96			Floudas and Reisinger 1999
Polyethylacrylate				0, -140	Huang <i>et al</i> 2002
Polyvinylchloride				-520	Huang <i>et al</i> 2002
Poly[(<i>o</i> -cresyl glycidyl ether) -co-formaldehyde]	285	0.65			Roland <i>et al</i> 2004
			3.3		Casalini and Roland 2004d

The activation enthalpy ratio can be calculated from various thermodynamic quantities. For example, it can be related to the isobaric activation energy and isothermal activation volume using (Dreyfus *et al* 2003)

$$\frac{E_V}{E_P} = \frac{(\partial\rho/\partial T)_P(\partial \ln \tau/\partial P)_T}{(\partial\rho/\partial P)_T(\partial \ln \tau/\partial T)_P}. \quad (36)$$

Or, as shown by Naoki *et al* (1987), the ratio

$$\frac{E_V}{E_P} = 1 - \left(\frac{\partial P}{\partial T}\right)_V \left(\frac{\partial T}{\partial P}\right)_\tau, \quad (37)$$

where the thermal pressure coefficient, $(\partial P/\partial T)_V$ is the ratio of the thermal expansion coefficient and the bulk compressibility, and $(\partial T/\partial P)_\tau$ is just the pressure coefficient of T_g . Comparing equations (35) and (37), we obtain

$$\gamma = T_g^{-1} \left[\frac{\beta}{dT_g/dP} - \alpha \right]^{-1}. \quad (38)$$

Thus, the exponent characterizing an important aspect of the dynamics can be calculated from EOS data alone, without recourse to actual relaxation measurements. The enthalpy ratio can also be expressed in terms of the isobaric, $\alpha_P = -\rho^{-1}(\partial\rho/\partial T)_P$, and isochronic, $\alpha_\tau = -\rho^{-1}(\partial\rho/\partial T)_\tau$ thermal expansivities (Casalini and Roland 2003a)

$$\frac{E_V}{E_P} = \frac{1}{1 - \alpha_P/\alpha_\tau}. \quad (39)$$

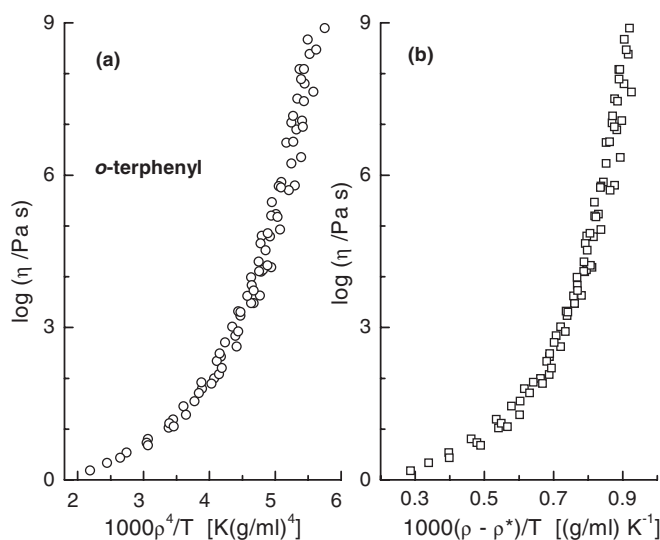


Figure 18. Viscosity of OTP measured at various temperatures as a function of pressures and plotted versus (a) the density raised to the 4th power divided by temperature (Dreyfus *et al* 2004); (b) the density minus a reference density equal to 0.86 g ml^{-1} (Tarjus *et al* 2004b). The two methods yield equivalent superpositioning of the data.

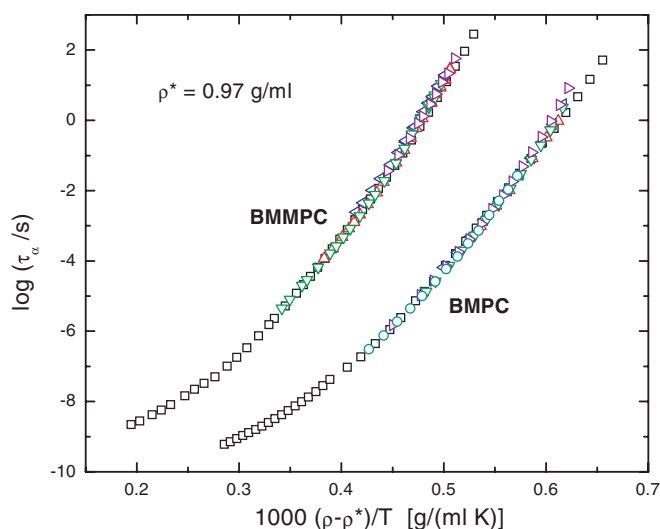


Figure 19. Master curves of the dielectric relaxation times of the molecular liquids BMPC and BMMPC, for a common reference density of 0.97 g ml^{-1} . These same data are equally well superposed using a power law, although the exponents are different: $\gamma = 7.0$ for BMPC and $= 8.5$ for BMMPC (see figure 16). Data from Roland and Casalini (2004).

The quantity $|\alpha_\tau|/\alpha_P$ is another common measure of the relative contributions of volume and thermal energy to the T -dependence of τ_α (Ferrer *et al* 1998, Roland and Casalini 2004a, Tarjus *et al* 2004a, 2004b). Both ratios are decreasing functions of temperature (Dreyfus *et al* 2003, Papadopoulos *et al* 2004), but the usual practice is to calculate E_V/E_P (or α_τ/α_P) for a constant value of the relaxation time near T_g ; e.g. $1 \leq \tau_\alpha \text{ (s)} \leq 100$.

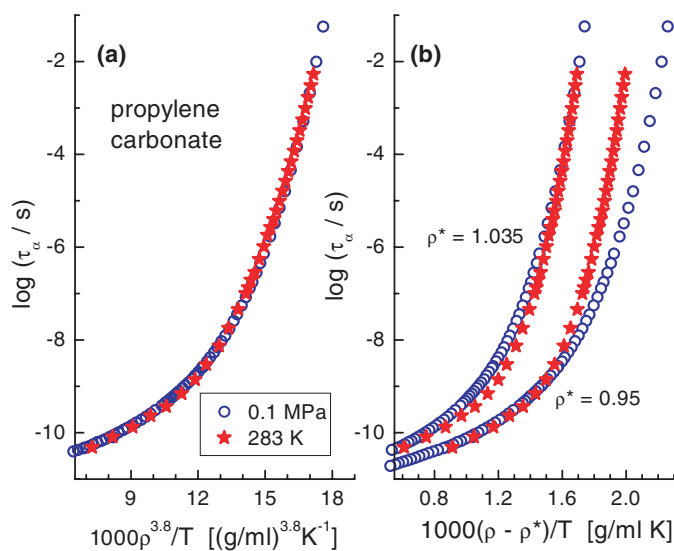


Figure 20. Dielectric relaxation times for propylene carbonate plotted versus (a) density raised to the power of 3.8 divided by temperature and (b) density minus a reference density divided by temperature. For the latter, two values of ρ^* are shown, illustrating that superpositioning cannot be achieved. Data from Roland and Casalini (2004).

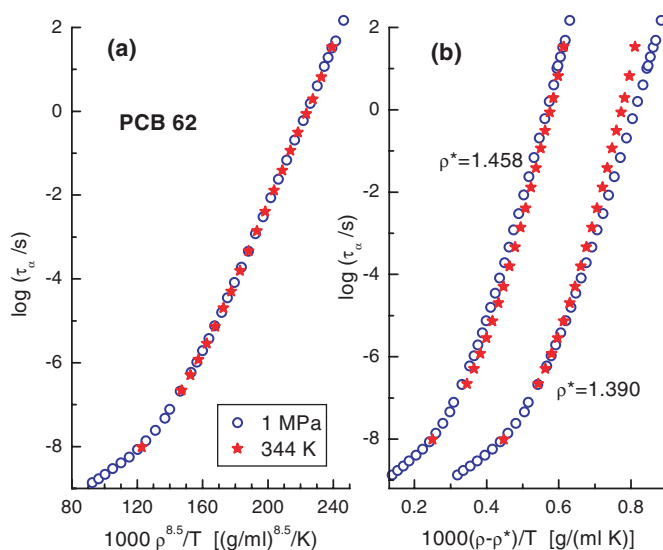


Figure 21. Dielectric relaxation times for a polychlorinated biphenyl (62% chlorine) plotted versus (a) density raised to the power of 8.5 divided by temperature and (b) density minus a reference density divided by temperature. For the latter, two values of ρ^* are shown, illustrating that superpositioning cannot be achieved. Data are from Roland and Casalini (2005).

Inspection of table 2 reveals that for most liquids and polymers, density and temperature both exert a significant influence on the relaxation times. For polymers, density has less influence than for molecular glass-formers. This is ironic, given the historic prominence of free volume theories in the study of polymer dynamics. The relatively weak influence

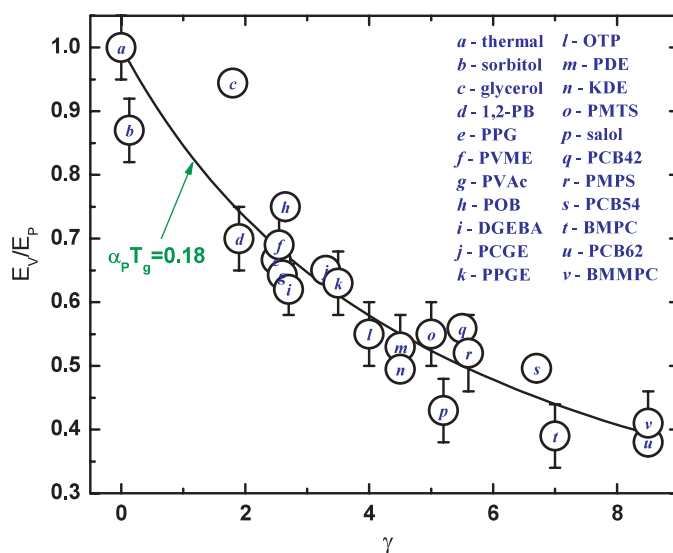


Figure 22. Ratio of isochoric and isobaric activation enthalpies versus the value of the exponent yielding superposition of $\tau_\alpha(T, P)$. Regression of equation (35) yields the indicated product of the thermal expansion coefficient and glass transition temperature (Casalini and Roland 2004d).

of volume arises from the fact that for polymers, two neighbouring segments are always covalently bonded. Interactions between directly bonded segments are only weakly sensitive to pressure, since it is difficult to change chemical bond lengths. Note that the end-to-end distance of a polymer chain is invariant to pressure. This confers a near pressure-independence of the normal mode dielectric strength (Roland *et al* 2003c, Casalini and Roland 2005b).

It is only for associated liquids (strong H-bonding) that temperature becomes the dominant control variable. Thermal energy reduces the degree of H-bonding, enhancing the direct effect temperature has on the relaxation times. On the other hand, higher pressure sometimes reduces hydrogen bonding (Naoki and Katahira 1991, Cook *et al* 1992, Poole *et al* 1994), since a smaller volume makes directional interactions more difficult. This serves to enhance molecular mobility, countervailing the direct effect of pressure on τ . The consequences may be twofold: structural relaxation in associated liquids is less sensitive to pressure (smaller activation volumes and smaller dT_g/dP), and the magnitude of τ in the supercooled regime is governed primarily by temperature. This dichotomy between normal and associated liquids was first pointed out by MacKenzie (1958), from an analysis of viscosity data on molecular liquids.

A popular scheme to classify the temperature-dependences of relaxation times (or viscosities), in particular quantifying the degree of departure from Arrhenius behaviour, is via a T_g -normalized Arrhenius plot. Such plots were first published by Oldekop (1957), showing viscosity data for ten inorganic glass-formers. Subsequently, Laughlin and Uhlmann (1972) reported a near correspondence of T_g -normalized Arrhenius plots of the viscosities of four organic liquids, along with similar results for seven inorganic oxide liquids. This classification scheme has been developed in detail by Angell (1991, 1995), who coined the term ‘fragility plot’, in allusion to the change in short or intermediate range order (local liquid structure) associated with heating through the supercooled regime. In this parlance, strong glass-formers are those having a weak (or more nearly Arrhenius) dependence of

τ_α (or η) on T_g/T , while for fragile liquids, τ_α and η depend strongly on the normalized temperature variable. Much of the interest in fragility arises from the possibility of identifying general principles which underlie the supercooled dynamics, by drawing correlations between fragility and other dynamic and thermodynamic properties. The isobaric fragility, defined as $m_P \equiv d \log \tau(T_g)/d(T_g/T)|_P$, has been shown to correlate with: (i) the breadth of the relaxation function (Böhmer *et al* 1993, Roland *et al* 2003b); (ii) the magnitude of the Debye–Waller factor (Roland and Ngai 1996); (iii) the T -dependence of the configurational entropy (Ito *et al* 1999); (iv) the liquid shear modulus (Dyre and Olsen 2004) or its value relative to the bulk modulus (Novikov and Sokolov 2004); (v) vibrational properties of the glass (Scopigno *et al* 2003); and (vi) the form of the interaction potential (Speedy 1999, Sastry 2001, Bordat *et al* 2004).

Although fragility is usually measured at constant (atmospheric) pressure, an interesting issue is the effect of pressure. For experimental reasons, relaxation times at elevated pressure are commonly measured as isotherms (versus P at constant T). This directly yields the activation volume (equation (3)) and the pressure coefficient of the glass transition temperature. The fragility can then be calculated using (Paluch *et al* 2001a)

$$m_P = \frac{\log(e)\Delta V^\#}{R(dT_g/dP)}. \quad (40)$$

An alternative is to take advantage of the fact that the relaxation times depend only on TV^γ , and calculate $\tau_\alpha(T)$ for any fixed P using ambient pressure measurements of $\tau_\alpha(T)$ together with the experimentally determined γ and EOS (Casalini and Roland 2005c). Listed in table 2 are pressure coefficients of fragility ($\lim P \rightarrow 0$) for various glass-forming materials. Overwhelmingly, $(dm_P/dP) \leq 0$; that is, densification reduces the fragility. The only exceptions to this appear to be the hydrogen-bonded materials, such as glycerol (Cook *et al* 1994, Paluch *et al* 2002c), polypropylene glycol (Andersson and Andersson 1998) and perhaps salol (Schug *et al* 1998, Casalini *et al* 2003a). Simulations also suggest an increase in fragility when the coordination number of SiO_2 is changed by pressure (Angell *et al* 1994). Thus, all cases of a positive pressure coefficient of m_P appear to involve a change in the chemical structure of the material, whereas the direct effect of P on the dynamics is to reduce m_P .

To isolate the effect of thermal energy, apart from the influence of local volume, it is of interest to examine $\tau_\alpha(T)$ under constant density conditions. Although direct experimental measurements are extremely difficult, isochoric relaxation times can be calculated from isothermal and isobaric data by interpolation (more precisely, by using the fact that τ_α is a function of TV^γ). Representative results are shown in figure 23. These allow calculation of the isochoric fragility, m_V .

Since relaxation times are uniquely determined by TV^γ , once γ is known, fragility curves are readily calculated for any thermodynamic condition (Casalini and Roland 2005c). In table 3 are collected isochoric fragilities for various glass-forming materials. The values correspond to an arbitrary specific volume, in the vicinity of T_g at atmospheric pressure. As expected, m_V is always less than m_P , since the former quantifies only the effect of temperature, while for the latter volume and temperature effects both contribute (and as we have seen, $(dm_P/dP) < 0$).

As shown in figure 24, there is a roughly linear relationship between the isochoric and isobaric fragilities (Casalini and Roland 2005d). As a consequence of this correlation and given that $E_V/E_P = m_V/m_P$, it follows that a large m_P corresponds to a large value of E_V/E_P . From the linear fit shown in this figure (excluding the two outliers), together with the fact that $0 \leq E_V/E_P \leq 1$, we find that $37 \pm 3 \leq m_P \leq 231 \pm 72$. This is equivalent to the range of experimental values reported in the literature for simple liquids and polymers, $40 \leq m_P \leq 191$ (Böhmer *et al* 1993).

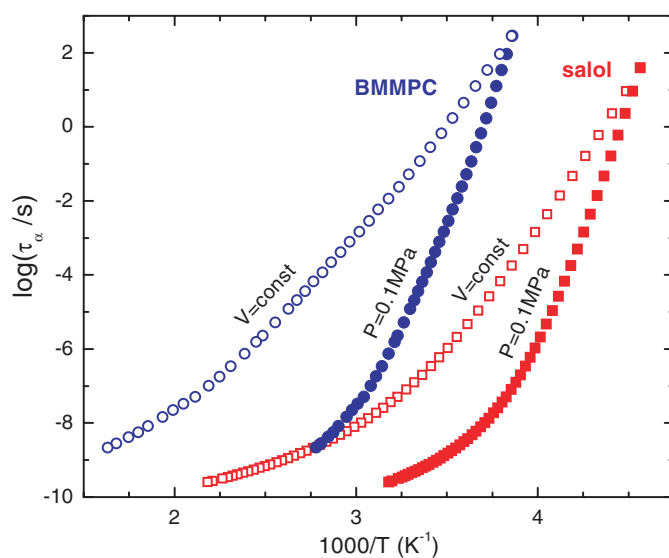


Figure 23. Isochoric (○, □) and isobaric (●, ■) $\tau_\alpha(T)$ for BMMPC and salol.

Table 3. Isobaric and isochoric fragilities.

Material	m_p	m_V	Reference
PDE	71	39	Casalini and Roland 2005a
KDE	64	34	Casalini and Roland 2005a
Polychlorinated biphenyl (62% Cl)	59	23	Casalini and Roland 2005a
Polychlorinated biphenyl (54% Cl)	59	29	Roland and Casalini 2005
Polychlorinated biphenyl (42% Cl)	59	33	Roland and Casalini 2005
Propylene carbonate	81	57	Casalini and Roland 2005a
BMMPC	58	25	Casalini and Roland 2005a
Salol	68	36	Casalini and Roland 2005a
BMPC	70	26	Casalini and Roland 2004b
1,2-polybutadiene	88	63	Casalini and Roland 2004b
Sorbitol	128	112	Casalini and Roland 2004b
Polymethylacrylate	122	94	Huang <i>et al</i> 2002
Polyethylacrylate	83	67	Huang <i>et al</i> 2002
Polyvinylacetate	130	130	Huang <i>et al</i> 2002
Polyvinylchloride	160	140	Huang <i>et al</i> 2002
Polystyrene	77	55	Huang <i>et al</i> 2002
Polyvinylacetate	95	61	Alba-Simionesco <i>et al</i> 2004
Polyepichlorohydrin	75	46	Alba-Simionesco <i>et al</i> 2004
Polyvinylmethylether	75	51	Alba-Simionesco <i>et al</i> 2004
1,4-polybutadiene	77	64	Alba-Simionesco <i>et al</i> 2004
Glycerol	40	38	Alba-Simionesco <i>et al</i> 2004
<i>o</i> -terphenyl	82	45	Alba-Simionesco <i>et al</i> 2004
Polypropylene oxide	74	41	Roland <i>et al</i> 2004e
Diglycidyl ether of bisphenol A	95	57	Roland <i>et al</i> 2004e
Polyvinylacetate	78	52	Roland <i>et al</i> 2004e
Poly[(phenol glycidyl ether)-co-formaldehyde]	95	60	Roland <i>et al</i> 2004e
Polymethyl acrylate	102	80	Roland <i>et al</i> 2004e
Poly[(<i>o</i> -cresol glycidyl ether)-co-formaldehyde]	130	84	Roland <i>et al</i> 2004e

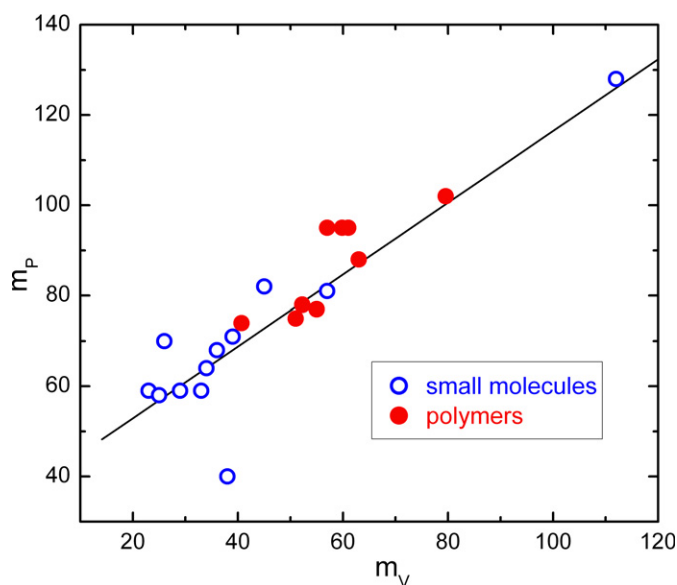


Figure 24. The isobaric fragility versus the isochoric fragility, both evaluated at T_g (data from table 3). Fit (solid line) gives $m_P = (37 \pm 3) + (0.84 \pm 0.05)m_V$ (Pearson correlation coefficient = 0.95).

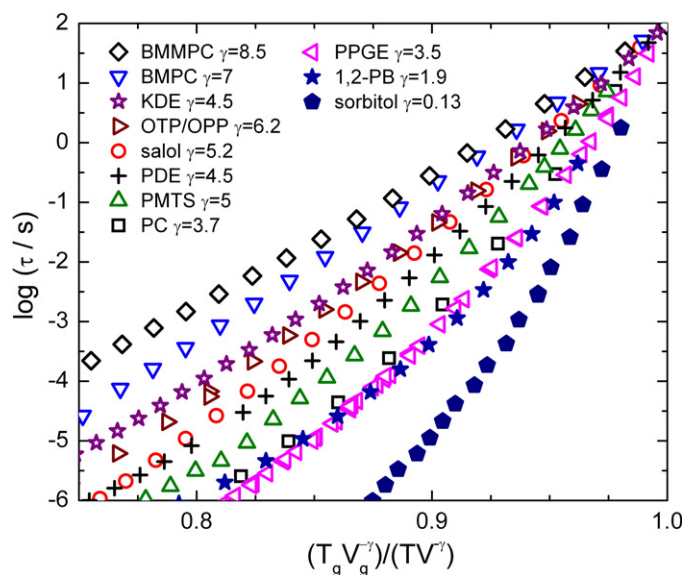


Figure 25. Modified fragility plot showing the dielectric relaxation time versus $T^{-1}V^{-\gamma}$ with the latter normalized by the value for which $\tau = 10^2$ s (Casalini and Roland 2004b).

Since unlike the usual isobaric fragility, the $T V^\gamma$ scaling delineates the respective T and V contributions to $\tau_\alpha(T)$, it is of interest to consider an alternative measure of fragility, employing the parameter γ . In figure 25, relaxation times are plotted versus $(T/T_g)^{-1}(V/V_g)^{-\gamma}$ (where $V_g \equiv V(T_g)$) (Casalini and Roland 2004b). The slopes at T_g of these curves are numerically

equal to m_V ; that is, the behaviour in a modified fragility plot has its origin in the effect of temperature alone.

7. Dynamic crossover

At temperatures above T_g , an interesting phenomenon is observed in most glass-formers. As first observed by Plazek and Magill (1966) (Magill and Plazek 1967) in *tris*-naphthylbenzene (TNB), there is a marked change in the temperature dependence of various properties, including both τ and η (Schneider *et al* 1999a, Angell *et al* 2000, Rault 2000, Novikov and Sokolov 2003). The temperature associated with this ‘dynamic crossover’, T_B , can be determined using a model-independent derivative function introduced by Stickel *et al* (1995)

$$\phi_T = \left[\frac{d \log(x)}{d(1000/T)} \right]^{-1/2}, \quad (41)$$

where x is τ_α or η . Various theoretical models anticipate, or at least interpret, the dynamic crossover: (i) the liquid–liquid transition postulated for polymers (Boyer 1985, Warner and Boyer 1992) (although it is not specific to polymers, not a thermodynamic phase transition, and some manifestations of Boyer’s crossover may be artefacts (Plazek 1982, Chen *et al* 1982, Orbon and Plazek 1982, Kisliuk *et al* 2000)); (ii) the crossover from free diffusion to landscape-dominated diffusion for τ on the order of ns, as predicted by the energy landscape model of Goldstein (1969); (iii) the percolation of ‘liquid-like cells’, according to the Cohen–Grest free-volume model (Cohen and Grest 1979, Grest and Cohen 1981, Paluch *et al* 2003c); (iv) a marked increase in the intermolecular cooperativity in the context of the coupling model (CM) (Ngai and Roland 2002, Casalini *et al* 2003d); (v) divergence of the viscosity according to MCT (Götze and Sjogren 1992), although a transition to hopping dynamics may prevent this divergence from being observed (Götze 1999); (vi) the emergence of thermal density fluctuations having a length scale larger than the liquid cage structure (Schweizer and Saltzman 2004a, 2004b). The general consensus is that below T_B , the dynamics become ‘fully cooperative’, although the non-Arrhenius character of $\tau(T)$ continues above T_B .

The dynamic crossover is also evident in measurements taken as a function of pressure at fixed temperature. In this case, the derivative function is (Casalini *et al* 2003e)

$$\phi_P = \left[\frac{d \log(x)}{dP} \right]^{-1/2}. \quad (42)$$

Experiments at elevated pressure reveal that at the dynamic crossover, the dielectric relaxation time (Casalini *et al* 2003b, 2003e) as well as the viscosity (Casalini and Roland 2004c), are constant; that is, T_B varies with pressure, but τ_B ($\equiv \tau_\alpha(T_B)$) or η_B is independent of T and P . This is illustrated in figures 26 and 27 for τ_α and η , respectively.

The fact that τ_α is a function of TV^γ can be exploited to calculate τ_B for materials for which the necessary high frequency data for $P > 0.1$ MPa are lacking (note that elevated pressure dielectric measurements are usually limited to about 1 MHz and below). For example, starting from atmospheric pressure measurements at varying temperature, the isobaric behaviour at any pressure \hat{P} (including $P < 0$) is calculated by finding the T such that $TV^\gamma(0.1 \text{ MPa}) = T\hat{V}^\gamma(\hat{P})$ (Casalini and Roland 2005c). In the same fashion, isochoric behaviour at a volume \hat{V} is determined from the value of the ambient pressure τ at a T conforming to the condition $TV^\gamma(0.1 \text{ MPa}) = T\hat{V}^\gamma$. It is emphasized that the calculations are done such that all relaxation times are within the measured range; that is, the TV^γ -superpositioning is used only to extrapolate the P - and V -dependences of τ_α . Results for various materials are listed in table 4. Of particular interest is the fact that not only is τ_B

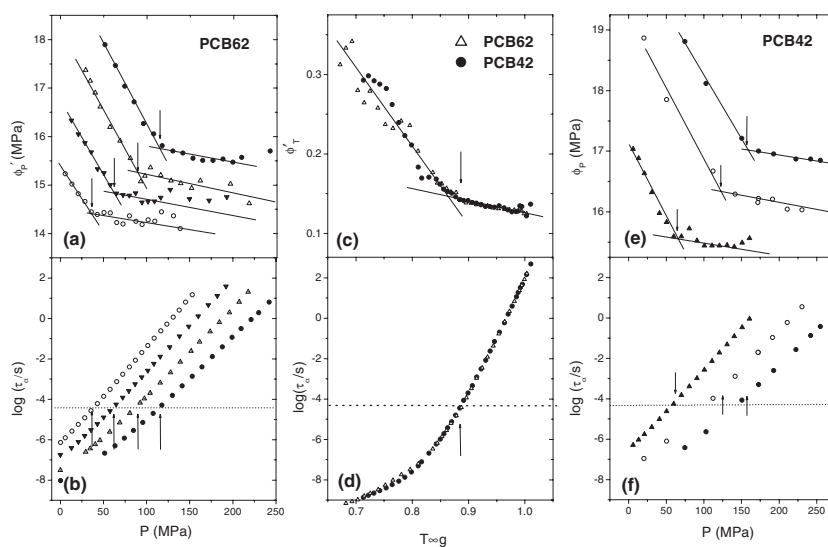


Figure 26. Dielectric relaxation time data for polychlorinated biphenyls having 42% and 62% by weight chlorine. (a) Derivative function ϕ_P for PCB62 versus pressure, calculated for isotherms at $T = 344$ (●), 334.5 (△), 325.1 (▼) and 317.4 K (○); (b) relaxation times for PCB62 versus pressure at four temperatures $T = 344$ (●), 334.5 (▲), 325.1 (▼) and 317.4 K (○); (c) derivative function ϕ_T versus inverse temperature normalized to T_g for PCB62 and PCB42; (d) relaxation time versus inverse temperature normalized to T_g for PCB62 and PCB42; (e) derivative function ϕ_P versus pressure, calculated at $T = 263$ (▲), 273.6 (○) and 283 K (●); (f) relaxation time versus pressure for PCB42 at $T = 263$ (▲), 273.6 (○) and 283 K (●). Data from Casalini and Roland (2005c) and Roland and Casalini (2005).

independent of pressure, but also the relaxation time at the dynamic crossover for constant density conditions is the same as the isobaric value (figure 28).

8. Secondary relaxations

In the broadband dielectric spectra of supercooled glass-formers, often several relaxation phenomena are observed (McCrum *et al* 1991, Wu 1991, Ediger *et al* 1996, Lunkenheimer and Loidl 2002). Even the simplest of glass formers, lacking internal degrees of freedom, usually reveal a peak in the dielectric loss, in addition to the prominent α -process. When the former is ascribed to reorientation of all atoms in the molecule, it is designated as the Johari–Goldstein (JG) process, since these authors were the first to report secondary relaxations in rigid molecules (Johari and Goldstein 1970, 1971, Johari 1973). When observed, the JG relaxation is the slowest of the secondary relaxations, involving restricted reorientations over smaller amplitudes than the primary α -process (Vogel and Rössler 2001). More generally, various secondary relaxations may be present in the spectrum, usually having weaker amplitudes than the α -relaxation and falling at higher frequencies. The general convention is to refer to these peaks using Greek letters in the order of increasing frequency, beginning with the structural relaxation peak as the α -process. The β -relaxation is a JG process if it involves motion of the entire molecule (or polymer repeat unit) (Kudlik *et al* 1999, Ngai and Paluch 2004). Unfortunately, in some literature any observed β -process is called the JG relaxation, without attempting to identify the underlying molecular motions. Part of the difficulty is that many of the properties of JG relaxations are seen in non-JG secondary relaxations, even though the latter

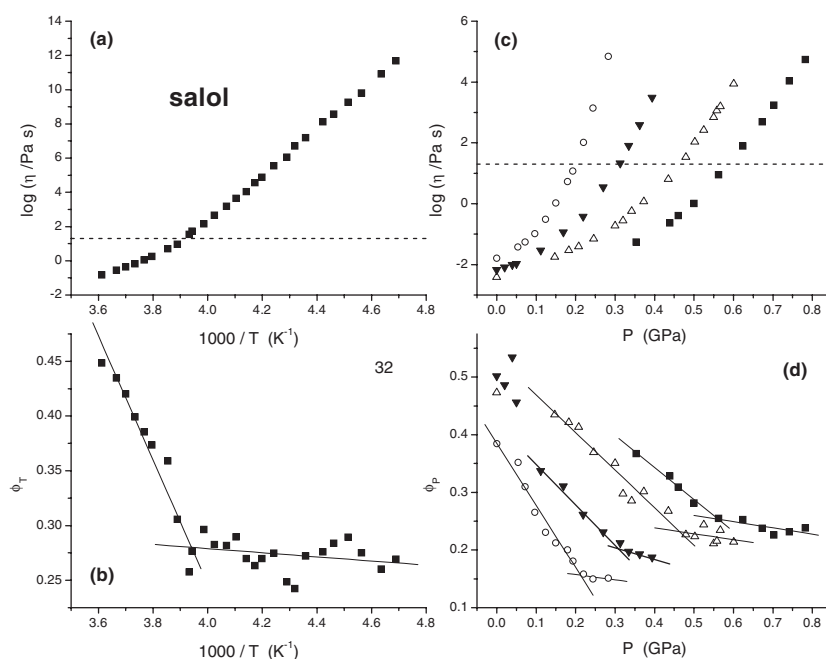


Figure 27. (a) Viscosities of salol at atmospheric pressure, where the horizontal dashed line corresponds to $\log \eta_B(T_B) = 1.3$ Pa s. (b) The derivative function used to determine $T_B = 254$ K at ambient pressure. (c) Viscosities of salol at $T = 363.2$ K (■), 343.2 K (△), 323.2 K (▼), and 303.2 K (○). The horizontal dashed line indicates the value at the dynamic crossover of $\log \eta_B = 1.3$ Pa s. (d) The derivative function used to determine the crossover pressure for each of the four isotherms (Casalini and Roland 2004c).

Table 4. Relaxation time at the dynamic crossover for isobaric and isochoric conditions (Casalini and Roland 2005c).

Materials	Range of P (MPa)	$\log(\tau_B/s)$
PDE	0.1 to 400	-3.8 ± 1
PDE	Isochoric 0.7285 ml g^{-1}	-3.7 ± 0.8
PCB62	0.1 to 600	-5.9 ± 0.4
PCB62	Isochoric 0.6131 ml g^{-1}	-5.8 ± 0.9
PC	0.1 to 1000	-7 ± 0.3
PC	Isochoric 0.7562 ml g^{-1}	-7.2 ± 0.7
KDE	0.1 to 1000	-6.4 ± 0.3
KDE	Isochoric 0.7562 ml g^{-1}	-6.3 ± 0.4
BMMPC	0.1 to 600	-6.1 ± 3
BMMPC	Isochoric 0.9032 ml g^{-1}	-6.2 ± 1
Salol	0.1 to 600	-6.4 ± 0.5
Salol	Isochoric 0.9032 ml g^{-1}	-6.3 ± 0.3

only reflect the motion of pendant groups or local moieties. BMPC (Meier *et al* 1991, Hansen *et al* 1997, Hensel-Bielówka *et al* 2002a) and di-5-hydroxypentylphthalate (Maślanka *et al* 2005) typify this situation. We also note that the JG relaxation is sometimes called the ‘slow’ β process. This is in deference to MCT, which predicts a fast (ps) signature in the dynamics of

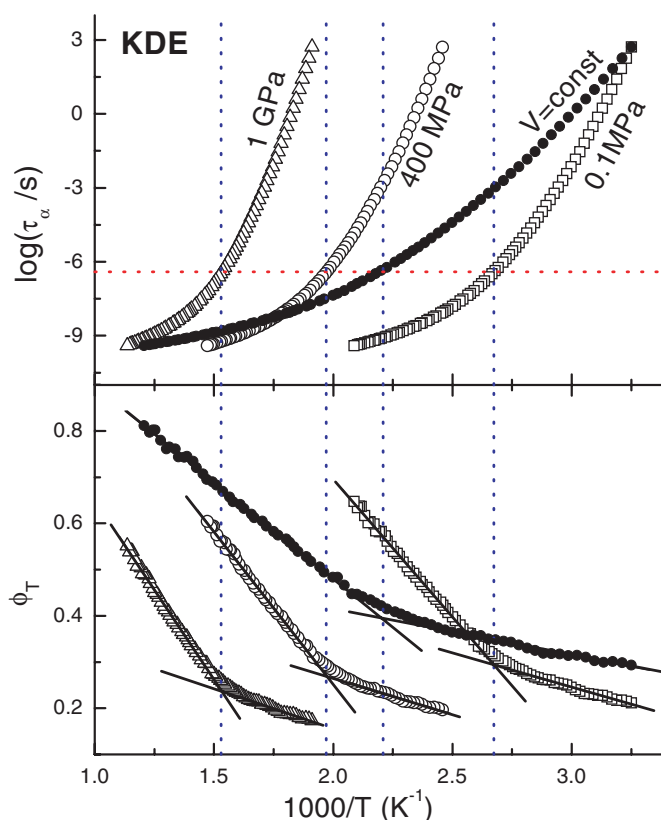


Figure 28. Upper panel: dielectric relaxation time for cresolphthalein-dimethylether (experimental data for 0.1 MPa; calculated isobars and isochoric curve at $V = 0.7709 \text{ ml g}^{-1}$). Dotted line indicates the average of $\log(\tau_B) = -6.35$ for the different curves. Lower panel: Stickel derivative function, with low and high T linear fits for the range $-4.62 < \log_{10}(\tau(s)) < 2.72$ and $-9.4 < \log_{10}(\tau(s)) < -7.28$, respectively. Vertical dotted lines indicate the dynamic crossover (Casalini and Roland 2005c).

glass-formers. However, strictly speaking, the fast MCT β process is not a relaxation (Götze and Sjogren 1992).

8.1. Johari–Goldstein secondary relaxation

The properties of the JG relaxation (some of which are shared by non-JG secondary relaxations) include a dielectric strength that increases with temperature, showing a change in slope at T_g (Johari *et al* 2002) and an Arrhenius behaviour below T_g , with an extrapolated merging with the α -relaxation at $T_{\alpha\beta} \sim (1.2\text{--}1.5) \times T_g$. This merging (or splitting) temperature is close to the temperature of the dynamic crossover (Hansen *et al* 1997), as discussed in section 7, although the extrapolation from the glassy into the liquid state used for determination of $T_{\alpha\beta}$ is incorrect (Paluch *et al* 2003d). While the JG relaxation is regarded as a noncooperative process, its properties reflect interactions with neighbouring molecules, indicating a possible relationship to the α -relaxation. There are two viewpoints: the same volume, temperature and entropy changes which engender structural relaxation are brought to bear on faster molecular motions; thus, some correlation in properties between the α - and JG-process is expected. However,

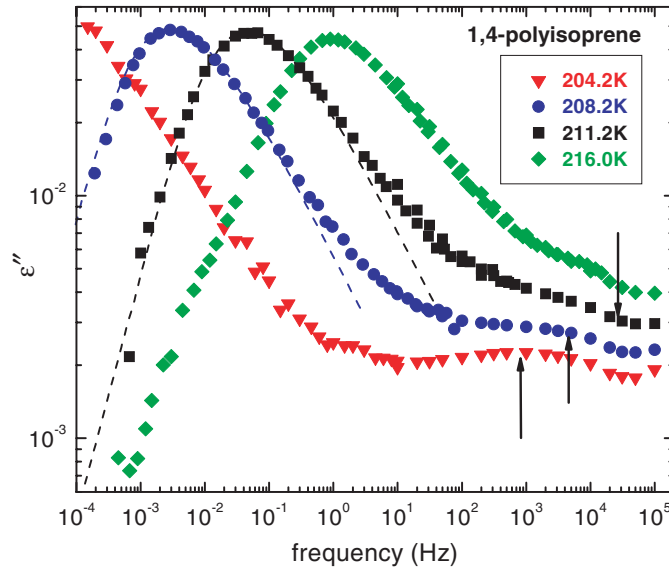


Figure 29. Dielectric loss spectra of PI at ambient pressure. The dashed lines are the fits to the KWW function ($\beta_{\text{KWW}} = 0.47$ independent of temperature), while the arrows mark the location of the JG peak calculated from equation (44) (Roland *et al* 2004b).

secondary relaxations (and other fast processes (Angell 2000)) seem to anticipate the glass transition, even though they occur earlier in time (Ngai 1998a, 2004). This suggests that the JG process may serve as the precursor of the intermolecularly cooperative α -relaxation (Bershtein *et al* 1985, 1997, Bershtein and Ryzhov 1994, Ngai 1998a, 2003, Ngai and Capaccioli 2004, Roland *et al* 2004b). If true, investigation of the JG relaxation can potentially yield unique insights into glass formation. Since β -relaxations have relatively short relaxation times, which change more slowly with temperature than the structural relaxation times, the JG process can be monitored in the glassy state over a wide range of temperatures. Hence, the β -process is also a source of information on the glassy state.

A theoretical description embodying the idea that the JG relaxation is the precursor of structural relaxation is derived from the CM (Tsang and Ngai 1997, Ngai and Tsang 1999). From the observation that the difference between the relaxation times for the α - and JG-relaxation were correlated with the breadth of the α -relaxation function (Ngai 1998a, 1998b), the JG relaxation time, τ_{JG} , is identified with the ‘primitive’ relaxation, τ_{CM} , of the CM model

$$\tau_{\text{JG}}(T, P) = \tau_{\text{CM}}(T, P). \quad (43)$$

Note that the JG relaxation is inhomogeneous, owing to the heterogeneity of the supercooled state. Thus, τ_{JG} corresponds to some average relaxation time. The observed correlation with the breadth of the α -relaxation peak arises from the CM relation

$$\tau_{\text{CM}} = t_c^{1-\beta_{\text{KWW}}} \tau_\alpha^{\beta_{\text{KWW}}}, \quad (44)$$

where $t_c \sim$ ps. From these two equations it follows that

$$\log \tau_\alpha - \log \tau_{\text{JG}} = (1 - \beta_{\text{KWW}})(\log \tau_\alpha - \log t_c) \quad (45)$$

and hence the observed correlation (Ngai 1998a, 1998b). This is illustrated in figures 29 and 30. A further prediction is that the activation energy for the JG process, E_{JG} , will also

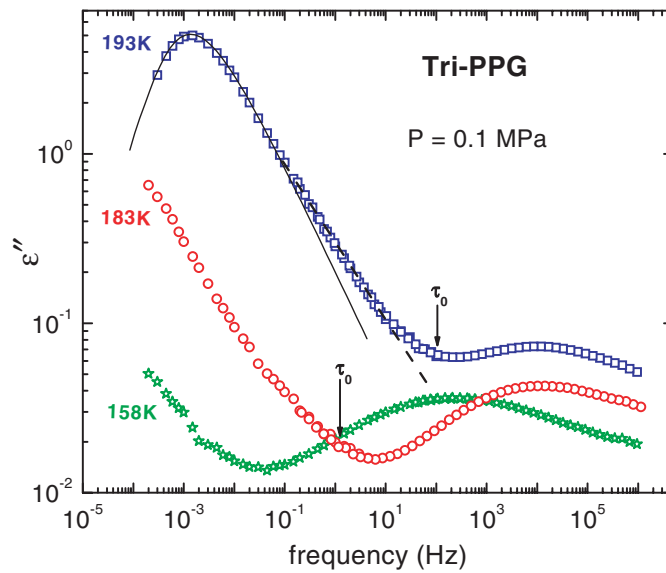


Figure 30. Dielectric loss curves for propylene glycol trimer measured at ambient pressure and the indicated temperatures. Solid line denotes KWW fit with $\beta_{\text{KWW}} = 0.63$. Arrows indicated the location of the JG relaxation time calculated using equation (44) (Casalini and Roland 2004c).

be (Ngai and Capaccioli 2004)

$$E_{\text{JG}} = 2.303RT_g(11.7 - 13.7\beta_{\text{KWW}} - \log \tau_0). \quad (46)$$

This equation, which assumes $\tau_\alpha(T_g) = 100$ s with τ_0 defined in equation (2), underlies the empirical observation of Kudlik *et al* (1997, 1999)

$$E_{\text{JG}} = 24RT_g. \quad (47)$$

The value of equation (46) is that it enables the value of the JG relaxation time to be determined from the properties of the α -relaxation. However, application of the model requires accurate determination of the stretch exponent, β_{KWW} . Problems arise when the α -relaxation peak is inhomogeneously broadened, for example, in blends or when the molecules have a complex structure with more than one dipole (Mašlanka *et al* 2005). Then the measured breadth does not reflect the intrinsic β_{KWW} for the α -process. Such a situation also occurs for copolymers (Roland 1992, Santangelo *et al* 1996), in which local segmental motion originates from the torsional motion of different repeat units.

The study of secondary relaxations has been significantly advanced by measurements at elevated pressure. Williams and co-workers (Williams and Watts 1971a, 1971b, Williams 1979, McCrum *et al* 1991) carried out many pressure-dependent experiments on polymers, and found that the β -relaxation in these materials is rather insensitive to pressure. However, many of the secondary relaxations in polymers correspond to motion of pendant groups; that is, they are not JG relaxations. Nevertheless, generally the β -relaxation, even in low molecular liquids, is less sensitive to pressure than the α -process. The consequence is that the separation between the α - and β -peaks increases under elevated pressure (figures 31 and 32) (Hensel-Bielówka and Paluch 2002, Hensel-Bielówka *et al* 2002a, 2002b, 2004, Casalini and Roland 2003b, 2004a, Sekula *et al* 2004). Experiments at high pressure facilitate the study of secondary relaxations, particularly when they are close in frequency to the α -process (Frick and Alba-Simionesco 1999, Casalini and Roland 2003b, 2004a, Roland *et al* 2003d). The differing

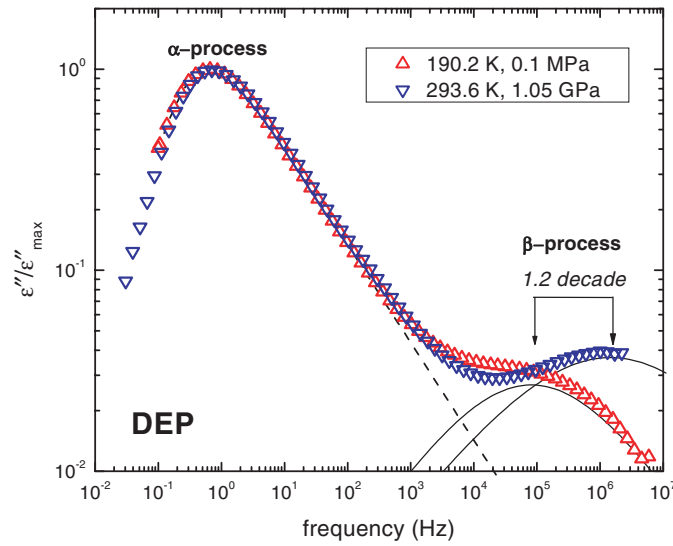


Figure 31. Dielectric spectra of diethyl phthalate measured at two conditions for which τ_α is roughly constant. The β -peak maxima is further from the α -peak for higher pressure and temperature (Pawlus *et al* 2003).

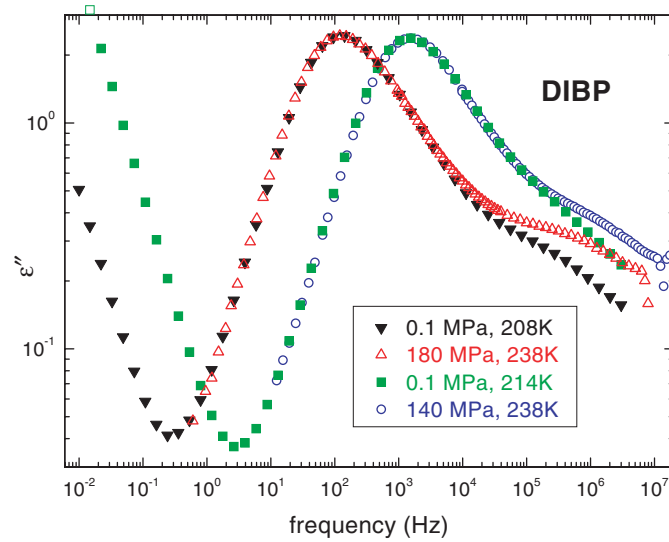


Figure 32. Dielectric spectra of diisobutyl phthalate obtained at conditions for which the α -peaks superpose, with greater separation from the secondary peak for higher pressure and temperature (Hensel-Bielówka and Paluch 2002).

pressure sensitivity follows from equation (44) of the CM, from which the relative magnitude of the activation volumes is given by (Casalini and Roland 2004a)

$$\Delta V_\alpha^\# = \beta_{\text{KWW}}(T, P) \Delta V_{\text{JG}}^\# \quad (48)$$

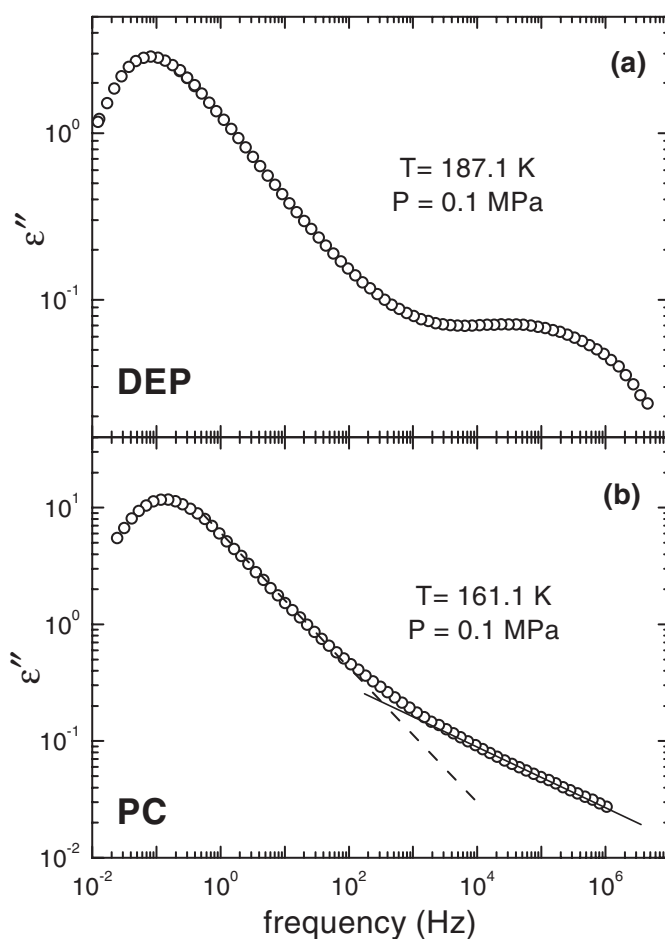


Figure 33. Dielectric spectra of (a) diethyl phthalate (Pawlus *et al* 2003), which has a resolved JG-peak, and (b) propylene carbonate (Pawlus *et al* 2004), which has an unresolved secondary relaxation (excess wing). The solid line in the lower graph shows the additional power law with a weaker slope than the α -relaxation (---).

8.2. The excess wing

Johari and Goldstein (1970) pointed out that since the β -relaxation exists in rigid molecules, it must be a general feature of the deeply supercooled and glassy state. And if the β -relaxations for molecular and polymeric glass formers have similar properties, they are likely to have a similar origin (Johari and Goldstein 1971). However, it was known even then that there exists a group of glass formers (e.g. glycerol and propylene carbonate) for which a β -process is absent, even far below T_g . In such materials, a new feature arises—the appearance of extra intensity on the high frequency side of the α -relaxation. This so-called ‘excess wing’ (EW), appearing about two decades above the α -peak maximum in the dielectric loss, has the form of a power law, $\epsilon'' \propto \nu^{-b}$ ($b < \beta_{KWW}$) (Dixon *et al* 1990, Leslie-Pelecky and Birge 1994, Lunkenheimer *et al* 1996, Leheny and Nagel 1997, Hensel-Bielowka and Paluch 2002). Representative dielectric loss curves for the two types of behaviour are shown in figure 33. Kudlik *et al* (1999) proposed a classification of glass formers, according to whether their dielectric spectra

showed a distinct β -peak ('type B') or only an excess wing ('type A'). However, as discussed below, high-pressure measurements show that such a distinction is artificial (Casalini and Roland 2003b).

The origin of the EW is one of the most disputed aspects of the glass transition dynamics. Early workers considered the EW to be an inherent part of the α -relaxation. This led to the proposal of a scaling procedure to superpose dielectric loss curves in the frequency range of the α -relaxation peak and the EW for different glass formers (Dixon *et al* 1990, Leheny and Nagel 1997). There was even theoretical support for the supposed scaling from models that treated the EW as an inherent part of the structural relaxation (Chamberlin 1993, Tarjus and Kivelson 1997).

Departures from the scaling of Nagel and Dixon have been noted (Schönals *et al* 1991), and the idea that the EW is a component of the α -process is at odds with the observation that materials having very similar α relaxations can have different EW (Casalini and Roland 2002). As first suggested by Johari and Pathmanathan (1986), the EW is the high frequency side of the β -peak, hidden by the dominant α -process. Even for putative type B materials, which exhibit a secondary relaxation, at high temperatures the secondary peak tends to merge with the α -peak. This means that there is a range of temperatures at which the partially-submerged JG peak assumes the appearance of an EW. More striking evidence that the EW is a separate process from the α -relaxation comes from physical ageing experiments and measurements at elevated pressure. Schneider and co-workers (Schneider *et al* 1999b, Lunkenheimer *et al* 2002) maintained various 'type A' glass formers for extended duration in glassy state, causing the α -peak to shift to lower frequencies, whereupon the EW develops into a shoulder. Such a transformation of an EW to a distinct feature in the dielectric loss spectrum can also be brought about by geometrical confinement (Bergman *et al* 2003, Svanberg *et al* 2003) or by the addition of a higher T_g diluent (Johari and Goldstein 1970, Blochowicz and Rössler 2004).

Experiments at high pressure have been especially useful in identifying the nature of the EW, since advantage can be taken of the different pressure sensitivities of the α - and β -peaks. Similar to ageing experiments, measurements under high pressure for glycerol show that the EW can be separated from the α -peak (Paluch *et al* 2002c). A more interesting situation is found for oligomers of propylene glycol. At ambient pressures, there is a secondary peak in the dielectric spectra of the dimer and trimer, which has sometimes been identified as a JG process (Johari 1986, León *et al* 1999). However, dielectric measurements under pressure reveal the existence of an excess wing, which evolves into a distinct peak upon physical ageing (Casalini and Roland 2003b, 2004a). This relaxation process occurs simultaneously with the higher frequency secondary relaxation observed at low pressure (figure 34). At low pressure, the higher frequency peak is the only observed secondary relaxation (see also figure 30); its insensitivity to pressure is consistent with its non-JG character. Application of pressure causes the emergence of the EW, which transforms into a distinct relaxation at sufficiently high pressure, low temperature and with physical ageing. Curiously, at higher pressures, and correspondingly higher temperatures so that the peaks are within the experimental window, the EW is less apparent (see figure 32). This may be owing to the effect of hydrogen bonding (Ngai and Paluch 2004).

Note that the glass-formers exhibiting an EW tend to have narrow relaxation functions. For example, $\beta_{\text{KWW}} = 0.73$ for PC, $\beta_{\text{KWW}} = 0.75$ for KDE, $\beta_{\text{KWW}} = 0.71$ for glycerol and $\beta_{\text{KWW}} = 0.71$ for PCB42. This property is in accordance with equation (44) (τ_{JG} is close to the α -relaxation time, so that only the high-frequency side of the JG-peak is visible), further supporting the identification of the EW as an unresolved JG process.

The large differences between $\Delta V_{\alpha}^{\#}$ and $\Delta V_{\text{JG}}^{\#}$ exploited in the works cited above involved hydrogen-bonded liquids. For simple van der Waals materials, the respective effects of pressure

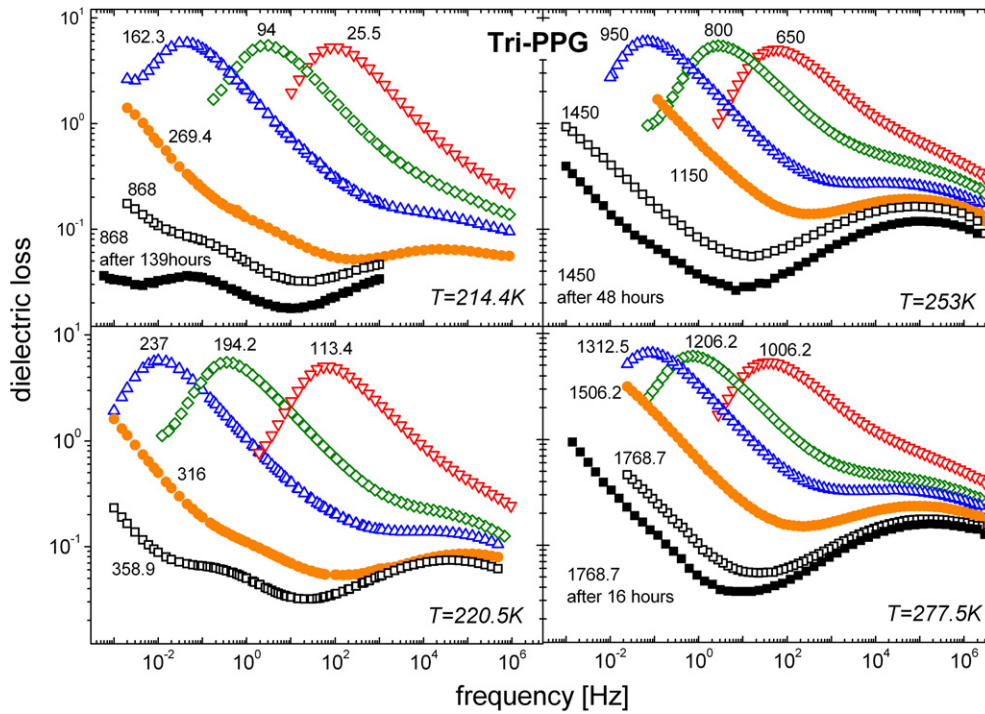


Figure 34. The evolution of the dielectric loss of propylene glycol trimer under high pressure at different temperatures. For the two lower temperatures, the intermediate JG-peak is well separated from both the α -peak and the higher frequency secondary peaks at higher pressures; however, for the two higher temperatures, the JG-relaxation is only resolved as a weak excess wing. The latter behaviour is also seen at ambient pressure (figure 30) (Pawlus *et al* 2005).

on the α - and β -relaxations are much weaker and more nearly in accordance with equation (44) (Paluch *et al* 2001b, Hensel-Bielówka and Paluch 2002, Roland *et al* 2003d, Hensel-Bielówka *et al* 2004, Ngai and Paluch 2004, Casalini and Roland 2004a). Thus, for glass formers such as KDE (figure 35), PDE, BMMPC (figure 36), PCB42 and PC, the dielectric spectra (both in the α -peak and the EW) for different conditions of constant τ_α fall on a master curve, independent of T and P . However, for associated liquids such as salol (figure 37), propylene glycols (figure 38) and polyalcohols (figure 39) temperature-pressure superpositioning fails. Under elevated pressure, the α -peaks become broader and the EW shifts. This behaviour is attributed to changes in the degree of hydrogen bonding. These may arise as a direct consequence of pressure (Poole *et al* 1994, Naoki and Katahira 1991), or owing to the higher temperature required for high P measurements (to maintain constant τ_α).

8.3. Temperature dependence of τ_{JG} near T_g

Many experimental results (Bergman *et al* 1998, Kudlik *et al* 1998, Rault 2000, Gomez *et al* 2001) have shown that the temperature dependence of τ_β follows an Arrhenius law below T_g

$$\tau_\beta = \tau_0 \exp\left(\frac{E_\beta}{RT}\right). \quad (49)$$

As temperature rises above T_g , the α - and β -relaxations merge, forming a single process. However, owing to the difficulty of resolving the overlapping peaks, the temperature evolution

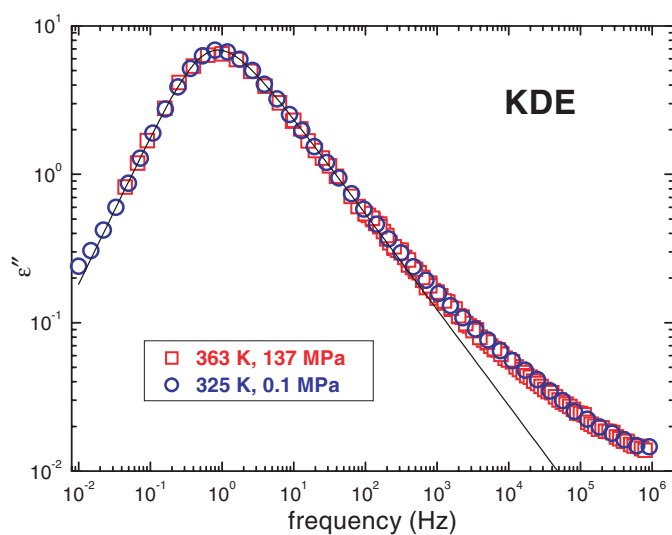


Figure 35. Dielectric spectra of cresolphthalein-dimethylether obtained at two conditions for which τ_α is roughly constant. Superposition of the α -peak is accompanied by superpositioning of the excess wing (Paluch *et al* 2001b).

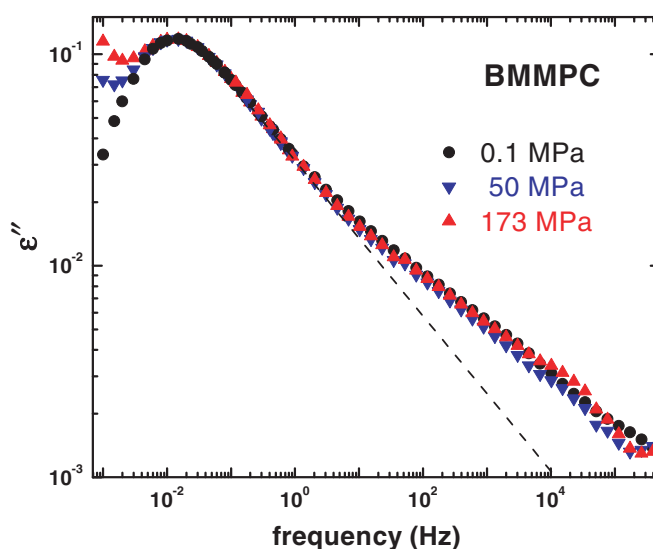


Figure 36. Dielectric spectra of 1,1'-di(4-methoxy-5-methylphenyl)cyclohexane obtained at three conditions for which τ_α is roughly constant. Superposition of the α -peak is accompanied by superpositioning of the excess wing (Roland *et al* 2003d).

of the τ_β in the equilibrium liquid state is uncertain. A common assumption is that the Arrhenius behaviour in the glassy state persists above T_g , whereby the merging temperature, $T_{\alpha\beta}$, at which τ_β becomes equal to the structural relaxation time, is well defined, at least operationally.

However, various experiments carried out at ambient pressure suggest that τ_β does not follow the Arrhenius dependence exhibited below T_g . From analysis of dielectric spectra

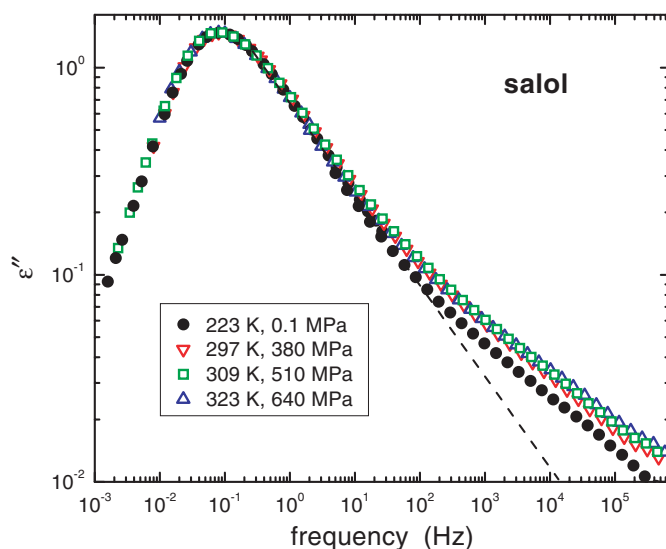


Figure 37. Dielectric spectra of salol obtained at conditions for which τ_α is roughly constant. There is a weak deviation of the excess wing for higher pressures (Roland *et al* 2003d).

of sorbitol by fitting the overlapping α - and β -peaks to the sum of two functions, several groups concluded that the Arrhenius dependence observed below T_g changes into a stronger temperature dependence above T_g (Wagner and Richert 1999, Fujima *et al* 2002, Nozaki *et al* 2002). Such results can be questioned because of the ambiguity associated with the method of separating the overlapping peaks (Bergman *et al* 1998). Most authors assume the α - and β -peaks superpose in the frequency domain (Garwe *et al* 1996), although there is an alternative procedure using an additive formula in the time domain (Williams 1979). From comparisons of the two analyses, some authors have reported little difference in fitting experimental data (Gomez *et al* 2001, Svanberg *et al* 2003), although different interpretations of the relationship between the α - and β -dynamics underlie the two methods (Donth *et al* 1999, Arbe *et al* 1999).

The situation improves when the measurements are carried out under elevated pressure. For example, the maximum in the dielectric loss for the secondary relaxation in sorbitol remains virtually unchanged with increasing pressure (figure 40(a)) (Paluch *et al* 2003d). Since the α -peak is moving toward lower frequency, the overlap of the two peaks is reduced by pressure (figure 40(b)). This facilitates an accurate determination of τ_β in the liquid state. The relaxation map (figure 41) clearly shows that secondary relaxation in sorbitol changes from one Arrhenius temperature dependence below T_g to a different one above T_g , with the latter having a larger activation energy. These results for sorbitol have been corroborated by analogous high-pressure dielectric measurements for xylitol (Paluch *et al* 2003d) and for a mixture of 17.2% chlorobenzene in decalin (Koplinger *et al* 2000), although in the latter case, the change in activated behaviour of the secondary relaxation times took place deep in the glassy state. Resolution of the secondary relaxation from the α -peak can also be brought about by the addition of a diluent, having a longer α -relaxation time. Exploiting this idea, Blochowicz and Rössler similarly found for 2-picoline mixed with tristyrene a stronger dependence of τ_{JG} in the liquid state than below T_g (Blochowicz and Rössler 2004).

We also note that a somewhat different analysis led Olsen and co-workers (Olsen 1998, Olsen *et al* 2000) to the conclusion that there is a near invariance to T of the secondary

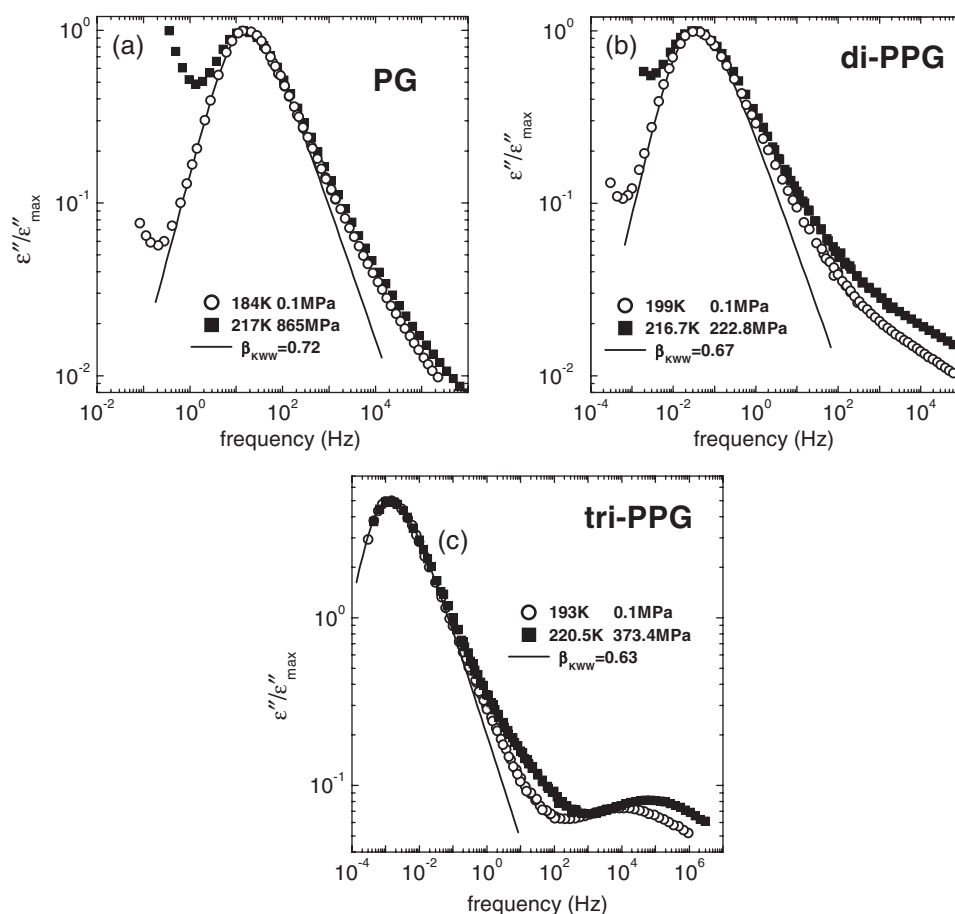


Figure 38. Comparison of the dielectric loss spectra of (a) propylene glycol, (b) propylene glycol dimer and (c) propylene glycol trimer measured at conditions for which the α -peaks approximately superpose. Solid lines are fits to KWW function, demarcating the excess wing; the latter is more prominent at higher pressure. For the trimer, there is also a secondary non-JG relaxation peak (Casalini and Roland 2004a).

relaxation times in the immediate vicinity of T_g (but below the merging temperature). These same investigators also reported a minimum in the secondary relaxation time of PG trimer; that is, in the vicinity of the glass transition, the secondary relaxation time *increased* with *increasing* temperature (Dyre and Olsen 2003). This peak is not a JG relaxation (Casalini and Roland 2003b, 2004a) as seen in figure 33, but this is still very unusual behaviour. These ambient pressure measurements were hindered by the strong overlap of a secondary peak with the close-lying, and much stronger, α -peak. From dielectric spectra at elevated pressure, in which the two peaks are much separated (although still overlapping), Pawlus *et al.* (2005) reached similar conclusions. Notwithstanding the details of the T -dependence of secondary relaxations in the liquid state, the important point is that the JG relaxation time in the equilibrium liquid does not follow the Arrhenius dependence seen below T_g . Accordingly, determinations of the merging temperature T_β by extrapolation from the glassy state must be in error.

There are some secondary relaxations which exhibit an Arrhenius temperature dependence that continues unchanged from the glassy to the liquid state. Examples are found in epoxy

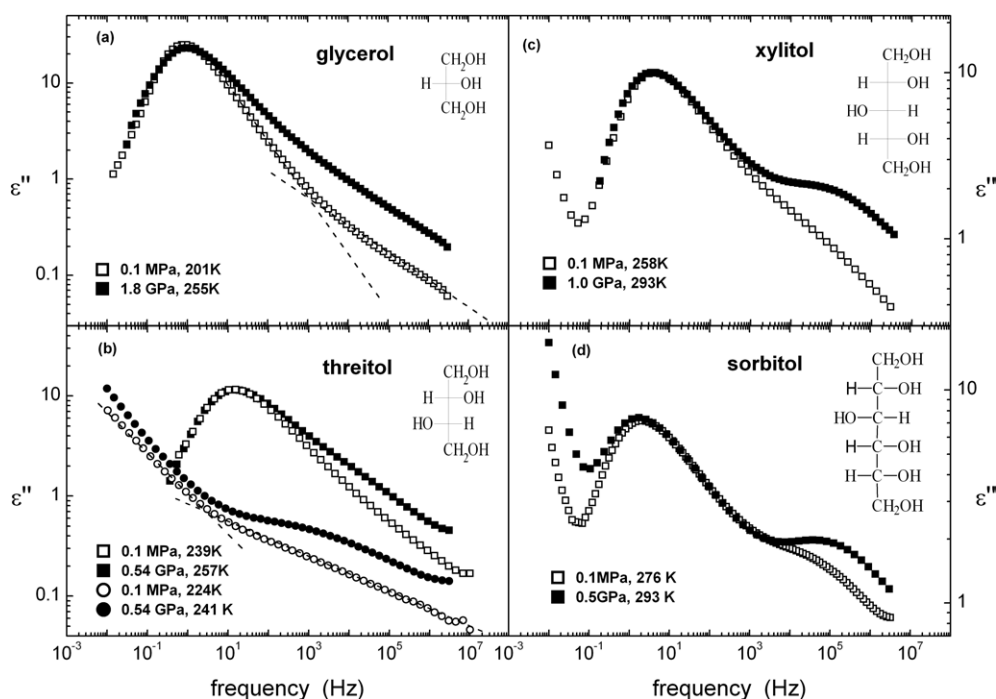


Figure 39. Dielectric loss of (a) glycerol, (b) threitol, (c) xylitol and (d) sorbitol obtained at ambient (\square , \circ) and elevated (\blacksquare , \bullet) pressure; the spectra were shifted slightly to make the α -peaks coincide. With increasing pressure and temperature the α -relaxation broadens, concomitant with increasing separation from the excess wing or secondary relaxation. For threitol some data obtained below T_g are included. (Hensel-Bielówka *et al* 2004).

resins (Pisignano *et al* 2001, Corezzi *et al* 2002), polyvinylmethylether (Chahid *et al* 1994) and fluorinated polyalkenes (Starkweather *et al* 1992). However, invariably these secondary relaxations do not involve intramolecular degrees of freedom; they are not JG processes.

Figure 42, showing isobaric and isothermal data for di-isobutylphthalate (DIBP), illustrates the different behaviour of the α - and secondary-relaxations. The pressure range for the upper abscissa scale was chosen to superimpose the $\tau_\alpha(P)$ with the $\tau_\alpha(T)$ data. Clearly, for DIBP the changes in τ_β with temperature greatly exceed the changes in τ_β with pressure. This is a characteristic feature seen in many glass-forming liquids (Hensel-Bielowka *et al* 2002b, Paluch *et al* 2003d, Hensel-Bielowka *et al* 2002a, Sekula *et al* 2004, Pawlus *et al* 2003, Casalini and Roland 2004a), reflecting the very weak effect of compression in the glassy state (perhaps related to the magnitude of the effective pressure when a glass is compressed). From figure 42 extrapolation of the isobaric relaxation times yields $\tau_\beta = 3 \times 10^{-9}$ s at $T = 253$ K (the temperature of the isothermal measurements); however, this value is about two decades shorter than the τ_β determined by (the weak) extrapolation of the isotherm. This seems to suggest dramatic changes in the P -dependence of τ_β for DIBP as T_g is traversed by decreasing pressure (as does $\tau_\beta(T)$ as described earlier). Alternatively, if the pressure dependence of τ_β were the same in the liquid and glassy states (i.e. there is always a negligible activation volume for the secondary relaxation), the implication is that the temperature dependence of the secondary relaxation departs markedly from the behaviour deduced from deconvoluting the dielectric spectra above T_g .

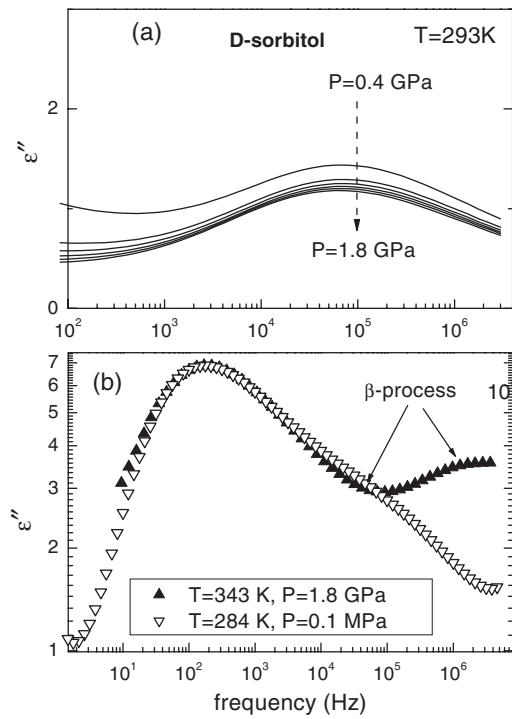


Figure 40. (a) Secondary relaxation of sorbitol as a function of pressure from 0.4 to 1.8 GPa at constant $T = 293$ K; τ_β is relatively invariant to pressure. (b) Dielectric loss spectra of sorbitol at ambient and high pressure and temperatures such that τ_α is constant. Note the reduced overlap of the α - and secondary-peaks at higher pressure (Paluch *et al* 2003d).

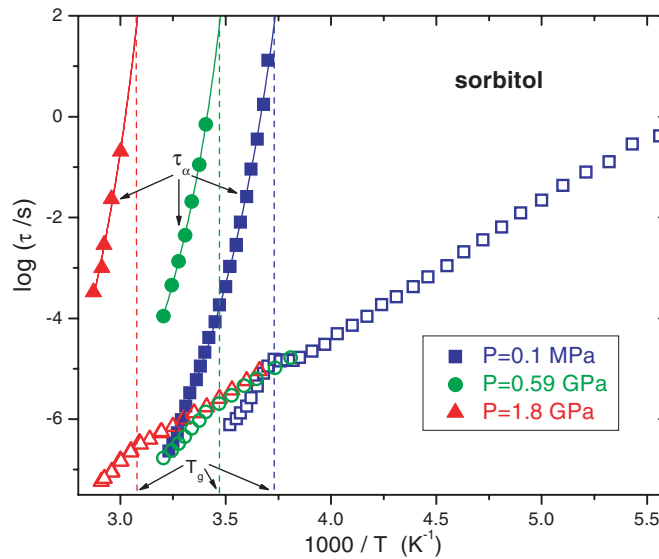


Figure 41. Relaxation times of sorbitol for the α -process (\blacksquare , \bullet , \blacktriangle) and the secondary β -process (\square , \circ , \triangle) at three pressures. Deviation of τ_β from Arrhenius behaviour is observed above the glass transition temperatures (with T_g latter denoted by the vertical dashed lines) (Paluch *et al* 2003d).

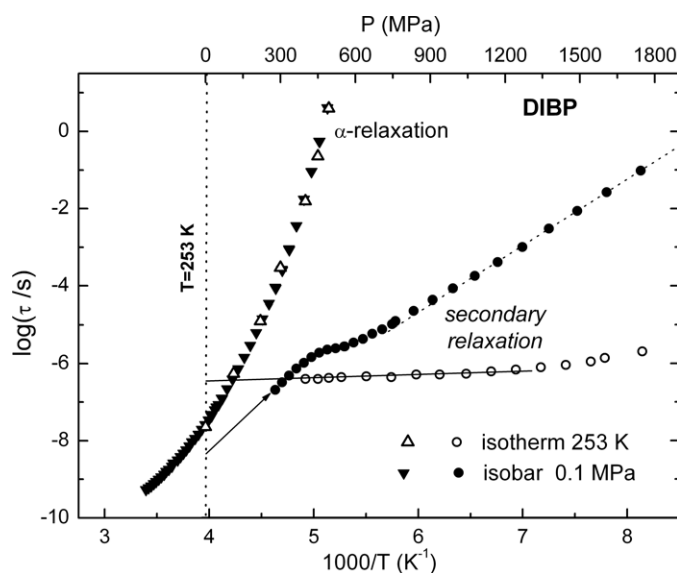


Figure 42. Temperature (\bullet , \blacktriangledown , lower axis, $P = 0.1$ MPa) and pressure (\circ , \triangle , upper axis, $T = 253$ K) dependences of the α - and secondary-relaxation time of di-isobutylphthalate. The abscissa scales were adjusted to superimpose the τ_α . The solid lines represent the extrapolation of secondary relaxation times above the glass transition (Paluch *et al* 2005).

8.4. Properties of secondary relaxations below T_g

Even though secondary relaxation times in the glassy state have a weaker temperature dependence and are relatively insensitive to pressure, neither their activation energy nor activation volume are zero. Interestingly, as shown by Olsen (1998) for glassy sorbitol, the relaxation time and the dielectric strength depend on the thermal history (notwithstanding the rough superpositioning seen in figure 40(b) for τ_β of sorbitol measured at different pressures below T_g). A similar dependence of secondary relaxation times on thermal and pressure history is seen for *m*-fluoroaniline (Reiser *et al* 2004) and DIBP (Paluch *et al* 2005): isothermal and isobaric quenching into the glassy state results in significantly different secondary relaxation times. Also, the activation energy for the secondary relaxations in DIBP are larger when the glass is formed at higher pressure. These results show clearly that the properties of the secondary relaxation in the glassy state depend upon the density.

9. Decoupling phenomena

A topic eliciting much interest over the past decade is the difference between translational and rotational diffusion in supercooled liquids (Rössler 1990, Ediger *et al* 1996, Sillescu 1999). The classical expressions are the Stokes–Einstein (SE) equation relating the translational diffusion coefficient, D_T , to the viscosity of the medium

$$D_T = \frac{kT}{6\pi\eta\bar{r}} \quad (50)$$

and the Debye–Stokes–Einstein (DSE) equation for the rotational diffusion correlation time, τ_R

$$\tau_R = \frac{4\pi\eta\bar{r}^3}{3kT} \quad (51)$$

(Einstein 1905, 1956, Debye 1929, Tyrell and Harris 1984). In these equations \bar{r} is the radius of the particle. Although these relations were derived from a simple hydrodynamic model for macroscopic (Brownian) particles, they have been successfully applied to molecular motions in (low viscosity) liquids and of probes surrounded by the host molecules of similar or smaller size. Since the product $D_T \tau_R$ is independent of the temperature and viscosity, the rotational and translational motions are expected to exhibit the same temperature dependence. However, as the temperature is lowered towards the glass transition temperature, the ratios $\eta/T \tau_R$ and $\eta D_T/T$ monotonically increase. Such departures from the SE and the DSE relations, referred to as decoupling phenomena, have been observed in many supercooled liquids (Rössler 1990, Fujara *et al* 1992, Fischer *et al* 1992, Chang *et al* 1994, Inoue *et al* 1995, Chang and Sillescu 1997, Swallen *et al* 2003). Interestingly, there are few materials (di-*n*-butylphthalate, tricresyl phosphate and squalene) for which no variation of $\eta/T \tau_R$ with temperature is seen (Dufour *et al* 1994, Behrens *et al* 1996, Deegan *et al* 1999).

It is commonly believed that spatially heterogeneous dynamics is responsible for the decoupling phenomena. Translational diffusion reflects the ‘fast’ molecules, whereas the mean rotational time is dominated by domains of ‘slow’ molecules (Cicerone and Ediger 1996, Chang and Sillescu 1997, Cicerone *et al* 1997). According to this interpretation, variation in the SE ratio reflects the temperature dependence of the characteristic length scale for the glass transition (Fischer *et al* 1992). However, this explanation cannot rationalize the decoupling phenomenon observed between the viscosity and dielectric relaxation time, since both sample the local environment. Moreover, in TNB, for example, which exhibits decoupling of diffusion and viscosity (Plazek and Magill 1966, Magill and Plazek 1967), the shape of the dielectric α -peak is invariant to temperature over the entire supercooled range (Richert *et al* 2003). Such a result is at odds with an interpretation of the decoupling phenomenon as arising from spatially heterogeneous dynamics (Richert *et al* 2003, Swallen *et al* 2003). An alternative explanation from the CM (Ngai 1999b, 1999c) shows the decoupling as a natural consequence of dynamic variables having different degrees of intermolecular cooperativity.

The decoupling phenomenon referred to above pertains to temperature dependences. However, the relaxation and transport properties of supercooled liquids also vary with pressure. Beyond the scientific merits of investigating the relative magnitudes of these pressure-dependences, the difficulty of measuring viscosity under large hydrostatic compression makes the correlation between η and dielectric relaxation times of practical value—determinations of the latter can be used to deduce the former (Suzuki *et al* 1997). Of course, the paucity of viscosity data at large pressure has limited the study of this topic.

Viscosity and dielectric relaxation measurements on salol as a function of pressure showed decoupling of η and τ_α (figure 43) (Casalini *et al* 2003a). Interestingly, the magnitude of the difference between their pressure dependences is lower at higher temperatures, even though these data correspond to very high pressure. The implication is that, at high temperature and low pressure the viscosity and relaxation times are coupled, consistent with results for ambient pressure (Stickel *et al* 1995, 1996).

Figure 44 shows data for DBP (Paluch *et al* 2003e, Cook *et al* 1993), for which the decoupling is absent at ambient pressure (Dufour *et al* 1994, Behrens *et al* 1996). The quantity $\eta/T \tau$, determined by interpolation of the viscosity data is constant over the entire pressure range, in conformance with the DSE relation (equation (51)). The origin of this behaviour is related to the nature of the intermolecular cooperativity in DBP (Paluch *et al* 2003e). As demonstrated for various glass formers, decoupling of relaxational and transport properties is correlated with the breadth of the relaxation function (Ngai 1999c). This indication is that the breakdown of the DSE equation is a manifestation of the strong intermolecular cooperativity that develops near T_g . For DBP, intermolecular cooperativity is relatively weak even near

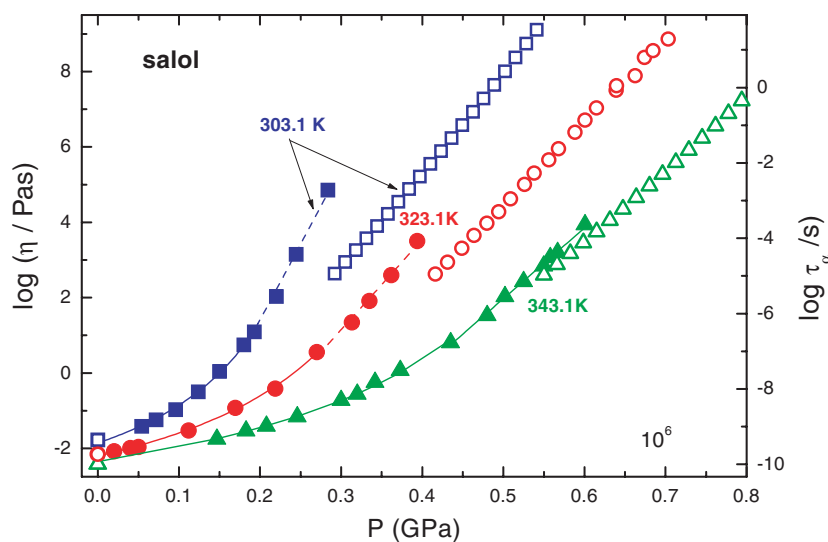


Figure 43. Viscosities (■, ▲, ●, left ordinate) from Schug *et al* (1998) and α -relaxation times (□, △, ○, right ordinate) from Casalini *et al* (2003a) for salol as a function of pressure. The ordinate scales were adjusted to make the atmospheric values of η and τ_α coincide. The lines through the viscosity points are only to guide the eyes.

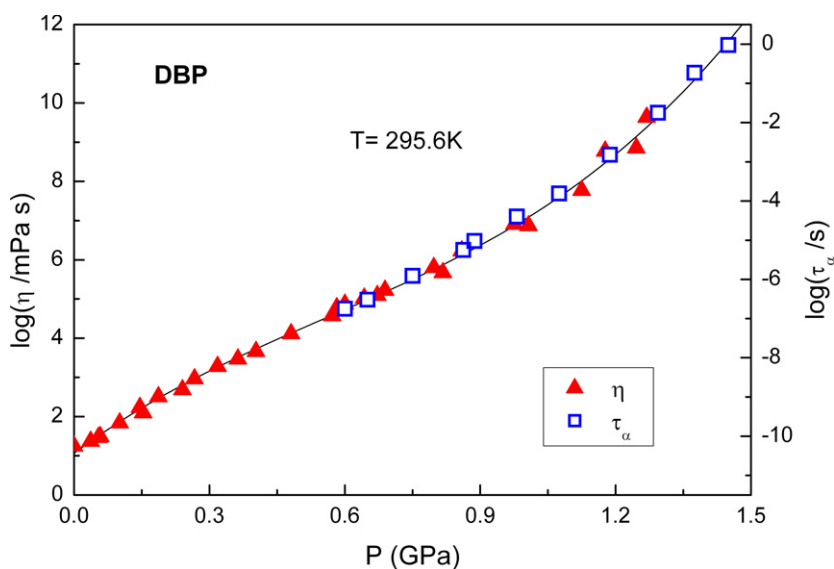


Figure 44. Dielectric α -relaxation times (□) from Paluch *et al* (2003e) and viscosities (▲) from Cook *et al* (1993) for dibutylphthalate as a function of pressure at $T = 295.6$ K. The solid line is a cubic polynomial fit.

T_g , as evidenced by its small fragility ($=69$) (Böhmer *et al* 1993) and narrow loss peak (FWHM < 1.8 decades) (Sekuła *et al* 2004). Thus, as T_g is approached by either cooling or compression, there is only a modest change in dynamics; consequently, no decoupling is observed.

Suzuki and co-workers compared dielectric relaxation times and viscosities at high pressures for a number of supercooled liquids, including dioctyl phthalate, tricresyl phosphate (Suzuki *et al* 2000) and naphthenic oil (Masuko *et al* 1997). Good agreement was found between the two quantities, suggesting the use of high pressure dielectric measurements to predict the viscosity behaviour under those conditions, using

$$\eta(T, P) = \eta_{\text{ref}}(T) \frac{K(T, P)\tau_{\alpha}(T, P)}{K_{\text{ref}}(T)\tau_{\text{ref}}(T)}, \quad (52)$$

where K is the bulk modulus, and the reference state refers to ambient pressure.

Another example of the relationship between the translational and rotational motions is the coupling/decoupling of the dielectric relaxation time and the dc conductivity, σ_{dc} ($=\varepsilon_0\omega\varepsilon''(\omega)$, where ε_0 is the permittivity of air). Since the conductivity is proportional to the diffusion constant of the ions (Nernst–Einstein relation), it follows from equations (50) and (51) that (Hansen and McDonald 1986)

$$\frac{\sigma_{\text{dc}}\tau_{\alpha}T}{c} = \text{constant} \quad (53)$$

in which c is the ion concentration. Near the glass transition, a temperature change of several degrees changes σ_{dc} and τ_{α} by orders of magnitude, so that the temperature factor can be neglected, giving (Stickel *et al* 1996)

$$\sigma_{\text{dc}}\tau_{\alpha} = \text{constant}. \quad (54)$$

This assumes the usual case that the number of charge carriers is constant. This relation is also referred to as the DSE relation, which can be misleading in light of equation (51). On the other hand, it should be stressed that equations (53) and (54) describe molecular motions of two different particles: the translational motion of ions (usually present as contaminants in any liquid) to the rotational motion of the host molecules. Since the dc conductivity is expected to be inversely proportional to the viscosity of the liquid, the relevant viscosity for both types of motion is the same. The advantage of broadband dielectric spectroscopy in assessing equation (54) is that both σ_{dc} and τ_{α} are measured simultaneously.

The relationship between σ_{dc} and τ has been examined for both low molecular weight and polymeric glass-formers. For some materials, at least in the investigated range, conformance to equation (54) was reported: propylene carbonate, salol (Stickel *et al* 1996), cresylglycidyl-ether (CGE) (Corezzi *et al* 1997, Capaccioli *et al* 1998). However, for other materials there is decoupling between σ_{dc} and τ_{α} : PDE (Stickel *et al* 1996), N,N-diglycidyl-4-glycidoyloxyaniline (DGGOA) (Corezzi *et al* 1999b) 3KNO₃-2Ca(NO₃)₂(CKN) (Pimenov *et al* 1996), diglycidylether of bisphenol A (DGEBA) oligomers (Koike 1993), and poly(propylene oxide) (Ratner *et al* 2000). When the DSE relation breaks down, a phenomenological equation can be used (Sasabe and Saito 1972, Koike and Tanaka 1991)

$$\sigma_{\text{dc}}\tau_{\alpha}^s = \text{constant}, \quad (55)$$

which is known as the fractional DSE equation (FDSE). The fractional exponent $s \leq 1$ is a measure of the enhancement of the ion diffusion relative to the rotational motion of the host molecules. From equation (3) and defining the activation volume for the conductivity as $\Delta V_{\sigma}^{\#} = -RT(d \ln \sigma / dP)|_T$, the FDSE exponent can be related to the ratio of the activation volume for the two dynamic quantities (Psurek *et al* 2002)

$$s = \frac{\Delta V_{\sigma}^{\#}}{\Delta V_{\tau}^{\#}}. \quad (56)$$

Since $s \leq 1$, this means that the activation volume for the α -relaxation is equal to or larger than for σ_{dc} . This is expected since the mobile ions are presumably more spherical and smaller than host molecules.

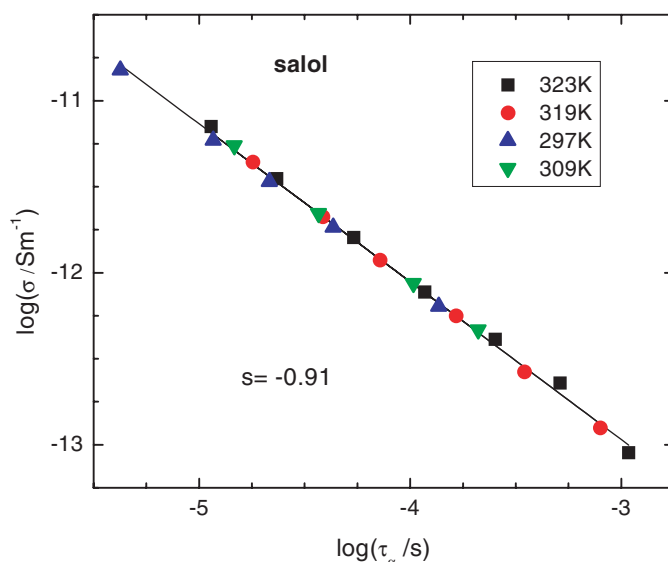


Figure 45. Double logarithmic plot of dc conductivity versus α -relaxation time for salol as a function of pressure at the indicated temperatures (Casalini *et al* 2003a).

It is of interest to assess conformity to equation (55) for data obtained at elevated pressure. Usually, the fractional exponent s is the same for variations of T (isobaric measurements) as for variations of P (isothermal measurements); however, there are some exceptions. For poly(propylene glycol)-bis(2,3-epoxypropyl ether) (Paluch 2000), s is smaller for measurements at high pressure. For salol the fractional exponent is unity (no decoupling) at atmospheric pressure (Stickel *et al* 1996), but at high pressure $s = 0.91 \pm 0.01$ (see figure 45 from the data in Casalini *et al* 2003a). Many high-pressure dielectric experiments have been made on epoxy resins, which are convenient because they tend not to crystallize, have large dipole moment (originating from the oxirane group) and have moderately high values of T_g . In figure 46 data for three isotherms and one (ambient pressure) isobar are shown for a bisphenol-A-propoxylate diglycidylether. All data fall on the same curve, yielding $s = 0.75$. There is enhancement of the translational motions over the rotations, and the degree of the decoupling is the same for the T - and P -dependences (Psurek *et al* 2002).

These findings are the general features of the supercooled dynamics. For example, isothermal data for three temperatures and isobaric measurements at two pressures on the epoxy poly((phenyl glycidyl ether)-co-formaldehyde showed that the FDSE equation describes all data with a common value of $s = 0.81$ (Paluch *et al* 2002g). For another series of epoxies, the exponent was independent of T and P , increasing systematically with molecular size (Psurek *et al* 2004). This is expected, given equation (56) and the fact that the activation volume for the α -relaxation generally increases with molecular size (Floudas *et al* 1999a, Hensel-Bielowka *et al* 2002b, Paluch *et al* 2002b, Casalini *et al* 2003c, Psurek *et al* 2004) (although only for a homologous series of chemically similar materials (Roland *et al* 2003a)).

A contrary example is found with propylene glycol and its oligomers (Casalini and Roland 2003c). From dielectric measurements at high pressure, s was found to be temperature and pressure independent. However, the FDSE exponent was invariant to molecular weight of the glycols, $s = 0.84 \pm 0.02$ (figure 47).

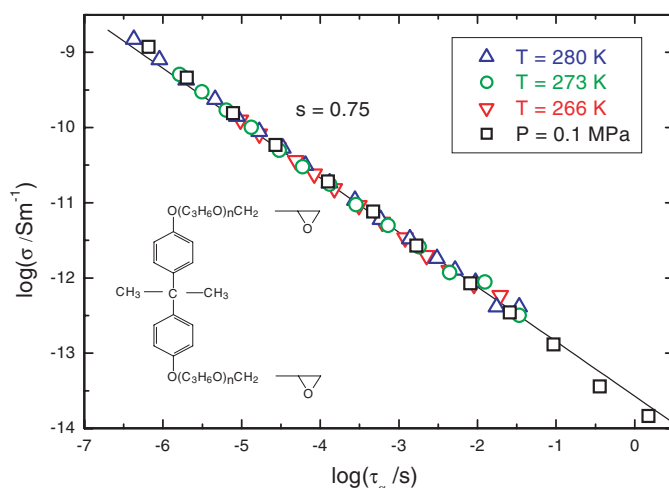


Figure 46. Double logarithmic plot of dc conductivity versus α -relaxation time for a bisphenol-A-propoxyate diglycidylether as a function of pressure at the indicated temperatures (Psurek *et al* 2002).

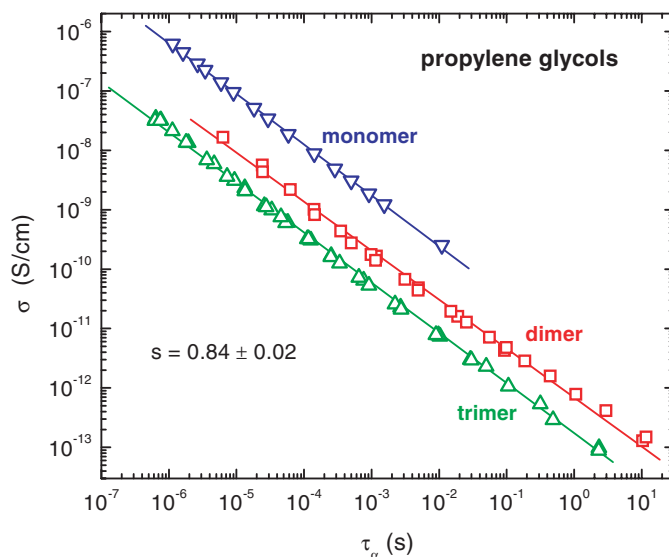


Figure 47. Double logarithmic plot of conductivity versus α -relaxation time for propylene glycol at $T = 216.7$ K and $65 < P$ (MPa) < 865 (∇); PPG dimer at $T = 216.8, 225.6$ and 238.4 K and $0.1 < P$ (MPa) < 594 (\square); and PPG trimer at $T = 223.5, 235.4$ and 245.3 K and $0.1 < P$ (MPa) < 632 (Δ). The power-law exponent is independent of molecular weight (Casalini and Roland 2003c).

10. Dielectric normal mode

The main focus of this review is the glass transition dynamics of polymers and molecular liquids; however, at lower frequencies in the dielectric spectra of type-A polymers (dipoles parallel to the chain backbone) a contribution to the loss is observed owing to global chain

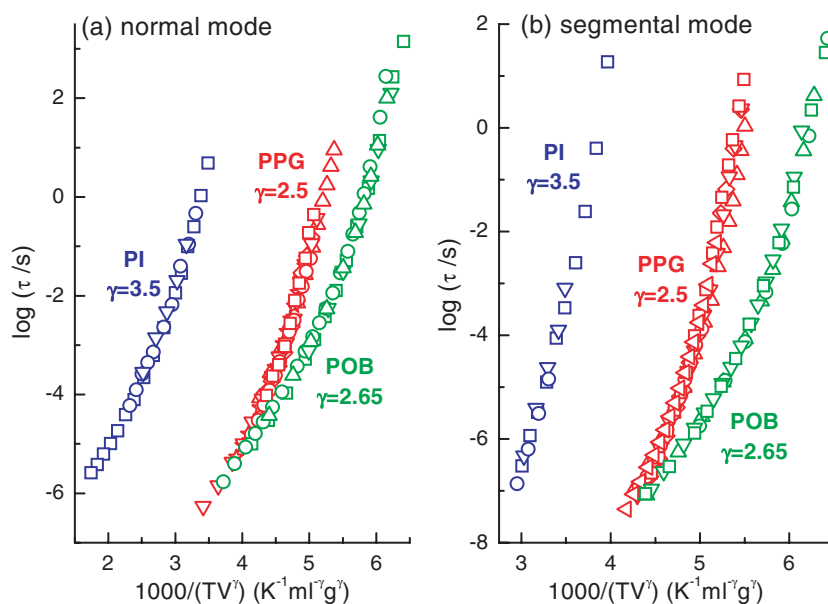


Figure 48. (a) Normal mode (b) segmental mode relaxation times for 1,4-polyisoprene, polypropylene glycol and polyoxybutylene, as a function of the reciprocal of the product of temperature and specific volume, with V raised to the indicated power. The different symbols refer to different measurement conditions of T and P (Roland *et al* 2004d, Casalini and Roland 2005b).

motions (Stockmayer 1967, Adachi and Kotaka 1993). These dielectric loss peaks are commonly referred to as the normal modes, in reference to the analysis of bead-spring models in terms of normal coordinates. Although according to most rheological models (Ferry 1980, Doi and Edwards 1986), global motions are governed by the same local friction coefficient associated with local segmental motion, it is well-known that the temperature dependence of the latter is stronger (Plazek 1965, 1966, Schönhalz 1993, Ngai and Plazek 1995, Santangelo *et al* 1996, Santangelo and Roland 1998, Roland *et al* 2001, 2004c, Mijovic *et al* 2002). In experiments, where both modes are simultaneously observed (usually requiring broad band measurements in the glass transition zone) there is a breakdown of time-temperature superpositioning results. Moreover, studies at elevated pressure show that both the pressure- and volume-dependences of the normal mode are also weaker than those for the segmental mode (Floudas and Reisinger 1999, Floudas *et al* 1999a, Roland *et al* 2003c, Casalini and Roland 2005b).

In figure 48(a), normal mode relaxation times for 1,4-polyisoprene (PI), polypropylene glycol (PPG4000) and polyoxybutylene (POB) are displayed versus TV^γ , along with the corresponding local segmental relaxation times in figure 48(b) (Roland *et al* 2004d, Casalini and Roland 2005b). It is of interest that the global (normal mode) relaxation times, measured at various temperatures and pressure, superpose as a function of TV^γ . However, more remarkable is the fact that the value of the exponent yielding superposition is the same for the two relaxation modes.

It may seem paradoxical that the normal and segmental mode relaxation times are functions of the same quantity, T^1V^γ , yet have different T - and P -dependences. In fact, the curves in figure 48(a) have different curvature than those in figure 48(b), implying that the T^1V^γ -dependences of the two relaxation times are also different. This is illustrated in

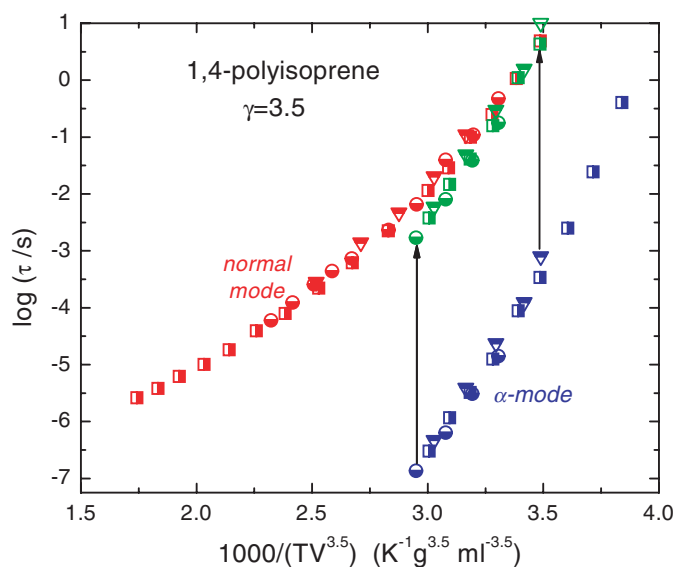


Figure 49. Data from figure 48 for PI. Vertical shifting of the local segmental relaxation times evidences their stronger variation with $TV^{3.5}$ in comparison with the dependence of the global relaxation times (Roland *et al* 2004d, Ngai *et al* 2005).

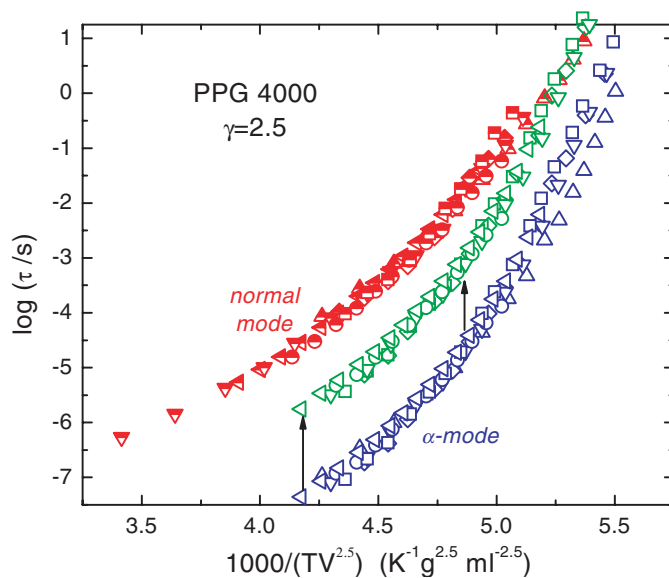


Figure 50. Data from figure 48 for PPG4000. Vertical shifting of the local segmental relaxation times evidences their stronger variation with $TV^{2.5}$ in comparison with the dependence of the global relaxation times (Roland *et al* 2004d, Ngai *et al* 2005).

figures 49–51, in which the τ_α are moved to coincide with the normal mode data at low T and high P . The respective curves diverge, reflecting the stronger dependence of τ_α on T^1V^γ .

An explanation accounting for this behaviour can be drawn from the coupling model. The idea is that the underlying non-cooperative relaxation time, τ_0 , of the model (which

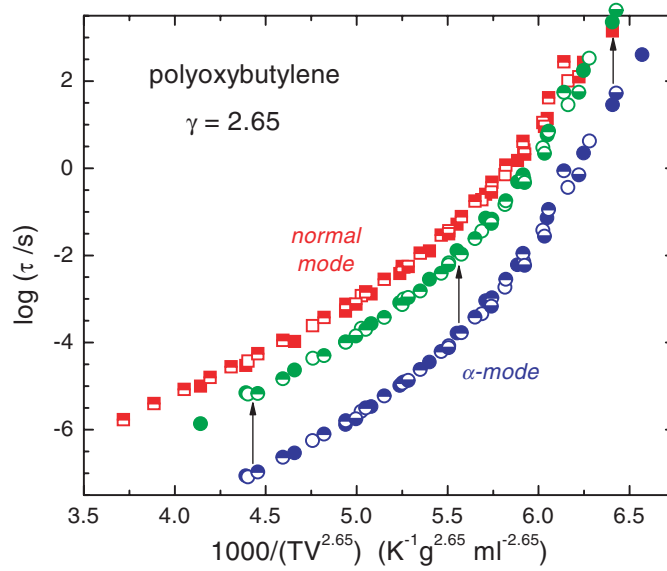


Figure 51. Data from figure 48 for POB. Vertical shifting of the local segmental relaxation times evidences their stronger variation with $TV^{2.65}$ in comparison with the dependence of the global relaxation times (Casalini and Roland 2005b, Ngai *et al* 2005).

can be identified with the JG relaxation, see section 8.1) is a function of the same product variable, T^1V^γ . However, the observed relaxation times are raised to a power of $1/\beta_{\text{KWW}}$ (equation (44)), so that the different $-T$, $-P$ (or $-V$) dependences are consequences of the different degree of intermolecular coupling, as reflected in the magnitude of the KWW stretch exponent for the two relaxation modes (Ngai *et al* 2005)

$$\tau = f([\tau_0(TV^\gamma)]^{1/\beta_{\text{KWW}}}). \quad (57)$$

Note that β_{KWW} is larger (weaker intermolecular coupling) for global motions, constrained by entanglement interactions, in comparison with the β_{KWW} for local segmental relaxation. This gives the prediction of weaker $-T$, $-P$ and $-TV^\gamma$ dependences for the chain dynamics.

11. Blends

Blends of low molecular weight liquids are used to study the supercooled state for materials having a tendency to crystallize, since mixing retards crystallization. Only a few studies of the dynamics of small molecule mixtures under pressure have been reported (Takahara *et al* 1999b, Köplinger *et al* 2000, Roland *et al* 2004a).

The miscibility (thermodynamic compatibility) is governed by the free energy of mixing

$$\Delta G_{\text{mix}} = \Delta H_{\text{mix}} - T \Delta S_{\text{mix}}, \quad (58)$$

where ΔG_{mix} is the change in Gibbs' free energy on mixing, ΔH_{mix} is the excess enthalpy and S_{mix} is the mixing entropy. A negative value of ΔG_{mix} indicates that the mixing occurs spontaneously. In the absence of specific interactions (van der Waals mixtures) an upper critical solution temperature (UCST) is expected, and pressure reduces miscibility because the positive (endothermic) interaction energy is increased (Rabeony *et al* 1998). However, even in such mixtures, pressure can enhance compatibility if the mixing volume is negative

(contraction upon blending) (Beiner *et al* 1998). For exothermic mixtures (which have a lower critical solution temperature, LCST), pressure enhances miscibility by promoting molecular interactions. Thus, pressure generally raises the critical temperature (higher UCST or LCST) (Rabeony *et al* 1998).

Generally, polymer blends are of the greatest interest because of their commercial significance. Blending can be a route for new materials, without the need to synthesize new polymers. The combinatorial entropy is small for polymers, so that the sign of ΔG_{mix} usually depends on ΔH_{mix} . This means that miscibility in polymer blends usually requires specific interactions, such as hydrogen bonding, between the components.

The theory of Flory–Huggins prediction for mixing free energy is

$$\frac{\Delta G_{\text{mix}}}{RT} = \frac{\phi}{V_A} \ln \phi + \frac{1-\phi}{V_B} \ln(1-\phi) + \chi \phi(1-\phi), \quad (59)$$

where V_A and V_B are the molecular volumes for the two components, ϕ is the volume fraction of the component A, and χ is the Flory–Huggins interaction parameter. The latter was originally considered to be purely enthalpic (equal to ΔH_{mix} normalized by thermal energy), which is true if the system is incompressible. However, experimental results such as neutron scattering (Janssen *et al* 1993) and photon correlation spectroscopy (Beiner *et al* 1998) show a strong dependence of critical temperature on pressure (of the order of 250 K GPa⁻¹). For chemically similar polymers close to their phase boundary, pressure enhances miscibility, in agreement with the findings that miscible polymer blends usually undergo densification on mixing. Thus, χ in equation (59) includes not only the mixing enthalpy but also the contribution from a change in volume upon mixing ('equation of state' effects (Flory *et al* 1968, Patterson 1982, Trask and Roland 1989)). In fact, a negative excess volume can give $\chi < 0$, even in the absence of specific chemical interactions (Trask and Roland 1988, Roland *et al* 1993).

Miscibility in blends implies a homogeneous morphology (and thus one T_g). Nevertheless, miscible polymer blends and disordered diblock copolymers can be dynamically heterogeneous. This means the blend components exhibit different τ_α and invariably requires that in the unmixed state, the components have very different glass transition temperatures (Colby 1989, Miller *et al* 1990, Roland and Ngai 1991). Two distinct α -relaxations have been observed in dielectric (Alegria *et al* 1994) and NMR (Chung *et al* 1994, Ngai and Roland 1995) spectra of miscible blends. Although each component experiences the same average environment (apart from chain connectivity), their response to the environment (intermolecular cooperativity) can differ, which, along with intrinsic mobility differences, gives rise to different relaxation behaviours (Roland and Ngai 1991, Cowie and Arrighi 1999). In general, the dynamic heterogeneity is controlled by both intramolecular and intermolecular interactions. The former are unimportant for small molecule mixtures, and for this reason, dynamic heterogeneity is only found in polymer blends.

There have been a few studies of the effect of pressure on the dynamics of blends and block copolymers. In dielectric measurements on poly(isoprene-*b*-vinylethylene) diblock copolymer (PI-*b*-PVE), Floudas *et al* (1999b) found that high pressure induces dynamic homogeneity; that is, under conditions of high P and T the spectrum is narrower. Under large hydrostatic pressure, the faster α -relaxation (due to the lower T_g PI block) shifts to lower frequency, merging with the peak due to the PVE. This was attributed to the larger activation volume for the PI segments compared with that of the PVE (Floudas *et al* 1999b).

However, in a dielectric study of blends of polystyrene with poly(vinyl methyl ether) (PS/PVME) (Alegria *et al* 2002, Floudas 2003), the application of pressure had no effect beyond increasing the blend T_g . The segmental relaxation time distributions (measured for the PVME only, since PS has a very weak dipole moment) were the same for different temperature-pressure conditions, when compared with a fixed value of the mean relaxation. Note that for

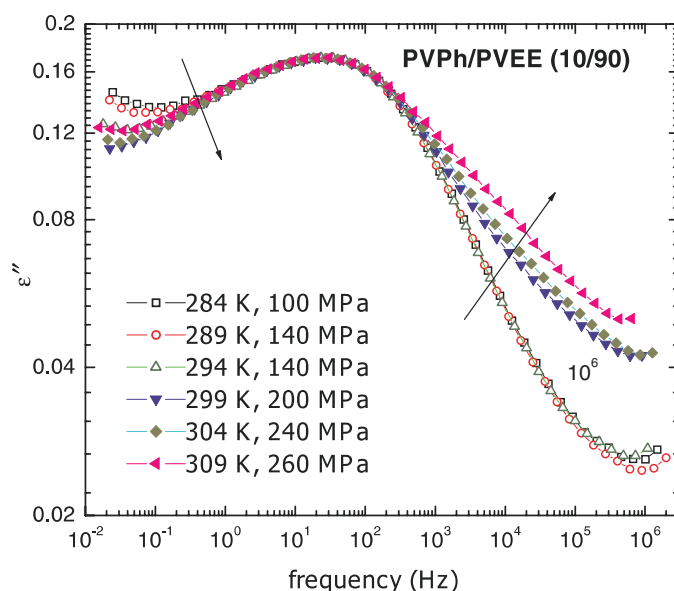


Figure 52. Dielectric α -relaxation peak for blends of 10% PVPh with 90% PVEE measured at different temperatures and pressures corresponding to a fixed τ_{α} . Arrows indicate the direction of increasing pressure (Mpoukouvalas *et al* 2005).

this blend, the component with the larger activation volume (PS) also has the higher T_g (Alegría *et al* 2002, Casalini and Roland 2003a, Roland and Casalini 2003b). The authors concluded that for a given value of the relaxation time, the shape of the α -peak was independent of the particular combination of temperature and pressure (Alegría *et al* 2002).

The presence of hydrogen bonding between the components not only enhances miscibility, but can also couple the component dynamics, making it more homogeneous. Since both pressure and temperature can affect the concentration of hydrogen bonds, such blends are of special interest for pressure studies. Hydrogen bonds are thermally-labile, and their strength always decreases with temperature. However, the effect of pressure is more complicated. There are data from experiments (Mammone *et al* 1980, Czelik and Jonas 1999) and molecular simulations (Root and Berne 1997), suggesting that pressure promotes formation of hydrogen bonds. However, other experiments (Naoki and Katahira 1991, Arencibia *et al* 2002) and Monte Carlo simulations (Jorgensen and Ibrahim 1982) indicate no effect from pressure or even a reduction in H-bonding. For water, the best-studied case, pressure clearly reduces the degree of H-bonding (Cook *et al* 1992, Poole *et al* 1994). Generally, the expectation is that there will be a higher concentration of hydrogen bonds at low temperature and low pressure, than at high pressure and high temperature. Typically, higher pressure experiments are conducted at higher temperatures, in order that the relaxation times fall within the measurement range. Thus, blends of poly(4-vinylphenol) (PVPh) with poly(vinyl ethyl ether) (PVEE) become more dynamically heterogeneous under elevated pressure, reflecting decreased H-bonding between the components (figure 52) (Mpoukouvalas *et al* 2005).

However, the opposite result is found for PVPh mixed with poly(ethylene-co-vinyl acetate) (EVA) (Zhang *et al* 2003). At high pressure and high temperature, the dielectric spectrum narrows, reflecting more homogeneous dynamics (figure 53). This is similar to the results for the PI-*b*-PVE block copolymer. However, the mechanism hypothesized therein, based on the difference in activation volumes, cannot apply to PVPh/EVA, since the higher T_g (i.e. slower)

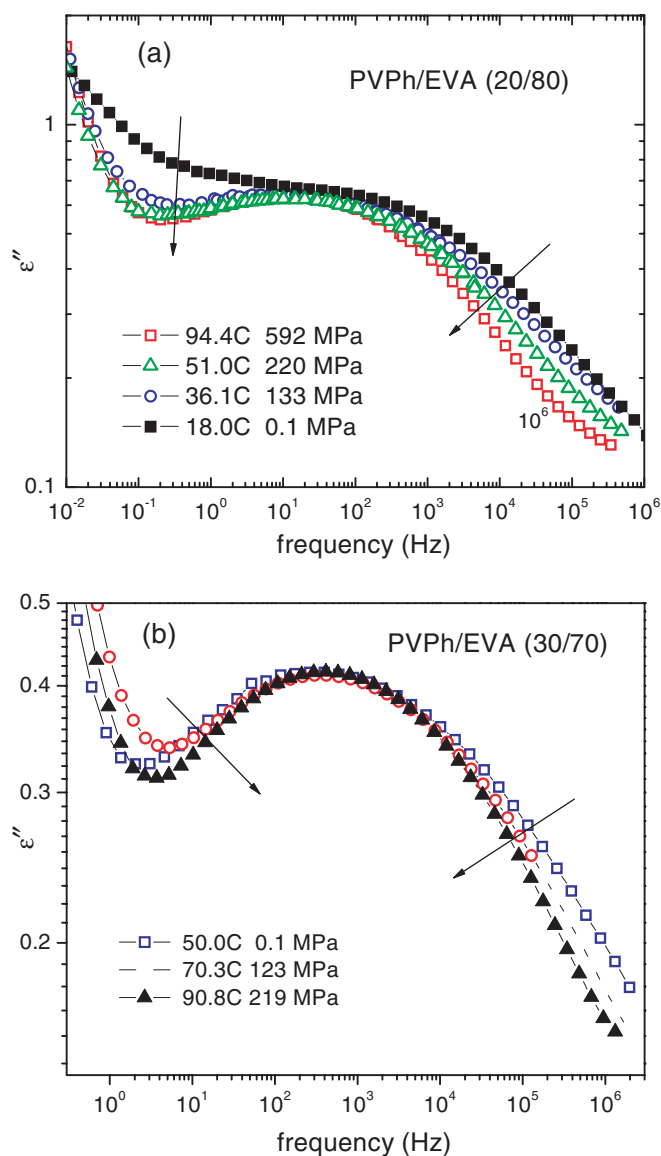


Figure 53. Dielectric α -relaxation peak for two blends of PVPh and EVA at different temperatures and pressures yielding a fixed τ_{α} : (a) 20% PVPh; (b) 30% PVPh. Arrows indicate the direction of increasing pressure (Zhang *et al* 2003).

component (PVPh) has the larger activation volume. Instead, the effect seems to relate to the presence of significant intramolecular hydrogen bonding in PVPh. At high T and P , these H-bonds tend to dissociate, making the blend more dynamically homogeneous (Zhang *et al* 2003).

In conclusion, even though the number of studies on blends under pressure is limited, very different behaviours have been observed. This demonstrates that the effect of pressure on the blend dynamics is complex, and future investigations should prove useful.

12. Summary

The use of hydrostatic pressure as an experimental variable allows investigation of aspects of the dynamics of glass-forming materials which otherwise could not be addressed. As a primary thermodynamic variable, pressure dependences are of fundamental importance for drawing structure-property relationships. Determination of the P -dependence of the dynamics, in combination with the EOS, enables the various factors (temperature, density, entropy, etc) governing τ_α to be quantified and intriguing phenomena such as the dynamic crossover and the decoupling of relaxation modes to be characterized and thus better understood. Beyond the primary relaxation, pressure facilitates study of other dynamic processes. For example, by taking advantage of different sensitivities to pressure, overlapping peaks can be resolved; such work has clarified the identity of the excess wing and JG processes as well as their relationship to the α -relaxation.

Notwithstanding the many experimental studies of the glass transition, including a limited number which utilize pressure, theoretical interpretations remain at the model-building stage. Herein we briefly discussed only those which offer predictions for the pressure behaviour of the structural relaxation. Unfortunately, application of these models usually requires adjustable parameters whose values cannot be corroborated directly by other means. Moreover, free-volume models also entail *ad hoc* corrections which are not easily justified. It seems that future theoretical progress will come from entropy models in combination with energy landscape ideas, since these can be more closely linked to measurable properties. In any event, the current limitations of theoretical descriptions of the glass transition underscore the need for continued experimental investigations, and certainly elevated pressure measurements will play an important role therein.

Acknowledgments

We thank J B Miller, K L Ngai and K S Schweizer for useful comments, and C Alba-Simionesco, C Dreyfus, G Floudas and J P Runt for kindly providing their data. The work at NRL was supported by the Office of Naval Research and that at Silesian University by the Committee for Scientific Research, Poland (KBN Grant #1 P03B 075 28).

References

- Adachi K and Kotaka T 1993 *Prog. Polym. Sci.* **18** 585
Adam G and Gibbs J H 1965 *J. Chem. Phys.* **43** 139
Alba-Simionesco C 1994 *J. Chem. Phys.* **100** 2250
Alba-Simionesco C, Fujimori H, Morineau D and Frick B 1997 *Prog. Theor. Phys. Suppl.* **126** 229
Alba-Simionesco C, Morineau D, Frick B, Higonencq N and Fujimori H 1998 *J. Non-Cryst. Solids* **235** 367
Alba-Simionesco C, Kivelson D and Tarjus G 2002 *J. Chem. Phys.* **116** 5033
Alba-Simionesco C, Cailliaux A, Alegria A and Tarjus G 2004 *Europhys. Lett.* **68** 58
Alegria A, Colmenero J, Ngai K J and Roland C M 1994 *Macromolecules* **27** 4486
Alegria A, Gómez D and Colmenero J 2002 *Macromolecules* **35** 2030
Andersson S P and Andersson O 1998 *Macromolecules* **31** 2999
Angell C A 1991 *J. Non-Cryst. Solids* **131–133** 13
Angell C A, Poole P H and Shao J 1994 *Nuovo Cimento D* **16** 993
Angell C A 1995 *Science* **267** 1924
Angell C A 2000 *J. Cond. Matter Phys.* **12** 6463
Angell C A, Ngai K L, McKenna G B, McMillan P F and Martin S F 2000 *J. Appl. Phys.* **88** 3113
Angell C A and Borick S 2002 *J. Non-Cryst. Solids* **307–310** 393
Arbe A, Richter D, Colmenero J and Farago B 1999 *Phys. Rev. E* **60** 1103
Arencibia A, Taravillo M, Pérez F J, Núñez J and Baonza V G 2002 *Phys. Rev. Lett.* **89** 195504

- Atake T and Angell C A 1979 *J. Phys. Chem.* **83** 3218
- Avramov I 2000 *J. Non-Cryst. Solids* **262** 258
- Babb S E 1963 *Rev. Mod. Phys.* **35** 400
- Ballard L, Yu A M, Reiner C and Jonas J 1998 *J. Magn. Reson.* **133** 190
- Barnett J D and Bosco C D 1969 *J. Appl. Phys.* **40** 3144
- Barnett J D, Block S and Piermarini G J 1973 *Rev. Sci. Instrum.* **44** 1
- Bartos J and Kristiak J 2000 *J. Phys. Chem. B* **104** 5666
- Bartos J, Kristiak J, Sausa O, Bandzuch P and Zrubcova J 2000 *Macromol. Symp.* **158** 111
- Behrens C F, Christiansen T G, Christensen T, Dyre J C and Olsen N B 1996 *Phys. Rev. Lett.* **76** 1553
- Beiner M, Fytas G, Meier G and Kumar S K 1998 *Phys. Rev. Lett.* **81** 594
- Bendler J T and Schlesinger M F 1987 *J. Mol. Liq.* **36** 37
- Bendler J T and Schlesinger M F 1988 *J. Stat. Phys.* **53** 531
- Bendler J T, Fontanella J J and Schlesinger M F 2001a *Phys. Rev. Lett.* **87** 195503
- Bendler J T, Fontanella J J, Schlesinger M F and Wintersgill M C 2001b *Electrochim. Acta* **46** 1615
- Bendler J T, Fontanella J J and Schlesinger M F 2003a *J. Chem. Phys.* **118** 6713
- Bendler J T, Fontanella J J, Schlesinger M F and Wintersgill M C 2003b *Electrochim. Acta* **48** 2267
- Bendler J T, Fontanella J J, Schlesinger M F and Wintersgill M C 2004 *Electrochim. Acta* **49** 5249
- Bergman R, Alvarez F, Alegria A and Colmenero J 1998 *J. Chem. Phys.* **109** 7546
- Bergman R, Mattson J, Svanberg C, Schwartz G A and Swenson J 2003 *Europhys. Lett.* **64** 675
- Bernu B, Hansen J P, Hiwatari Y and Pastore G 1987 *Phys. Rev. A* **36** 4891
- Bershtein V A, Egorov V M, Podolsky A F and Stepanov V A 1985 *J. Polym. Sci. Polym. Lett. Edn* **23** 371
- Bershtein V A and Ryzhov V A 1994 *J. Adv. Polym. Sci.* **114** 43
- Bershtein V A, Egorova L M and Prud'homme R E 1997 *J. Macromol. Sci. Phys. B* **36** 513
- Blochowicz T and Rössler E A 2004 *Phys. Rev. Lett.* **92** 225701
- Böhmer R, Ngai K L, Angell C A and Plazek D J 1993 *J. Chem. Phys.* **99** 4201
- Bordat P, Affouard F, Descamps M and Ngai K L 2004 *Phys. Rev. Lett.* **93** 105502
- Boyer R F and Spencer R S 1944 *J. Appl. Phys.* **15** 398
- Boyer R F 1985 *J. Polym. Sci. Polym. Phys. Edn* **23** 21
- Bridgman P W 1926 *Proc. Am. Arts Sci.* **61** 57
- Bridgman P W 1964 *Collected Experimental Papers* (Cambridge, MA: Harvard University Press)
- Calliaux A, Alba-Simonesco C, Frick B, Willner L and Goncharenko I 2003 *Phys. Rev. E* **67** 010802
- Cangialosi D, Wubbenhorst M, Schut H, Van Veen A and Picken S J 2004 *Proc. Mater. Sci. Forum* **445–6** 271
- Capaccioli S, Corezzi S, Gallone G, Rolla P A, Comez L and Fioretto D 1998 *J. Non-Cryst. Solids* **235–237** 576
- Caprion D and Schober H R 2002 *J. Chem. Phys.* **117** 2814
- Casalini R, Capaccioli S, Lucchesi M, Rolla P A and Corezzi S 2001a *Phys. Rev. E* **63** 031207
- Casalini R, Capaccioli S, Lucchesi M, Rolla P A, Paluch M, Corezzi S and Fioretto D 2001b *Phys. Rev. E* **64** 041504
- Casalini R and Roland C M 2002 *Phys. Rev. B* **66** 180201
- Casalini R, Capaccioli S, Lucchesi M, Paluch M, Corezzi S and Rolla P A 2002a *J. Non-Cryst. Solids* **307–310** 264
- Casalini R, Paluch M, Fontanella J J and Roland C M 2002b *J. Chem. Phys.* **117** 4901
- Casalini R and Roland C M 2003a *J. Chem. Phys.* **119** 4052
- Casalini R and Roland C M 2003b *Phys. Rev. Lett.* **91** 015702
- Casalini R and Roland C M 2003c *J. Chem. Phys.* **119** 11951
- Casalini R, Roland C M and Paluch M 2003a *J. Phys. Chem. A* **107** 2369
- Casalini R, Paluch M and Roland C M 2003b *J. Phys.: Condens. Matter* **15** S859
- Casalini R, Paluch M and Roland C M 2003c *Phys. Rev. E* **67** 031505
- Casalini R, Ngai K L and Roland C M 2003d *Phys. Rev. B* **68** 014201
- Casalini R, Paluch M and Roland C M 2003e *J. Chem. Phys.* **118** 5701
- Casalini R and Roland C M 2004a *Phys. Rev. B* **69** 094202
- Casalini R and Roland C M 2004b *Phys. Rev. E* **69** 062501
- Casalini R and Roland C M 2004c *Phys. Rev. Lett.* **92** 245702
- Casalini R and Roland C M 2004d *Colloid Polym. Sci.* **283** 107
- Casalini R, Paluch M, Psurek T and Roland C M 2004 *J. Mol. Liq.* **111** 53
- Casalini R and Roland C M 2005a *Phys. Rev. B* **71** 073501
- Casalini R and Roland C M 2005b *Macromolecules* **38** 1779
- Casalini R and Roland C M 2005c *Phys. Rev. B* **71** 014210
- Casalini R and Roland C M 2005d *Preprint cond-mat/0503489*
- Castro P and Delsuc M A 1998 *Magn. Reson. Chem.* **36** 833
- Chahid A, Alegria A and Colmenero J 1994 *Macromolecules* **27** 3282

- Chamberlin R V 1993 *Phys. Rev. B* **48** 15638
- Chandler D and Weeks J D 1970 *Phys. Rev. Lett.* **25** 149
- Chandler D, Weeks J D and Andersen H C 1983 *Science* **220** 4599
- Chang I, Fujara F, Heuberger B G G, Mangel T and Sillescu H 1994 *J. Non-Cryst. Solids* **172–174** 248
- Chang I and Sillescu H 1997 *J. Phys. Chem. B.* **101** 8794
- Chen J, Kow C, Fetters L J and Plazek D J 1982 *J. Polym. Sci. Polym. Phys. Edn* **20** 1565
- Chung G-C, Kornfield J A and Smith S D 1994 *Macromolecules* **27** 5729
- Cicerone M T and Ediger M D 1996 *J. Chem. Phys.* **104** 7210
- Cicerone M T, Wagner P A and Ediger M D 1997 *J. Phys. Chem. B* **101** 8727
- Cohen M H and Grest G S 1979 *Phys. Rev. B* **20** 1077
- Cohen M H and Grest G S 1984 *J. Non-Cryst. Solids* **61/62** 749
- Cohen M H and Turnbull D 1959 *J. Chem. Phys.* **31** 1164
- Colby R H 1989 *Polymer* **30** 1275
- Colucci D M, McKenna G B, Filiben J J, Lee A, Curlis D B, Bowman K B and Russell J D 1997 *J. Polym. Sci. B* **35** 1561
- Comez L, Fioretto D, Kriegs H and Steffen W 2002 *Phys. Rev. E* **66** 032501
- Comez L, Corezzi S, Fioretto D, Kriegs H, Best A and Steffen W 2004 *Phys. Rev. E* **70** 011504
- Cook R E, King H E and Peiffer D G 1992 *Phys. Rev. Lett.* **69** 3072
- Cook R L, Herbst C A and King H E 1993 *J. Phys. Chem.* **97** 2355
- Cook R L, King H E, Herbst C A and Herschbach D R 1994 *J. Chem. Phys.* **100** 5178
- Corezzi S, Capaccioli S, Gallone G, Livi A and Rolla P A 1997 *J. Phys.: Condens. Matter* **9** 6199
- Corezzi S, Rolla P A, Paluch M, Ziolo J and Fioretto D 1999a *Phys. Rev. E* **60** 4444
- Corezzi S, Campani E, Rolla P A, Capaccioli S and Fioretto D 1999b *J. Chem. Phys.* **111** 9343
- Corezzi S, Capaccioli S, Casalini R, Fioretto D, Paluch M and Rolla P A 2000 *Chem. Phys. Lett.* **320** 113
- Corezzi S, Beiner M, Huth H, Schroter K, Capaccioli S, Casalini R, Fioretto D and Donth E 2002 *J. Chem. Phys.* **117** 2435
- Cowie J M G and Arrighi V 1999 in *Polymer Blends and Alloys* ed G O Shonaike and G P Simon (New York: Dekker) chapter 4
- Cummins H Z 1996 *Phys. Rev. E* **54** 5870
- Cummins H Z, Li G, Hwang Y H, Shen G Q, Du W M, Hernandez J and Tao N J 1997 *Z. Phys. B* **103** 501
- Czelik C and Jonas J 1999 *Chem. Phys. Lett.* **302** 633
- Dalal E N and Phillips P J 1983 *Macromolecules* **16** 890
- Dasgupta C and Ramaswamy S 1992 *Physica A* **186** 314
- Dasgupta C, Indrani A V, Ramaswamy S and Phani M K 1991 *Europhys. Lett.* **15** 307
- Debenedetti P G and Stillinger F H 2001 *Nature* **410** 259
- Debenedetti P G, Stillinger F H, Truskett T M and Roberts C J 1999 *J. Phys. Chem. B* **103** 7390
- Debye P 1929 *Polar Molecules* (New York: Dover)
- Deegan R, Leheny R L, Menon N, Nagel S R and Venerus D C 1999 *J. Phys. Chem. B* **103** 4066
- Delangen M and Prins K O 1995 *Rev. Sci. Instrum.* **66** 5218
- De Michele C, Sciortino F and Coniglio A 2004 *J. Phys.: Condens. Matter* **16** L489
- Dixon P K, Wu L, Nagel S R, Williams B D and Carini J P 1990 *Phys. Rev. Lett.* **65** 1108
- Dlubek G, Kilburn D, Bondarenko V, Pionteck J, Krause-Rehberg R and Alam M A 2004a *Macromol. Symp.* **210** 11
- Dlubek G, Kilburn D and Alam M A 2004b *Electrochim. Acta* **49** 5241
- Dlubek G, Kilburn D and Alam M A 2005a *Electrochim. Acta* **50** 2351
- Dlubek G, Wawryszczuk J, Pionteck J, Gowrek T, Kaspar H and Lochhass K H 2005b *Macromolecules* **38** 429
- Doi M. and Edwards S F 1986 *The Theory of Polymer Dynamics* (Oxford: Clarendon)
- Donth E, Schroter K and Kahle S 1999 *Phys. Rev. E* **60** 1099
- Donth E, Huth H and Beiner M 2001 *J. Phys.: Condens. Matter* **13** L451
- Doolittle A K and Doolittle D B 1957 *J. Appl. Phys.* **28** 901
- Dreyfus C, Aouadi A, Gapinski J, Matos-Lopes M, Steffen, W, Patkowski A and Pick R M 2003 *Phys. Rev. E* **68** 011204
- Dreyfus C, Le Grand A, Gapinski J, Steffen W and Patkowski A 2004 *Eur. J. Phys.* **42** 309
- Drozd-Rzoska A, Rzoska S J, Paluch M, Pawlus S, Ziolo J, Santangelo P G and Roland C M 2005 *Phys. Rev. E* **71** 011508
- Dufour J, Jorat L, Bondeau A, Sibilini A and Noyel G 1994 *J. Mol. Liq.* **62** 75
- Dyre J and Olsen N B 2003 *Phys. Rev. Lett.* **91** 155703
- Dyre J C and Olsen N B 2004 *Phys. Rev. E* **69** 042501
- Ediger M D, Angel C A and Nagel S R 1996 *J. Phys. Chem.* **100** 13200

- Einstein A 1905 *Ann. Phys. (NY)* **17** 549
- Einstein A 1956 *Investigations on the Theory of Brownian Motion* (New York: Dover)
- Ellison C J, Mundra M K and Torkelson J M 2005 *Macromolecules* **38** 767
- Faupel F, Kanzow J, Gunther-Schade K, Nagel C, Sperr P and Kogel G 2004 *Proc. Mater. Sci. Forum* **445–6** 219
- Ferrer M L, Lawrence C, Demirjian B G, Kivelson D, Alba-Simionesco C and Tarjus G 1998 *J. Chem. Phys.* **109** 8010
- Ferry J D 1980 *Viscoelastic Properties of Polymers* (New York: Wiley)
- Fischer E W, Donth E and Steffen W 1992 *Phys. Rev. Lett.* **68** 2344
- Floudas G and Reisinger T 1999 *J. Chem. Phys.* **111** 5201
- Floudas G, Gravalides C, Reisinger T and Wegner G 1999a *J. Chem. Phys.* **111** 9847
- Floudas G, Fytas G, Reisinger T and Wegner G 1999b *J. Chem. Phys.* **111** 9129
- Floudas G 2003 *Broadband Dielectric Spectroscopy* ed F Kremer and A Schonhals (Berlin: Springer) chapter 8
- Floudas G, Mierzwa M and Schonhals A 2003 *Phys. Rev. E* **67** 031705
- Floudas G 2004 *Prog. Polym. Sci.* **29** 1143
- Flory P J, Ellenson J L and Eichinger B E 1968 *Macromolecules* **1** 279
- Forsman H, Andersson P and Bäckström G 1986 *J. Chem. Soc. Faraday Trans. II* **82** 857
- Frick K and Alba-Simionesco C 1999 *Physica B* **266** 53
- Frick K, Alba-Simionesco C, Andersen K H and Willner L P 2003 *Phys. Rev. E* **67** 051801
- Fujara F, Geil B, Sillescu H and Fleischer G 1992 *Z. Phys. B* **88** 195
- Fujima T, Frusawa H and Ito K 2002 *Phys. Rev. E* **66** 031503
- Fujiwara S and Yonezawa F 1996 *Phys. Rev. E* **54** 644
- Fulcher G S 1923 *J. Am. Ceram. Soc.* **8** 339
- Fytas G, Dorfmueller Th and Wang C H 1983 *J. Phys. Chem.* **87** 5041
- Fytas G, Patkowski A, Meier G and Dorfmueller Th 1982a *Macromolecules* **15** 21
- Fytas G, Patkowski A, Meier G and Dorfmueller Th 1982b *Macromolecules* **15** 870
- Fytas G, Meier G, Patkowski A and Dorfmueller Th 1982c *Colloid Polym. Sci.* **260** 949
- Fytas G, Patkowski A, Meier G and Dorfmueller Th 1984 *J. Chem. Phys.* **80** 2214
- Gapinski J, Paluch M and Patkowski A 2002 *Phys. Rev. E* **66** 011501
- Garwe F, Schonhals A, Lockwenz H, Beiner M, Schroter K and Donth E 1996 *Macromolecules* **29** 247
- Gilchrist A, Earley J E and Cole R H 1957 *J. Chem. Phys.* **26** 196
- Gitsas A, Floudas G and Wegner G 2004 *Phys. Rev. E* **69** 041802
- Goldstein M 1969 *J. Chem. Phys.* **51** 4767
- Goldstein M 2005 *Phys. Rev. B* **71** 136201
- Gomez D, Alegria A and Colmenero J 2001 *Macromolecules* **34** 503
- Götze W and Sjögren L 1992 *Rep. Prog. Phys.* **55** 241
- Götze W 1999 *J. Phys.: Condens. Matter* **11** A1
- Grabow M H and Andersen H C 1986 *Ann. NY Acad. Sci.* **484** 96
- Grest G S and Cohen M H 1980 *Phys. Rev. B* **21** 4113
- Grest G S and Cohen M H 1981 *Adv. Chem. Phys.* **48** 455
- Hansen J P and McDonald I R 1986 *Theory of Simple Liquids* 2nd edn (London: Academic)
- Hansen C, Stöckel F, Berger T, Richert R and Fischer E W 1997 *J. Chem. Phys.* **107** 1086
- Hempel E, Hempel, G, Hensel A, Schick C and Donth E 2000 *J. Phys. Chem. B* **104** 2460
- Hensel-Bielówka S and Paluch M 2002 *Phys. Rev. Lett.* **89** 025704
- Hensel-Bielówka S, Ziolo J, Paluch M and Roland C M 2002a *J. Chem. Phys.* **117** 2317
- Hensel-Bielówka S, Ziolo J, Paluch M and Roland C M 2002b *J. Phys. Chem. B* **106** 12459
- Hensel-Bielówka S, Pawlus S, Roland C M, Ziolo J and Paluch M 2004 *Phys. Rev. E* **69** 050501
- Hoffman J D, Williams G and Passaglia E 1966 *J. Polym. Sci. C* **14** 173
- Hollander A G S and Prins K O 2001 *J. Non-Cryst. Solids* **286** 1
- Hoover W G and Ross M 1971 *Contemp. Phys.* **12** 339
- Huang D, Colucci D M and McKenna G B 2002 *J. Chem. Phys.* **116** 3925
- Huber H, Mali M, Roos J and Brinkmann D 1984 *Rev. Sci. Instrum.* **55** 1325
- Imre A R, Maris H J and Williams P R (ed) 2002 *Liquids Under Negative Pressure* (Boston: Kluwer) ISBN 1-4020-0896-1
- Inoue T, Cicerone M T and Ediger M D 1995 *Macromolecules* **28** 3425
- Ito K, Moynihan C T and Angell C A 1999 *Nature* **398** 492
- Jäckle J 1986 *Rep. Prog. Phys.* **49** 171
- Janssen S, Schwahn D, Mortensen K and Springer T 1993 *Macromolecules* **26** 5587
- Jayaraman A 1983 *Rev. Mod. Phys.* **55** 65
- Jin H J, Gu X J, Wen P, Wang L B and Lu K 2003a *Acta Mater.* **51** 6219

- Jin H J, Wen P and Lu K 2003b *Appl. Phys. Lett.* **83** 3284
- Jobling A and Lawrence A S C 1951 *Proc. R. Soc. Lond. A* **206** 257
- Johari G P and Goldstein M 1970 *J. Chem. Phys.* **53** 2372
- Johari G P and Goldstein M 1971 *J. Chem. Phys.* **55** 4245
- Johari G P and Whalley E 1972 *Faraday Symp. Chem. Soc.* **6** 23
- Johari G P 1973 *J. Chem. Phys.* **58** 1766
- Johari G P 1986 *Polymer* **27** 866
- Johari G P and Pathmanathan K 1986 *J. Chem. Phys.* **85** 6811
- Johari G P, Powers G and Vij J K 2002 *J. Chem. Phys.* **116** 5908
- Johari G P 2003 *J. Chem. Phys.* **119** 635
- Jonsson H and Andersen H C 1988 *Phys. Rev. Lett.* **60** 2295
- Jorgensen W L and Ibrahim M 1982 *J. Am. Chem. Soc.* **104** 373
- Kamwer K, Rusch R and Johnson W L 1999 *Phys. Rev. Lett.* **82** 580
- King H E Jr, Herbolzheimer E and Cook R L 1992 *J. Appl. Phys.* **71** 2071
- King H E Jr and Prewitt C T 1980 *Rev. Sci. Instrum.* **51** 1037
- Kisliuk A, Mathers R T and Sokolov A P 2000 *J. Polym. Sci. Polym. Phys. Edn* **38** 2785
- Kob W and Andersen H C 1995 *Phys. Rev. E* **52** 4134
- Kob W, Barrat J L, Sciortino F and Tartaglia P 2000 *J. Phys.: Condens. Matter* **12** 6385
- Koike T and Tanaka R 1991 *J. Appl. Polym. Sci.* **42** 1333
- Koike T 1993 *Polym. Sci. Eng.* **33** 1301
- Koplinger J, Kasper G and Hunklinger S 2000 *J. Chem. Phys.* **113** 4701
- Koran F and Dealy J M 1999 *J. Rheol.* **43** 1279
- Kudlik A, Tschirwitz C, Benkhof S, Blochowicz T and Rössler E 1997 *Europhys. Lett.* **40** 649
- Kudlik A, Tschirwitz C, Blochowicz T, Benkhof S and Rössler E 1998 *J. Non-Cryst. Solids* **235** 406
- Kudlik A, Benkhof S, Blochowicz T, Tschirwitz C and Rössler E 1999 *J. Mol. Struct.* **479** 201
- Kulik A S and Prins K O 1993 *Polymer* **34** 4629
- Laughlin W T and Uhlmann D R 1972 *J. Phys. Chem.* **76** 2317
- Leheny R L and Nagel S R 1997 *Europhys. Lett.* **39** 447
- León C, Ngai K L and Roland C M 1999 *J. Chem. Phys.* **110** 11585
- Leslie-Pelecky D L and Birge N O 1994 *Phys. Rev. Lett.* **72** 1232
- Lewis L J and Wahnström G 1994 *Phys. Rev. E* **50** 3865
- Leyser H, Schulte A, Doster W and Petry W 1995 *Phys. Rev. E* **51** 5899
- Li W-X and Keyes T 1999 *J. Chem. Phys.* **111** 328
- Li M 2000 *Phys. Rev. B* **62** 13979
- Lovesey S W 1984 *Theory of Neutron Scattering from Condensed Matter* (Oxford: Clarendon)
- Lunkenheimer P, Pimenov A, Schiener B, Bohmer R and Loidl A 1996 *Europhys. Lett.* **33** 611
- Lunkenheimer P and Loidl A 2002 *Chem. Phys.* **284** 205
- Lunkenheimer P, Wehn R, Riegger T and Loidl A 2002 *J. Non-Cryst. Solids* **307–310** 336
- Macedo P B and Litovitz T A 1965 *J. Chem. Phys.* **42** 245
- MacKenzie J D 1958 *J. Chem. Phys.* **28** 1037
- Magill J H and Plazek D J 1967 *J. Chem. Phys.* **46** 3757
- Malhotra B D and Pethrick R A 1983 *Phys. Rev. B* **28** 156
- Mammone J F, Sharma S K and Nicol M 1980 *J. Phys. Chem.* **84** 3130
- March N H and Tosi M P 2003 *Introduction to Liquid State Physics* (Singapore: World Scientific)
- Martinez L M and Angell C A 2002 *Nature* **410** 663
- Mašlanka S, Paluch M, Sułkowski W W and Roland C M 2005 *J. Chem. Phys.* **122** 084511
- Masuko M, Suzuki A, Hanai S and Okabe H 1997 *Japan. J. Tribol.* **42** 286
- McCrum N G, Read B E and Williams G 1991 *Anelastic and Dielectric Effects in Polymeric Solids* (New York: Dover)
- Meier G, Gerharz B, Boese D and Fischer E W 1991 *J. Chem. Phys.* **94** 3050
- Middleton T F and Wales D J 2001 *Phys. Rev. B* **64** 024205
- Middleton T F and Wales D 2002 *J. Chem. Phys.* **118** 4583
- Mijovic J, Sun M and Han Y 2002 *Macromolecules* **35** 6417
- Miller J B, McGrath J, Roland C M, Trask C A and Garroway A N 1990 *Macromolecules* **23** 4543
- Miller J B, Walton J H and Roland C M 1993 *Macromolecules* **26** 5602
- Miller J B and Roland C M 1995 *Appl. Magn. Reson.* **8** 535
- Miyoshi T, Takegoshi K and Terao T 2002 *Macromolecules* **35** 151
- Mpoukouvalas K and Floudas G 2003 *Phys. Rev. E* **68** 031801
- Mpoukouvalas K, Floudas G, Zhang S H and Runt J 2005 *Macromolecules* **38** 552

- Mueser M H, Loeding D, Nielaba P and Binder K 1998 *Ferroelectrics* **208–209** 293
- Mukherjee A, Bhattacharyya S and Bagchi B 2002 *J. Chem. Phys.* **116** 4577
- Munro R G, Piermarini G J and Block S 1978 *J. Appl. Phys.* **50** 3180
- Naoki M and Matsushita M 1983 *Bull. Chem. Soc. Japan* **56** 5628
- Naoki M and Owada A 1984 *Polymer* **25** 75
- Naoki M, Matsumoto K and Matsushita M 1986 *J. Phys. Chem.* **90** 4423
- Naoki M, Endou H and Matsumoto K 1987 *J. Phys. Chem.* **91** 4169
- Naoki M and Katahira S 1991 *J. Phys. Chem.* **95** 431
- Nauroth M and Kob W 1997 *Phys. Rev. E* **55** 657
- Ngai K L and Roland C M 1993 *Macromolecules* **26** 6824
- Ngai K L and Plazek D J 1995 *Rubber Chem. Tech.* **68** 376
- Ngai K L and Roland C M 1995 *Macromolecules* **28** 4033
- Ngai K L 1998a *J. Chem. Phys.* **109** 6982
- Ngai K L 1998b *Physica A* **261** 36
- Ngai K L 1999a *J. Phys. Chem. B* **103** 5895
- Ngai K L 1999b *Phil. Mag. B* **79** 1783
- Ngai K L 1999c *J. Phys. Chem. B* **103** 10684
- Ngai K L and Tsang K Y 1999 *Phys. Rev. E* **60** 4511
- Ngai K L, Bao L-R, Yee A F and Soles C L 2001 *Phys. Rev. Lett.* **87** 215901
- Ngai K L and Roland C M 2002 *Polymer* **43** 567
- Ngai K L 2003 *J. Phys.: Condens. Matter* **15** S1107
- Ngai K L 2004 *Phil. Mag.* **84** 1341
- Ngai K L and Paluch M 2004 *J. Chem. Phys.* **120** 857
- Ngai K L and Capacioli S 2004 *Phys. Rev. E* **69** 031501
- Ngai K L, Casalini R and Roland C M 2005 *Macromolecules* at press
- Novikov V N and Sokolov A P 2003 *Phys. Rev. E* **67** 031507
- Novikov V N and Sokolov A P 2004 *Nature* **431** 961
- Nozaki R, Zenitani H, Minoguchi A and Kitai K 2002 *J. Non-Cryst. Solids* **307–310** 349
- Olabisi O and Simha R 1975 *Macromolecules* **8** 206
- Oldekop V W 1957 *Glastec. Ber.* **30** 8
- Oliver W F, Herbst C A, Lindsay S M and Wolf G H 1991 *Phys. Rev. Lett.* **67** 2795
- Olsen N B 1998 *J. Non-Cryst. Solids* **235–237** 399
- Olsen N B, Christensen T and Dyre J C 2000 *Phys. Rev. E* **62** 4435
- Omi H, Nagasaka B, Miyakubo K, Ueda T and Eguchi T 2004 *Phys. Chem. Chem. Phys.* **6** 1299
- Orbon S J and Plazek D J 1982 *J. Polym. Sci. Polym. Phys. Edn* **20** 1575
- O'Reilly J M 1962 *J. Polym. Sci.* **57** 429
- Pakula T 2000 *J. Mol. Liq.* **86** 109
- Pakula T and Teicmann J 1997 *Mater. Res. Soc. Symp. Proc.* **455** 211
- Paluch M, Rzoska S J, Habdas P and Ziolo J 1998 *J. Phys.: Condens. Matter* **10** 4131
- Paluch M, Hensel-Bielowka S and Ziolo J 1999 *J. Chem. Phys.* **110** 10978
- Paluch M 2000 *J. Phys.: Condens. Matter* **12** 9511
- Paluch M, Patkowski A and Fisher E W 2000a *Phys. Rev. Lett.* **85** 2140
- Paluch M, Hensel-Bielowka S and Psurek T 2000b *J. Chem. Phys.* **113** 4374
- Paluch M, Hensel-Bielowka S and Ziolo J 2000c *Phys. Rev. E* **61** 526
- Paluch M 2001 *J. Chem. Phys.* **115** 10029
- Paluch M, Gapinski J, Patkowski A and Fischer E W 2001a *J. Chem. Phys.* **114** 8048
- Paluch M, Ngai K L and Hensel-Bielowka S 2001b *J. Chem. Phys.* **114** 10872
- Paluch M, Roland C M and Pawlus S 2002a *J. Chem. Phys.* **116** 10932
- Paluch M, Pawlus S and Roland C M 2002b *Macromolecules* **35** 7338
- Paluch M, Casalini R, Hensel-Bielowka S and Roland C M 2002c *J. Chem. Phys.* **116** 9839
- Paluch M, Psurek T and Roland C M 2002d *J. Phys.: Condens. Matter* **14** 9489
- Paluch M, Roland C M and Best A 2002e *J. Chem. Phys.* **117** 1188
- Paluch M, Casalini R, Best A and Patkowski A 2002f *J. Chem. Phys.* **117** 7624
- Paluch M, Psurek T and Roland C M 2002g *J. Phys.: Condens. Matter* **14** 9489
- Paluch M and Roland C M 2003 *J. Non-Cryst. Solids* **316** 413
- Paluch M, Roland C M, Gapinski J and Patkowski A 2003a *J. Chem. Phys.* **118** 3177
- Paluch M, Roland C M, Casalini R, Meier G and Patkowski A 2003b *J. Chem. Phys.* **118** 4578
- Paluch M, Casalini R and Roland C M 2003c *Phys. Rev. E* **67** 021508

- Paluch M, Roland C M, Pawlus S, Ziolo J and Ngai K L 2003d *Phys. Rev. Lett.* **91** 115701
- Paluch M, Sekula M, Pawlus S, Rzoska S J, Ziolo J and Roland C M 2003e *Phys. Rev. Lett.* **90** 175702
- Paluch M, Pawlus S, Hensel-Bielowka S, Sekula M, Psurek T, Rzoska S J and Ziolo J 2005 unpublished
- Pan M X, Wang J G, Yao Y S, Zhao D Q and Wang W H 2004 *Appl. Phys. Lett.* **78** 601
- Papadopoulos P, Peristeraki D, Floudas G, Koutalas G and Hadjichristidis N 2004 *Macromolecules* **37** 8116
- Parry E J and Tabor D 1973 *J. Phys. D: Appl. Phys.* **6** 1328
- Pasterny K, Paluch M, Grzybowka K and Grzybowski A 2004 *J. Mol. Liq.* **109** 137
- Patkowski A, Paluch M and Kriegs H 2002 *J. Chem. Phys.* **117** 2192
- Patkowski A, Paluch M and Gapinski J 2003 *J. Non-Cryst. Solids* **330** 259
- Patkowski A, Gapinski J and Meier G 2004 *Colloid Polym. Sci.* **282** 874
- Patterson D 1982 *Polym. Sci. Eng.* **22** 64
- Pawlus S, Paluch M, Sekula M, Ngai K L, Rzoska S J and Ziolo J 2003 *Phys. Rev. E* **68** 021503
- Pawlus S, Casalini R, Roland C M, Paluch M, Rzoska S J and Ziolo J 2004 *Phys. Rev. E* **70** 061501
- Pawlus S, Hensel-Bielowka S, Ziolo J and Paluch M 2005 *Phys. Rev. B* submitted
- Piermarini G J, Forman R A and Block S 1978 *Rev. Sci. Instrum.* **49** 1061
- Pimenov A, Lunkenheimer P, Kohlhaas R, Loidl A and Bohmer R 1996 *Phys. Rev. E* **54** 676
- Pisignano D, Capaccioli S, Casalini R, Lucchesi M, Rolla P A, Justl A and Rossler E 2001 *J. Condens. Matter Phys.* **13** 4405
- Plazek D J 1965 *J. Phys. Chem.* **69** 3480
- Plazek D J 1996 *J. Rheol.* **40** 987
- Plazek D J and Magill J H 1966 *J. Chem. Phys.* **45** 3038
- Plazek D J 1982 *J. Polym. Sci. Polym. Phys. Edn* **20** 1533
- Poole P H, Sciortino F, Grande T, Stanley H E and Angell C A 1994 *Phys. Rev. Lett.* **73** 1632
- Prevosto D, Lucchesi M, Capaccioli S, Casalini R and Rolla P A 2003 *Phys. Rev. B* **67** 174202
- Prevosto D, Lucchesi M, Capaccioli S, Casalini R and Rolla P A 2005 *Phys. Rev. B* **71** 136202
- Prigogine I and Mathot V 1952 *J. Chem. Phys.* **20** 49
- Psurek T, Hensel-Bielowka S, Ziolo J and Paluch M 2002 *J. Chem. Phys.* **116** 9882
- Psurek T, Ziolo J and Paluch M 2004 *Physica A* **331** 353
- Rabeony M, Lohse D J, Garner R T, Han S J, Graessley W W and Migler K B 1998 *Macromolecules* **31** 6511
- Ratner M A, Johansson P and Shriver D F 2000 *MRS Bull.* **25** 31
- Rault J 2000 *J. Non-Cryst. Solids* **271** 177
- Rehage G and Oels H-J 1977 *High Temp. High Press.* **9** 545
- Reinsberg S A, Qiu X H, Wilhelm M, Spiess H W and Ediger M D 2001 *J. Chem. Phys.* **114** 7299
- Reiser A, Kasper G and Hunklinger S 2004 *Phys. Rev. Lett* **92** 125701
- Reisinger T, Zarski M, Meyer W H and Wegner G 1997 *Novocontrol Dielectric Newsletter* (November issue)
- Richert R and Angell C A 1998 *J. Chem. Phys.* **108** 9016
- Richert R, Duvvuri K and Duong L-T 2003 *J. Chem. Phys.* **118** 1828
- Rizos A K and Ngai K L 1999 *Phys. Rev. E* **59** 612
- Roland C M and Ngai K L 1991 *Macromolecules* **24** 2261
- Roland C M 1992 *Macromolecules* **25** 7031
- Roland C M, Miller J B and McGrath K J 1993 *Macromolecules* **26** 4967
- Roland C M, Ngai K L and Lewis L J 1995 *J. Chem. Phys.* **103** 4632
- Roland C M and Ngai K L 1996 *J. Chem. Phys.* **104** 2967
- Roland C M, Ngai K L, Santangelo P G, Qiu X H, Ediger M D and Plazek D J 2001 *Macromolecules* **34** 6159
- Roland C M and Casalini R 2003a *Macromolecules* **36** 1361
- Roland C M and Casalini R 2003b *J. Chem. Phys.* **119** 1838
- Roland C M, Casalini R, Santangelo P, Sekula M, Ziolo J and Paluch M 2003a *Macromolecules* **36** 4954
- Roland C M, Paluch M and Rzoska S J 2003b *J. Chem. Phys.* **119** 12439
- Roland C M, Psurek T, Pawlus S and Paluch M 2003c *J. Polym. Sci. Polym. Phys. Edn* **41** 3047
- Roland C M, Casalini R and Paluch M 2003d *Chem. Phys. Lett.* **367** 259
- Roland C M and Casalini R 2004 *J. Chem. Phys.* **121** 11503
- Roland C M, Capaccioli S, Lucchesi M and Casalini R 2004a *J. Chem. Phys.* **120** 10640
- Roland C M, Schroeder M J, Fontanella J J and Ngai K L 2004b *Macromolecules* **37** 2630
- Roland C M, Ngai K L and Plazek D J 2004c *Macromolecules* **37** 7051
- Roland C M, Casalini R and Paluch M 2004d *J. Polym. Sci. Polym. Phys. Edn* **42** 4313
- Roland C M, Paluch M, Pakula T and Casalini R 2004e *Phil. Mag.* **84** 1573
- Roland C M and Casalini R 2005 *J. Chem. Phys.* **122** 134505
- Root L J and Berne B J 1997 *J. Chem. Phys.* **107** 4350

- Roots J E, Ma K T, Higgins J S and Arrighi V 1999 *Phys. Chem. Chem. Phys.* **1** 137
- Rössler E 1990 *Phys. Rev. Lett.* **65** 1595
- Rössler E, Sillescu H and Spiess H W 1985 *Polymer* **26** 203
- Roux J N, Barrat J L and Hansen J P 1989 *J. Phys.: Condens. Matter* **1** 7171
- Sampoli M, Benassi P, Eramo R, Angelani L and Ruocco G 2003 *J. Phys.: Condens. Matter* **15** S1227
- Saito S, Sasabe H, Nakajima T and Yada K 1968 *J. Polym. Sci. Polym. Phys. Edn* **6** 1297
- Santangelo P G, Ngai K L and Roland C M 1996 *Macromolecules* **29** 3651
- Santangelo P G and Roland C M 1998 *Macromolecules* **31** 3715
- Sasabe H and Saito S 1968 *J. Polym. Sci. Polym. Phys. Edn* **6** 1401
- Sasabe H, Saito S, Asahina M and Kakutani H 1969 *J. Polym. Sci. Polym. Phys. Edn* **7** 1405
- Sasabe H and Saito S 1972 *Polym. J. (Tokyo)* **3** 624
- Sastry S 2001 *Nature* **409** 164
- Sastry S, Debenedetti P G and Stillinger F H 1998 *Nature* **393** 554
- Scala A, Starr F W, La Nave E, Sciortino F and Stanley H E 2000 *Nature* **406** 166
- Schneider U, Lunkenheimer P, Brand R and Loidl A 1999a *Phys. Rev. E* **59** 6924
- Schneider U, Brand R, Lunkenheimer P and Loidl A 1999b *Phys. Rev. B* **56** R5713
- Schönals A, Kremer F and Schlosser E 1991 *Phys. Rev. Lett.* **67** 999
- Schönhals A 1993 *Macromolecules* **26** 1309
- Schroeder M J and Roland C M 2002 *Macromolecules* **35** 2676
- Schug K U, King H E Jr and Böhmer R 1998 *J. Chem. Phys.* **109** 1472
- Schweizer K S and Saltzman E J 2004a *J. Chem. Phys.* **121** 1984
- Schweizer K S and Saltzman E J 2004b *J. Phys. Chem. B* **108** 19729
- Scopigno T, Ruocco G, Sette F and Monaco G 2003 *Science* **302** 849
- Sekula M, Pawlus S, Hensel-Bielówska S, Zioło J, Paluch M and Roland C M 2004 *J. Phys. Chem. B* **108** 4997
- Shell M S, Debenedetti P G, La Nave E and Sciortino F 2003 *J. Chem. Phys.* **118** 8821
- Shimokawa S and Yamada E 1983 *J. Magn. Reson.* **51** 103
- Shumway S, Clarke A S and Jonsson H 1995 *J. Chem. Phys.* **102** 1796
- Sillescu H 1999 *J. Non-Cryst. Solids* **243** 81
- Simha R and Somcynsky T 1969 *Macromolecules* **2** 342
- Skorodumov V F and Godovskii Y K 1993 *Polym. Sci.* **35** 562
- Solunov C A 2002 *J. Phys.: Condens. Matter* **14** 7297
- Speedy R J 1999 *J. Phys. Chem. B* **103** 4060
- Starkweather W H, Avakian P, Fontanella J J and Wintersgill M C 1992 *Macromolecules* **25** 7145
- Stickel F, Fischer E W and Richert R 1995 *J. Chem. Phys.* **102** 6251
- Stickel F, Fischer E W and Richert R 1996 *J. Chem. Phys.* **104** 2043
- Stillinger H, Debenedetti P G and Truskett T M 2001 *J. Phys. Chem. B* **105** 11809
- Stockmayer W H 1967 *Pure Appl. Chem.* **15** 539
- Suzuki A, Masuko M, Nakayama T and Okabe H 1997 *J. Japan Soc. Tribol.* **42** 294
- Suzuki A, Masuko M and Nikkuni T 2000 *Tribol. Int.* **33** 107
- Suzuki A, Masuko M and Wakisaka K 2002 *Tribol. Int.* **35** 55
- Svanberg C, Bergman R and Jacobsson P 2003 *Europhys. Lett.* **64** 358
- Swallen S F, Bonvallet P A, McMahon R J and Ediger M D 2003 *Phys. Rev. Lett.* **90** 015901
- Takahara S, Yamamuro O and Suga H 1994 *J. Non-Cryst. Solids* **171** 259
- Takahara S, Yamamuro O, Ishikawa M, Matsuo T and Suga H 1998 *Rev. Sci. Instrum.* **69** 185
- Takahara S, Ishikawa M, Yamamuro O and Matsuo T 1999a *J. Phys. Chem. B* **103** 792
- Takahara S, Ishikawa M, Yamamuro O and Matsuo T 1999b *J. Phys. Chem. B* **103** 3288
- Tammann V G and Hesse W 1926 *Z. Anorg. Allg. Chem.* **156** 245
- Tarjus G and Kivelson D 1997 *Supercooled Liquids: Advances and Novel Applications* ed J T Fourkas *et al* (Washington, DC: American Chemical Society)
- Tarjus G, Kivelson D, Mossa S and Alba-Simionesco C 2004a *J. Chem. Phys.* **120** 6135
- Tarjus G, Mossa S and Alba-Simionesco C 2004b *J. Chem. Phys.* **121** 11505
- Theobald S, Schwarzenberger P and Pechhold W 1994 *High Pressure Res.* **13** 133d
- Theobald S, Pechhold W and Stoll B 2001 *Polymer* **42** 289
- Thiessen P A and Kirsch W 1938 *Rubber Chem. Technol.* **26** 387
- Tölle A, Schober H, Wuttke J, Randl O G and Fujara F 1998 *Phys. Rev. Lett.* **80** 2374
- Tölle A 2001 *Rep. Prog. Phys.* **64** 1473
- Tracht U, Wilhelm M, Heuer A and Spiess H W 1999 *J. Magn. Reson.* **140** 460
- Trask C A and Roland C M 1988 *Polym. Commun.* **29** 332

- Trask C A and Roland C M 1989 *Macromolecules* **22** 256
- Tribone J J, O'Reilly J M and Greener J 1989 *J. Polym. Sci. B: Polym. Phys.* **27** 837
- Tsang K Y and Ngai K L 1997 *Phys. Rev. E* **54** 3067
- Tyrell H J V and Harris K R 1984 *Diffusion in Liquids* (London: Butterworths)
- Urbanowicz P, Rzoska S J, Paluch M, Sawicki B, Szulc A and Ziolo J 1995 *Chem. Phys.* **201** 575
- Van Krevelen D W 1990 *Properties of Polymers* (New York: Elsevier)
- Van Krevelen D W 1997 *Properties of Polymers* (Amsterdam: Elsevier)
- Vass S, Patkowski A, Fischer E W, Stüvegh K and Vértes A 1999 *Europhys. Lett.* **46** 815
- Vogel H 1921 *Phys. Z.* **222** 645
- Vogel M and Rössler E 2001 *J. Chem. Phys.* **114** 5802
- Vollmayr-Lee K 2004 *J. Chem. Phys.* **121** 4781
- Vollmayr-Lee K, Kob W, Binder K and Zippelius A 2002 *J. Chem. Phys.* **116** 5158
- Warner C M and Boyer R F 1992 *J. Polym. Sci. Polym. Phys. Edn* **301** 1177
- Wagner H and Richert R 1999 *J. Phys. Chem. B* **103** 4071
- Weeks J D, Chandler D and Andersen H C 1971 *J. Chem. Phys.* **54** 5237
- Wen P, Wang W H, Zhao Y H, Zhao D Q, Pan M X, Li F Y and Jin C Q 2004 *Phys. Rev. B* **69** 092291
- Widom B 1967 *Science* **157** 375
- Widom B 1999 *Physica A* **263** 500
- Williams G 1964a *Trans. Faraday Soc.* **60** 1548
- Williams G 1964b *Trans. Faraday Soc.* **60** 1556
- Williams G 1965 *Trans. Faraday Soc.* **61** 1564
- Williams G 1966a *Trans. Faraday Soc.* **62** 1321
- Williams G 1966b *Trans. Faraday Soc.* **62** 2091
- Williams G and Edwards D A 1966 *Trans. Faraday Soc.* **62** 1329
- Williams G and Watts D C 1970 *Trans. Faraday Soc.* **66** 80
- Williams G and Watts D C 1971a *Trans. Faraday Soc.* **67** 2793
- Williams G and Watts D C 1971b *Trans. Faraday Soc.* **67** 1971
- Williams E and Angell C A 1977 *J. Phys. Chem.* **81** 232
- Williams G 1979 *Adv. Polym. Sci.* **33** 60
- Williams G 1997 *Dielectric Spectroscopy of Polymeric Materials* ed J P Runt and J J Fitzgerald (Washington, DC: American Chemical Society)
- Wu L 1991 *Phys. Rev. B* **43** 9906
- Yamamuro O, Takahara S and Suga H 1995 *J. Non-Cryst. Solids* **183** 144
- Zahl A, Igel P, Weller M and van Eldik R 2004 *Rev. Sci. Instrum.* **75** 3152
- Zhang S H, Casalini R, Runt J and Roland C M 2003 *Macromolecules* **36** 9917
- Zoller P 1986 *Encyclopedia of Polymer Science and Engineering* 2nd edn, vol 5 ed H Mark *et al* (New York: Wiley) p 69
- Zoller P and Walsh D J 1995 *Standard Pressure–Volume–Temperature Data for Polymers* (Lancaster: Technomic)